Natural Climate Solutions: Essays on Climate Mitigation in Agriculture, Forestry, and Land Use

By

EMILY MCGLYNN
DISSERTATION

Submitted in partial satisfaction of the requirements for the degree of

DOCTOR OF PHILOSOPHY

in

Agricultural and Resource Economics

in the

OFFICE OF GRADUATE STUDIES

of the

UNIVERSITY OF CALIFORNIA

DAVIS

Approved:

Michael Springborn, Chair

Aaron Smith

Frances Moore

Committee in Charge

2022

Acknowledgements

This material is based upon work supported by the National Science Foundation Graduate Research Fellowship under Grant No. 1650042. Any opinion, findings, and conclusions or recommendations expressed in this material are those of the author(s) and do not necessarily reflect the views of the National Science Foundation.

Work on Chapter 1 was funded by the Doris Duke Charitable Foundation.

For Lucas.

Table of Contents

Abstract

Policy makers around the world have recognized the role that agriculture, forestry, and land use can play in addressing climate change. These sectors are a growing source of greenhouse gases (GHGs), emitting one quarter of global anthropogenic GHG emissions annually. However, global integrated assessment models estimate that enhancing natural land-based CO_2 sinks, avoiding deforestation, and using bioenergy to avoid fossil fuel use could provide nearly one third of GHG abatement required to avoid the most extreme impacts of climate change. Through dedicated management and preservation, natural and managed landscapes can remove CO_2 from the atmosphere through photosynthesis, storing carbon in trunks, branches, roots, soils, and detritus for decades and even centuries.

Yet outside the confines of optimization models, federal, state, and local policy makers are often unsure how to efficiently deploy natural climate solutions, given the many markets, laws, landowners, and natural systems that influence net GHG outcomes and the potential for negative impacts to ecosystems and social welfare. In this dissertation, I provide three essays that inform natural climate solutions policy, accounting for important sources of real-world complexity.

- **Chapter 1. Addressing uncertainty and bias in land use, land use change, and forestry greenhouse gas inventories.** National GHG inventories (NGHGIs) are the primary tool for tracking anthropogenic GHG emissions for individual countries, sectors, and sources. I propose an analytical framework for implementing the uncertainty provisions of the UN Paris Agreement Enhanced Transparency Framework, with a view to

identifying the largest sources of land use, land use change, and forestry uncertainty in National GHG Inventories and prioritizing methodological improvements. This chapter was published in *Climatic Change*.[*]

- **Chapter 2. Conserving carbon: Evaluating term-limited conservation programs.** I develop a structural model of the landowner decision to participate in a voluntary, term-limited conservation program that constrains the optimal timing of land use change and that allows for re-enrollment, addressing a key literature gap in the evaluation of climate and conservation policy in forestry and agricultural sectors.
- **Chapter 3. The problem with pricing "carbon": exploring forest-driven albedo effects in DICELAND.** I update the Dynamic Integrated model for Climate and the Economy (DICE) to endogenously control global forest carbon sequestration activity. I use the so-called DICELAND model to estimate efficient global carbon prices and forest CO_2 mitigation levels when accounting for albedo (land-darkening) effects of global forest expansion.

[*] McGlynn, E., Li, S., F. Berger, M. *et al.* Addressing uncertainty and bias in land use, land use change, and forestry greenhouse gas inventories. *Climatic Change* **170,** 5 (2022). https://doi.org/10.1007/s10584-021-03254-2

1. Addressing uncertainty and bias in land use, land use change, and forestry greenhouse gas inventories*

Abstract

National greenhouse gas inventories (NGHGIs) will play an increasingly important role in tracking country progress against United Nations (U.N.) Paris Agreement commitments. Yet uncertainty in land use, land use change, and forestry (LULUCF) NGHGHI estimates may undermine international confidence in emissions reduction claims, particularly for countries that expect forests and agriculture to contribute large near-term GHG reductions. In this paper, we propose an analytical framework for implementing the uncertainty provisions of the U.N. Paris Agreement Enhanced Transparency Framework, with a view to identifying the largest sources of LULUCF NGHGI uncertainty and prioritizing methodological improvements. Using the United States as a case study, we identify and attribute uncertainty across all U.S. NGHGI LULUCF "uncertainty elements" (inputs, parameters, models, and instances of plot-based sampling) and provide GHG flux estimates for omitted inventory categories. The largest sources of uncertainty are distributed

* Co-authored with Serena Li, Michael Berger, Meredith Amend, and Kandice Harper. Emily McGlynn (lead author) developed research objectives and analytical methods for all land use categories, wrote manuscript, and carried out analysis for Wetlands and Alaska, Hawaii, and U.S. Territories. Serena Li carried out analysis for Cropland and Grasslands sections, including the expert survey. Michael Berger developed and oversaw analysis for Settlements. Meredith Amend coded the Monte Carlo analysis in R for Settlements analysis. Kandice Harper developed and carried out analysis for Forests section and provided support for all other analysis.

across LULUCF inventory categories, underlining the importance of sector-wide analysis: forestry (tree biomass sampling error; tree volume and specific gravity allometric parameters; soil carbon model), cropland and grassland (DayCent model structure and inputs) and settlement (urban tree gross to net carbon sequestration ratio) elements contribute over 90% of uncertainty. Net emissions of 123 MMT CO_2e could be omitted from the U.S. NGHGI, including: Alaskan grassland and wetland soil carbon stock change (90.4 MMT CO_2); urban mineral soil carbon stock change (34.7 MMT CO_2); and federal cropland and grassland N_2O (21.8 MMT CO_2e). We explain how these findings and other ongoing research can support improved LULUCF monitoring and transparency.

1. Introduction

National greenhouse gas (GHG) inventories (NGHGIs) are the primary tool for tracking anthropogenic (human-induced) GHG emissions at the country, sector, and source category level. Over the coming decade and beyond, NGHGIs will support setting and measuring progress against each country's "nationally determined contributions" (NDCs) for reducing GHG emissions under the United Nations (U.N.) Paris Agreement, while also supporting domestic climate policy development and evaluation (U.N. Framework Convention on Climate Change (UNFCCC) 2019a; UNFCCC 2019b; Andersson et al. 2008). In particular, NGHGI accounting for land use, land use change, and forestry (LULUCF) is a priority for many countries: the first round of NDCs indicates that LULUCF will provide 25% of planned GHG reductions leading to 2030 (Grassi et al. 2017). Global integrated assessment models project that enhancing natural land-based sinks, avoided

deforestation, and bioenergy could provide 30% of GHG abatement required to keep temperature increase below 1.5 C by 2050 (Roe et al. 2019).

Yet LULUCF is a large source of uncertainty in estimating anthropogenic GHG emissions (Friedlingstein et al. 2020, Pulles 2017, Jonas et al. 2014, National Research Council 2011). To ensure international confidence in national GHG reporting, significant improvements in LULUCF NGHGI estimation methods and transparency will be required. In this paper, we demonstrate an analytical framework for identifying, quantifying, and reporting on sources of LULUCF uncertainty and bias in NGHGI inventories at the level of individual datasets, models, submodels, and other inputs ("uncertainty elements"). Using the United States as a case study, we suggest countries can use this analytical framework to comply with U.N. Paris Agreement guidelines in two ways:

(1) Transparently reporting on LULUCF NGHGI uncertainty estimation methods, including clarifying which uncertainty elements are accounted for and how LULUCF uncertainty is calculated; and

(2) Identifying the largest uncertainty elements as a first step in prioritizing inventory improvements.

In our framework, we identify and attribute uncertainty across all U.S. LULUCF GHG source and sink (collectively, flux) estimates and provide initial GHG flux estimates for omitted inventory categories.[†] We make three contributions: (1) we propose and demonstrate an analytical

[†] In this paper, "flux" or "flux estimate" refers to a GHG source or sink calculation, over any geography, sector, subsector, or gas; "inventory category" refers to the most disaggregated level of flux estimates reported in an NGHGI.

framework that countries can use to fulfill U.N. Paris Agreement transparency provisions, (2) we advance the large literature concerning NGHGI uncertainty by focusing on so-called individual "uncertainty elements," which allows for better targeting data and research needs, and (3) we demonstrate a set of uncertainty attribution methods that can be applied across inventory categories with varying methodological complexity, including the most sophisticated (Tier 3) methods.[‡]

1.1 Evidence of global and national LULUCF uncertainty

LULUCF estimation uncertainty results from a combination of structural and conceptual challenges, including: (1) large heterogeneity in fluxes across time and space, driven by complex biological, geochemical, and physical processes combined with variable anthropogenic and natural disturbances, (2) the inability to continuously observe fluxes over time and over large areas, and (3) differences in definitions and accounting methods across countries and studies (Rypdal and Winiwarter 2001, Grassi et al. 2018). These dynamics drive higher proportional and absolute uncertainty when compared to GHG sources for which census data is available, underlying processes are better understood, and available GHG accounting guidance is more prescriptive (Pulles 2017).

[‡] Tiers 1, 2, and 3 refer to Intergovernmental Panel on Climate Change (IPCC) methodologies for estimating national GHG fluxes by source and sink categories (2006, 2019). Tiers 1 and 2 multiply activity data by an emissions factor. Tier 2 applies country-specific emissions factors while Tier 1 uses IPCC-recommended defaults. LULUCF Tier 3 methods include using country-specific models, repeated field sampling and/or remote monitoring, and methods that account for climatic dependency. IPCC guidance posits that Tier 3 methods are likely to provide higher accuracy than lower tiers (2006, 2019).

NGHGIs play a useful role in tracking anthropogenic LULUCF GHG emissions. Alternative methods (global land use change bookkeeping models and dynamic global vegetation models (DGVMs)) exhibit large multi-model uncertainty for total atmosphere-to-land CO_2 fluxes, with a standard deviation equal to 10% of annual global anthropogenic GHG emissions (4.0 Gigatonnes (Gt) CO_2 yr^{-1} over average, 2010-2019) (Friedlingstein et al. 2020). The disagreement is driven in part by conflicting definitions of anthropogenic LULUCF fluxes. Combining global bookkeeping models and DGVMs to align with the definition used by NGHGIs (all LULUCF fluxes on managed land) achieves results consistent with aggregate NGHGI estimates (within 0.8 Gt CO_2 yr^{-1}) (Grassi et al. 2018).[§] As such, NGHGIs appear to be able to collectively validate the LULUCF estimates of global models and vice versa.

However, individual NGHGIs vary widely in quality and precision, which creates challenges in tracking country-level emissions trends and therefore NDC progress. The NGHGIs of major-emitting countries reviewed in Table 1 cover 40% of global LULUCF fluxes (in absolute value, see Supplementary Material (SM) Section 1). Reviewed countries report proportional LULUCF uncertainty ranging from 12% (Colombia) to 102% (Cambodia). Of the 5 major-emitting countries with the largest LULUCF fluxes, we find that four (China, United States,

[§] IPCC (2006, 2019) NGHGI guidelines recommend that anthropogenic LULUCF GHG fluxes be defined as all GHG fluxes occurring on managed lands, the so-called "managed land proxy." Given the objective of NGHGIs to quantify all anthropogenic GHG fluxes, the managed land proxy has recognized flaws, including the presence of naturally-occurring GHG fluxes on managed lands (e.g., wildfires) and indirect human-induced fluxes on unmanaged lands (e.g., methane emissions due to permafrost thaw). However, several rounds of IPCC review have found the managed land proxy to be the most pragmatic approach to delineating anthropogenic emissions in the LULUCF sector. For a useful review of the managed land proxy, see Grassi et al. (2018).

Russia, India) exhibit sufficiently large uncertainty that the LULUCF emissions reductions proposed in their first NDCs are at risk of failing statistical significance at the 95% confidence level (Jonas et al. 2010, see SM Section 1 for further discussion).

Furthermore, there is significant heterogeneity in uncertainty estimation methods, making it difficult to compare precision across NGHGIs and to know how well uncertainty values reflect true variance of the flux point estimate. Challenges include not reporting LULUCF uncertainty at all (India, South Korea), not reporting uncertainty for inventory categories (China, Brazil), and, most commonly, providing insufficient information on how uncertainties were calculated (no reporting on uncertainty measures for emissions factors or activity data; no information on how uncertainty measures were estimated).

(1)	(2)	(3)	(4)	(5) Uncertainty reported?			(6)	(7)	(8)
Country	LULUCF, MMT CO_2e	Economy-wide emissions, incl. LULUCF, MMT CO_2e	% Tier 3, LULUCF	Sector	Gas	Inventory Category	LULUCF uncertainty (%)	Half CI, MMT CO_2e	NDC LULUCF, MMT CO_2e
China	-1,103	11,484	4	X			21	232	160
United States	-789	5,798	97	X		X	27[§]	213	20
Indonesia†	639	1,513	0			X	34	217	450
Russia	-533	1,614	1	X		X	32	171	80
India	-307	2,647	0				NR		50
Nigeria	307	648	0			X	22	68	
Brazil	403	1,577	0		X		67	270	300
Malaysia	-241	81	0	X		X	17	41	
Mexico	-148	551	0	X		X	19	28	60
Cambodia	131	166	0	X		X	102	134	0
Thailand††	-91	270	0				56	51	
Peru†	76	174	0			X	80	61	
Turkey	-84	425	0	X		X	51	43	0
Chile	-64	51	0	X		X	65	42	50
Colombia†	64	226	0			X	12	8	20
Japan	-50	1,161	94	X		X	14	7	30
South Korea	-44	656	0				NR		
Italy†	-42	438	82			X	28	12	
Spain	-38	280	0	X		X	48	18	
Vietnam†	-39	317	74			X	72	28	

Table 1. LULUCF NGHGI uncertainty for 20 major emitting countries. Column (4) is calculated by taking the absolute value of fluxes for all LULUCF inventory categories and finding the proportion of flux absolute values labeled Tier 3. Column (6) reflects one direction of the 95% confidence interval (CI) as percentage of central value (column (2)). NR = Not reported. Column (7) shows half of the 95% CI range, derived from columns (2) and (6). Column (8) shows LULUCF GHG reductions between 2010 and 2030, consistent with countries' first NDCs (Grassi et al. 2018). Not all countries quantify LULUCF actions in the first NDC. Gray rows indicate countries with estimation error (column (7)) larger than NDC LULUCF reductions (column (8)). For additional detail on sources and derivations, see Supplementary Material Section 1, Table 1-1. †LULUCF sector uncertainty is not reported, so column (6) is calculated using error propagation and inventory category uncertainty. ††Uncertainty is calculated using error propagation and total inventory uncertainty with and without LULUCF. [§]United States reports non-symmetric 95% CI, 27% reflects average of 35% lower bound and 19% upper bound; however column (7) reflects the non-symmetric CI.

The large majority of LULUCF fluxes reported in NGHGIs are calculated using lower order (Tier 1 and 2) methods, which likely limit accuracy (Ogle et al. 2003, Ogle et al. 2006). As countries look to improve LULUCF monitoring methods, uncertainty estimation will become more complex. Indeed, uncertainty estimates may increase to more closely approximate true variability, particularly as more sources of uncertainty are accounted for. Therefore, it will be important for countries to simultaneously improve NGHGI methods, transparently report uncertainty, and identify opportunities for increasing precision to ensure NDC emissions reduction claims are well-supported.

To date, non-Annex I (developing) countries have lacked mandates and resources to report NGHGIs in a format comparable to Annex I countries, which has driven large heterogeneity in non-Annex I NGHGIs.[**] Going forward, however, Parties to the U.N. Paris Agreement have agreed to implement an Enhanced Transparency Framework, under which both Annex I and non-Annex I countries will regularly submit NGHGIs using 2006 Intergovernmental Panel on Climate Change (IPCC) Guidelines for National Greenhouse Gas Inventories and the 2019 Refinement (IPCC 2006, IPCC 2019, UNFCCC 2015, UNFCCC 2019a, UNFCCC 2019b). All Parties are required to estimate uncertainty for all inventory categories and inventory totals, and to report on uncertainty estimation methods and underlying assumptions (UNFCCC 2019a, Decision 18/CMA.1). Developing countries are given some flexibility to qualitatively discuss uncertainty for key inventory categories, where data are unavailable.

[**] Annex I is defined under the UNFCCC as countries that were members of the Organisation for Economic Cooperation and Development (OECD) in 1992.

To support the Enhanced Transparency Framework, countries can use the methods demonstrated in this paper to both transparently report on NGHGI uncertainty methods and to identify the largest sources of LULUCF uncertainty as a way to prioritize inventory improvements. We use the United States as a case study due to the scale of U.S. LULUCF fluxes (the largest of all Annex I countries, Mooney et al. (in press)), the proportion of LULUCF fluxes calculated using Tier 3 methods (97%, Table 1), and the degree of transparency in the U.S. NGHGI. The methods and data underlying the U.S. LULUCF inventory are based on over 130 peer-reviewed articles and government reports and improvements made over 25 NGHGI reports since 1996 (U.S. NGHGI 2021). The United States encompasses a large variety of land uses and climatic regions, making it a useful basis for studying GHG estimation methods across LULUCF inventory categories. The United States is also active in LULUCF carbon credit markets, generating over 25% of LULUCF credits issued globally under existing voluntary and compliance carbon crediting mechanisms (see SM Section 1, Table 1-3).

1.2 Defining and quantifying NGHGI uncertainty

We are interested in a quantitative measure of the potential difference between an NGHGI flux estimate and the true value of the flux being estimated, referred to as model outcome uncertainty or prediction error (Walker 2003, Harmon et al. 2015). Our analysis focuses on two ways model outcome uncertainty can manifest: (1) random error around the true flux, and (2) bias or systematic error between the estimate and the true flux.

As recommended by IPCC (2006, 2019) guidelines, NGHGI uncertainty assessments often assume flux estimates are unbiased, that is, the true GHG flux can be recovered in expectation

(Magnussen et al. 2014). Using this assumption and standard statistical inference methods, one can calculate a 95% confidence interval (CI) for each estimate, a measure of random error which indicates the bounds within with the true flux will be located 95% of the time, assuming data could be randomly sampled many times over relevant populations.

Previous work has relaxed the unbiasedness assumption by comparing independent calculations for the same inventory category (Petrescu et al. 2020, Erb et al. 2013, Shvidenko et al. 2010, Smith et al. 2008). Even if unbiasedness holds for individual flux estimates, NGHGIs as a whole can be biased by omitting inventory categories due to lack of knowledge, data, or technical capacity. Inventory-wide bias has been estimated by comparing aggregate NGHGI flux estimates across historical inventory recalculations (Hamal 2010), a method which captures bias from changes in inventory methods and inventory category omissions, but this approach will not be useful for identifying potential inventory improvements.

Many studies have assessed uncertainty across entire NGHGIs (e.g., Bun et al. 2010, Winiwarter and Muik 2010, Lieberman et al. 2007) and with a focus on agricultural and forestry inventory sectors (e.g., Petrescu et al. 2020, Shvidenko et al. 2010, Leip 2010, Nilsson et al. 2007, Monni et al. 2007a, Monni et al. 2007b), yet uncertainty estimates are limited to the level of sector, gas (CO_2, CH_4, N_2O), or flux. Few studies have performed more detailed uncertainty attribution for agriculture and forestry sectors, and where this analysis occurs it is limited to Tier 2 inventory methods (Monni et al. 2007a, Winiwarter and Rypdal 2001, Winiwarter and Muik 2010). Studies that assess uncertainty for individual inventory categories provide useful context and inputs for our analysis (Peltoniemi et al. 2006, Ogle et al. 2010).

We look to build on these literature strands in two ways: (1) identifying individual sources of uncertainty which we term "uncertainty elements," for each NGHGI flux estimate, with a goal of resolving uncertainty attribution at a level that is meaningful for setting programmatic, research, and budgetary priorities, and (2) attributing uncertainty across all elements as consistently as possible for the entire LULUCF sector. While for most fluxes we are unable to account for bias, we suggest a measure of NGHGI bias by providing initial estimates of omitted GHG fluxes.

2. Methods

Our analytical scope aligns with the IPCC (2006, 2019) definition of LULUCF fluxes, encompassing all GHG sources and sinks from U.S. managed lands. We also broaden LULUCF to include N_2O and CH_4 emissions from agricultural soil management and rice methane for two reasons: (1) the United States uses a single model, DayCent, to jointly calculate carbon stock change and non-CO_2 fluxes on agricultural soils, and (2) previous studies identified agricultural soil N_2O emissions as the largest source of economy-wide NGHGI uncertainty (Ramírez et al. 2008, Winiwarter and Muik 2010, Petrescu et al. 2020), so including these inventory categories would likely impact our analysis.

We describe here the two components of our analysis:

- **Uncertainty attribution**: We quantify the contribution of each uncertainty element to the 95% CIs of all relevant LULUCF inventory categories.

- **Omitted flux estimation**: We provide initial estimates of known omitted fluxes, using literature review, expert input, and Tier 1 and 2 methods.

2.1 **Uncertainty attribution**

To identify sources of NGHGI uncertainty we must first justify an uncertainty taxonomy tailored to the LULUCF NGHGI context. Based on the literature review described in SM Section 2, chapter 1.2, we define an uncertainty element as an individual input, parameter, model or submodel, and any instance of design-based sampling error. We refer to input, parameter, and model structure uncertainty collectively as model uncertainty, as distinct from sampling error. In some cases, we aggregate uncertainty elements into a group of inputs or parameters for ease of analysis and interpretation.

Given this taxonomy, we review methods for each LULUCF inventory category and identify all uncertainty elements. For inventory categories where it was possible to recalculate the central flux estimate given available data, we attribute uncertainty to each element using the contribution index method (Equation 1).

Equation 1: Contribution index

$$Index\ i,k\ = \frac{Range\ \ full,k\ - Range(i,k)}{\sum_{j=1}^{J} Range\ \ full,k\ - Range(j,k)} \times 100$$

Where

i = 1,…,J	refers to uncertainty element *i*;
Range(full,k)	is inventory category *k* 95% CI magnitude (97.5th quantile minus 2.5th quantile);

Range(i,k) is inventory category *k* 95% CI magnitude holding element *i* at its mean or point estimate; and

Index(i,k) is percentage contribution of element *i* to *Range(full,k)*.

Other methods for uncertainty attribution have been utilized in the literature, including sensitivity analysis (McRoberts et al. 2016, Rypdal and Flugsrud 2001), uncertainty importance elasticities (Smith and Heath 2001, Winiwarter and Muik 2010), regression correlation coefficients (Peltoniemi et al. 2006, Winiwarter and Muik 2010), and Gaussian error propagation (Harmon et al. 2007, Phillips et al. 2000). We chose the contribution index method for its ability to account for full probability distributions, to allow for non-linear relationships between elements and model outputs and dependencies among uncertainty elements, and because we would be able to use previously-published analyses for some inventory categories (Smith and Heath 2001, Ogle et al. 2003, Skog et al. 2004).

Where flux estimate recalculation was not possible, due to lack of access to data or methods, we use published uncertainty attribution results or, in the case of Tier 3 cropland and grassland fluxes, expert elicitation. U.S. EPA recognizes expert elicitation as one method for NGHGI quality assurance and uncertainty analysis (U.S. EPA 2002). We tailored U.S. EPA (2002) NGHGI expert elicitation guidance to the objectives of our study (methods described in more detail below).

Uncertainty elements that we identified but were not able to quantify are listed in SM Table 2-1. Table 2 summarizes the uncertainty attribution methods used for each LULUCF inventory category.

Land category	GHG flux category	Uncertainty attribution method			
		Recalculation + Contribution Index	Expert Elicitation	Literature	NGHGI (2018)
Forests	*Living and standing dead biomass*	✓			
	Litter	✓		✓	
	Soil	✓		✓	
	Non-CO_2 from forest fires	✓			
	Harvested wood products			✓	
	N_2O from N additions to soils				✓
	Drained organic soils				✓
Croplands and Grasslands	*Tier 3 soils*		✓		
	Tier 1 and 2 soils			✓	
	Non-CO_2 from grassland fires	✓			
Settlements	*Urban trees*	✓			
	Yard trimmings and food scraps	✓			
	N_2O from soils				✓
	Drained organic soils				✓
Wetlands	*Peatlands*				✓
	Coastal wetlands				✓

Table 2. Uncertainty attribution methods for each GHG flux category.

2.2 Omitted GHG flux estimation

Most of the omitted fluxes identified in this paper are already recognized in the U.S. LULUCF GHG inventory as planned improvements. We identified additional omitted fluxes by reviewing IPCC (2006, 2019) guidance, by including prompts to identify omitted GHG fluxes in the cropland and grassland expert elicitation survey, and by prompting U.S. LULUCF NGHGI inventory compilers to identify omitted GHG fluxes through direct communication.

For each identified omitted flux, we reviewed the literature to identify activity data and emission factors. The resulting omitted GHG flux estimates are meant to be useful only for purposes of prioritizing future work.

2.3 Methods by land use and inventory categories

We briefly summarize the methods used for each LULUCF inventory category here, with further details provided in the SM. Our analysis is based on the 2018 U.S. NGHGI report, which covers inventory years 1990 to 2016 and which was the most complete inventory report available while the majority of our analytical work was completed. In the SM we note any significant methodological updates in more recent U.S. NGHGI reports, none of which meaningfully influence our findings.

Forests

Above- and belowground biomass in living and standing dead trees (SM Section 2, chapter 2.1): We recalculate the carbon stock change flux and 95% CI for above- and belowground tree biomass and standing dead trees (hereafter, tree biomass), accounting for uncertainty in nine groups of allometric model parameters (Table 2-2) as well as sampling error. We use Forest Inventory and Analysis (FIA) data and allometric models specific to eastern Texas as the basis for analysis to reduce Monte Carlo computational burden. Eastern Texas was chosen as a representative region for national forest carbon fluxes, encompassing both shrub species common in the western United States and hardwood and softwood species present in higher precipitation regions. We find that eastern Texas tree biomass exhibits similar proportional uncertainty to national uncertainty reported in the U.S. NGHGI (see SM Section 2, chapter 2.1 for more detail).

Litter and soil (SM Section 2, chapter 2.2 and 2.3): Using literature estimates of mean litter carbon stocks by forest type (Domke et al. 2016), and the reported model prediction uncertainty for litter carbon stocks (U.S. NGHGI 2018), we use Monte Carlo simulation to estimate the national 95% CI for litter carbon stock change. Similar methods were used for soils, accounting for model prediction uncertainty from estimating soil carbon stocks to 100 cm depth at a subset of FIA plots as well as the Random Forest model used to extrapolate soil carbon stock estimates to all FIA plots (Domke et al. 2017). A significant shortcoming of our approach for both litter and soil carbon pools is that it requires assuming covariance of carbon stocks between two time periods, because the U.S. NGHGI does not report 95% CIs by forest carbon pool. For this reason, we provide sensitivity analysis for different levels of intertemporal covariance.

Non-CO_2 from forest fires (SM Section 2, chapter 2.4): We recalculate the CH_4 and N_2O emissions from forest fires and their respective 95% CIs, using Monte Carlo simulation to account for uncertainty from four input variables (burned area, fuel availability, combustion factor, and emissions factor) using standard deviations reported in the U.S. NGHGI (2018) and IPCC (2006).

Harvested wood products (SM Section 2, chapter 2.5): We modify contribution index results from Skog et al. (2004) to focus on inputs and parameters used in Skog (2008), which most closely aligns with U.S. NGHGI (2018) methods.

Cropland and Grassland

The U.S. NGHGI uses consistent methods across many cropland and grassland inventory categories, so we collapse analysis across the two land uses. The U.S. NGHGI uses Tier 3 methods

on 78% of managed cropland and grassland soils, and Tier 1 and 2 on organic soils, federal grasslands, shaley and gravelly soils, and minor crop types.

Carbon stock change, N_2O, and rice CH_4 on Tier 3 soils (SM Section 2, chapter 3.1): It was not possible to recalculate Tier 3 fluxes, due to National Resources Inventory (NRI) dataset confidentiality. Therefore, we use expert elicitation to identify the largest sources of uncertainty stemming from inputs and structure of the biogeochemical model DayCent as well as scaling NRI plot estimates to population area. The expert elicitation included prompts to identify primary research, model development and intermodel comparison, and data priorities for reducing cropland and grassland Tier 3 flux uncertainty. Participation in uncertainty attribution sections of the survey required knowledge of Century, DayCent or similar biogeochemical soil models and IPCC GHG accounting guidance. Respondents were asked to confirm that they possessed this knowledge before completing the survey. Respondent expertise was concentrated in soil science (87%), biogeochemistry (67%), and the carbon cycle (67%); 53% worked in academia, 33% in government, and the remainder in NGO or private sectors. Details on the expert elicitation protocol and results are provided in the SM Section 2, chapter 3.1 and the full expert elicitation survey is available in SM Section 3.

Carbon stock change and N2O in Tier 1, 2 soils (SM Section 2, chapter 3.2): We apply contribution index results from Ogle et al. (2003) to 95% CIs reported in the U.S. NGHGI (2018).

Non-CO_2 from grassland fires (SM Section 2, chapter 3.3): We recalculate 2014 CH_4 and N_2O emissions, the most recent year for which burned grassland area estimates are available, and follow methods similar to the forest fire inventory category.

Omitted cropland and grassland GHG fluxes (SM Section 2, chapter 3.4): We use IPCC (2006) default equations and literature emissions factors to estimate carbon stock change in woody biomass and litter (USDA 2012, Udawatta and Jose 2012); non-CO_2 emissions from woody biomass in grassland fires (U.S. NGHGI 2018, IPCC 2006); soil microbial CH_4 sink (Dutaur and Verchot 2007, Del Grosso et al. 2000); and select GHG sinks and sources on federal cropland and grassland (U.S. NGHGI 2018).

Settlements

Carbon stock change in urban trees (SM Section 2, chapter 4.1): We recalculate the CO_2 flux and 95% CI attributable to carbon stock change in urban trees (Nowak et al. 2008, Nowak et al. 2013). We attribute uncertainty to all inputs (Table 2-30) using error propagation and contribution index methods.

Carbon stock change in yard trimmings and food scraps (SM Section 2, chapter 4.2): We recalculate CO_2 fluxes and 95% CIs attributable to yard trimmings and food scraps discarded in landfills (U.S. NGHGI 2018, Cruz and Barlaz 2010), accounting for uncertainty from all inputs. *Omitted settlement GHG fluxes* (SM Section 2, chapter 4.5): We estimate CO_2 emissions resulting from U.S. settlement mineral soils, which is omitted from the U.S. NGHGI due to lack of data, consistent with IPCC (2006) guidelines. Using Tier 1 methods and IPCC (2006) default values, we provide an initial estimate of this flux.

Wetlands

The U.S. NGHGI (2018) indicates there are 43 million hectares of wetlands in the United States, yet GHG fluxes are calculated for only 2.9 million hectares of wetlands. The omission is

due to lack of data that would allow for designating non-coastal wetlands as managed (that is, wetlands directly created by human activity or areas where the water level has been artificially altered) (U.S. NGHGI 2018). Due to this data gap we were not able to estimate omitted wetland fluxes (SM Section 2, chapter 5).

Alaska, Hawaii, and U.S. territories

Alaska, Hawaii, and U.S. territories comprise nearly 20 percent of the total U.S. land base (nearly all of this in Alaska), but they are not completely accounted for in the U.S. NGHGI. The 2019 U.S. NGHGI included forest carbon stock changes in interior Alaska for the first time, an area covering 24.5 million acres (9% of U.S. managed forest area). We provide estimates for omitted fluxes in Alaska, Hawaii, and Puerto Rico (the largest U.S. territory), based on IPCC (2006) guidance, emissions data derived from the U.S. NGHGI (2018, 2019), and literature review (SM Section 2, chapter 6).

3. Results

Uncertainty contribution results are reported as the uncertainty element's contribution index value (%) multiplied by its respective inventory category 95% CI range (MMT CO_2e). We present the 10 largest sources of uncertainty for each land use category, then collectively show omitted GHG flux results. Complete results for all inventory categories and uncertainty elements are available in the SM.

3.1 Forests

The largest source of forest GHG flux uncertainty is design-based sampling error in estimating tree biomass carbon stock change (434.3 MMT CO_2e) (Table 3). Two groups of allometric parameters are the largest sources of uncertainty in estimating individual tree biomass (together, 131.9 MMT CO_2e), which govern the conversion of tree diameter and height to gross bole volume (volume coefficients) and the conversion of bole volume to biomass (wood and bark specific gravities).

While we find that allometric volume coefficients are a large source of forest carbon stock change uncertainty, we were not able to find an empirical estimate of volume coefficient uncertainty. Sensitivity analysis of the coefficient of variation (5%, 10% (base case), and 20%) found this assumption has large impacts on both the tree biomass 95% CI and the uncertainty contribution ranking of allometric parameter groups (SM Table 2-4).

Model uncertainty for soil and litter carbon stock change are substantial (together, 91.7 to 288.9 MMT CO_2e); we report a range for these pools to reflect sensitivity to carbon stock intertemporal covariance (SM Section 2, chapter 2.2 and 2.3).

Element	*Type*	*Description*	*Uncertainty contribution (MMT CO_2e)*
Tree biomass	Sampling	Design-based sampling error derived from post-stratified variance of above-and belowground biomass on *Forest Remaining Forest.*	434.3
Forest soils[a]	Model (aggregate)	Total model prediction error in estimating soil carbon flux on *Forest Remaining Forest.*	81.2-255.7
Forest tree biomass: Volume coefficients[b]	Parameter	Uncertainty associated with species-specific parameters used to estimate tree stem volume from height and diameter measurements.	16.9-77.7
Forest tree biomass: Wood and bark specific gravities	Parameter	Uncertainty associated with species-specific parameters used to convert tree stem volume to biomass.	54.2
Forest litter[a]	Model (aggregate)	Total model prediction error in estimating litter carbon flux on *Forest Remaining Forest.*	10.5-33.2
Forest fire input: Fuel availability, CONUS	Input	Uncertainty associated with input specifying mass of dry matter available for combustion per unit area in the conterminous United States.	28.7
Harvested wood products: Solid wood products data	Input	Uncertainty associated with input specifying annual solid wood products production.	14.0
Harvested wood products: Solid wood products conversion to carbon	Parameter	Uncertainty associated with the parameter used to estimate carbon in solid wood products.	13.2
Forest fires: Emission factors	Parameter	Uncertainty associated with parameters that specify the mass of CH_4 and N_2O gas emitted per mass of dry matter combusted.	6.0
Harvested wood products: Paper data	Input	Uncertainty associated with input specifying annual paper production.	4.7

Table 3. Forest GHG flux uncertainty elements. a. Accounts for sensitivity to carbon stock covariance between time steps; low value reflects 99.99% covariance as percentage of variance; high estimate reflects 99.9% (see SM sections 2.2 and 2.3). b. Accounts for sensitivity to coefficient of variation assumption; low estimate reflects COV =5%, high estimate reflects COV= 10% (see SM Section 2, chapter 2.1).

3.2 Cropland and Grassland

The DayCent model accounts for the vast majority of cropland and grassland soil carbon stock change, agricultural N_2O, and rice methane uncertainty (Table 4). DayCent model structure and parameters (including organic matter formation and decomposition; nitrification and denitrification; leaching, runoff, and volatilization) collectively contribute 117.2 MMT CO_2e, while DayCent inputs (including tillage, fertilization management, and manure and organic fertilizer application) contribute 222.0 MMT CO_2e. Input uncertainty is primarily driven by randomly assigning management activities to NRI plots consistent with county-level statistics (Ogle et al. 2010).

Element	*Type*	*Description*	*Uncertainty contribution (MMT CO_{2e})*
DayCent: Soil properties	Input	Uncertainty in soil texture and natural drainage capacity for each NRI survey location derived from the Soil Survey Geographic Database (not accounted for in NGHGI 95% CI).	31.3
DayCent: Leaching, runoff, and volatilization	Input, Model (aggregate)	Uncertainty associated with DayCent inputs, parameters, and model structure used to estimate N lost through leaching, runoff and volatilization (not accounted for in NGHGI 95% CI).	28.6
DayCent: Organic matter formation and decomposition	Model structure	Uncertainty associated with DayCent submodel used to simulate soil organic C and N dynamics across discrete litter and soil pools.	25.6
DayCent: Nitrification and denitrification	Model structure	Uncertainty associated with DayCent submodel structure used to simulate soil mineral N dynamics.	24.1
DayCent: Manure and other organic fertilizer applications	Input	Uncertainty in occurrence of manure and organic fertilizer application, application rates, and interaction with mineral fertilizer application at NRI survey locations.	23.4
DayCent: Tillage	Input	Uncertainty in tillage practices (conventional, reduced, no-till) at NRI survey locations.	23.4
DayCent: Fertilization management	Input	Uncertainty in mineral N application rates at NRI survey locations by crop and land use type, derived from USDA Agricultural Resource Management Surveys.	21.9
DayCent: Soil and water temperature regimes	Model structure	Uncertainty associated with the DayCent submodel used to simulate water flows and changes in soil water availability.	15.7

Table 4. Cropland and grassland GHG flux uncertainty elements.

3.3 Settlements

Urban tree gross to net sequestration ratio contribution is an order of magnitude larger than any other settlement uncertainty element (Table 5). This uncertainty arises due to a majority of states lacking data on net urban tree growth rates, requiring use of a national average (Nowak et al. 2013).

Yard trimmings and food scraps carbon stock change inputs account for less than 12% of settlement GHG flux uncertainty, with negligible contributions from remaining fluxes (carbon stock change on drained organic soils and N_2O emissions from soil N additions).

Element	*Type*	*Description*	*Uncertainty contribution (MMT CO_2e)*
Urban tree: gross to net sequestration ratio	Input	Uncertainty in state-level input reflecting proportion of urban tree carbon lost to downed branches or tree decay. Where state-level data is lacking, a national average value is used.	86.5
Urban tree: gross sequestration rate	Input	Uncertainty in state-level input reflecting mass of carbon per area stored in urban trees.	7.0
Urban tree: Urban/developed land area	Input	Uncertainty associated with deriving state-level urban/developed land area from Census/NLCD data, used to expand urban tree carbon stock change estimates.	6.5
Yard trimmings and food scraps: Food scraps multiplier	Parameter	Uncertainty in the proportion of total biological waste assumed to be food scraps.	6.3
Urban tree: Tree cover percentage	Input	Uncertainty in state-level input reflecting percentage of urban/developed land with tree cover.	4.3
Yard trimmings and food scraps: Percent carbon stored in organic waste	Parameter	Uncertainty in parameters reflecting amount of carbon stored in each organic waste type, given decay rate.	3.8
Yard trimmings and food scraps: Moisture content of organic waste	Parameter	Uncertainty in parameters reflecting moisture content of each organic waste type.	1.8
Yard trimmings and food scraps: Yard trimmings multiplier	Parameter	Uncertainty in volume of grass, leaves, and branches as percentage of yard trimmings volume.	1.6
Settlement soils: Direct N_2O emissions from N additions to soils	Total	Total uncertainty in N input data, NRI data, default IPCC emission factors, and surrogate data extrapolation in estimating N_2O emissions.	1.3

Table 5. Settlement GHG flux uncertainty elements.

3.4 Uncertainty attribution synthesis

Our findings suggest higher LULUCF uncertainty in the U.S. NGHGI than is currently reported. While our recalculated uncertainty estimates generally align with reported values, two notable exceptions are forest carbon stock change and cropland and grassland Tier 3 fluxes, where we found 5-27% (with sensitivity to litter and soil carbon stock change uncertainty) and 94% larger CI ranges, respectively. Total LULUCF CI magnitude could be 18-35% higher than U.S. NGHGI (2018) reported values (Figure 1).

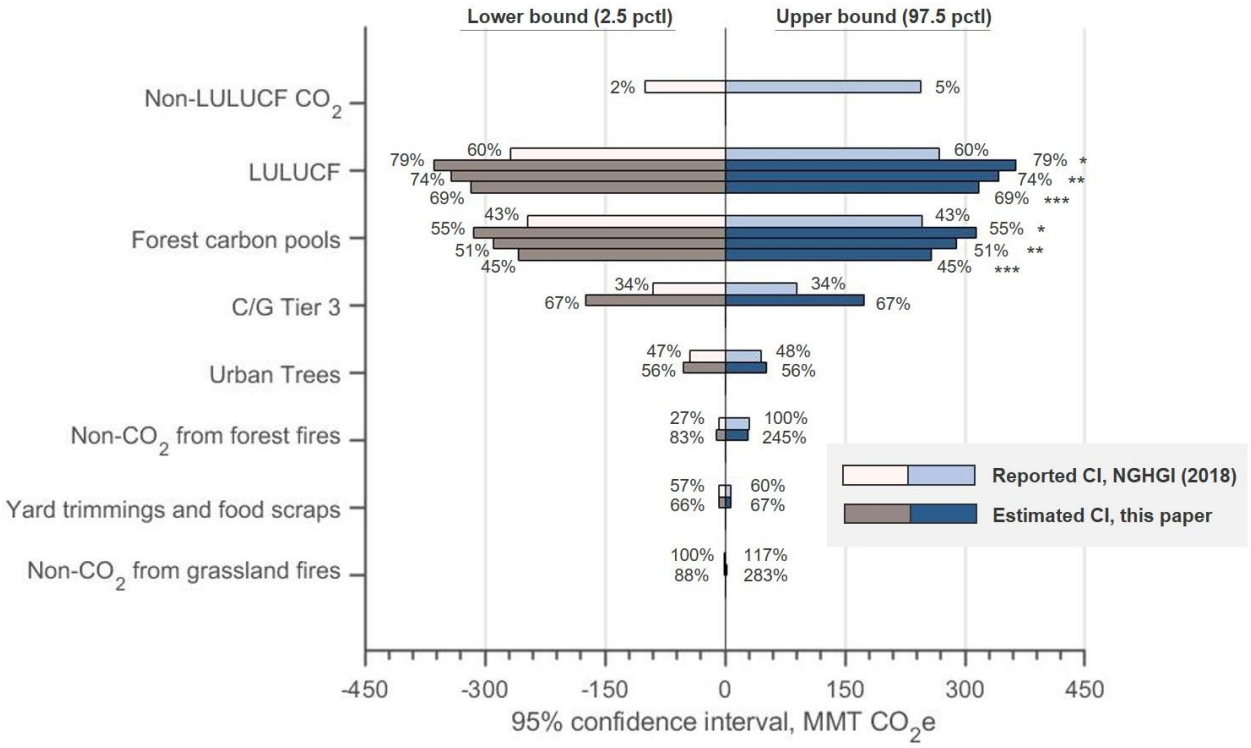

Fig. 1. Reported and recalculated confidence intervals (CI) by inventory category. Magnitude of one-direction CI as percentage of the point estimate is shown at the end of each bar. U.S. NGHGI (2018) values for "LULUCF" reflect only inventory categories assessed in this paper, and so is inconsistent with U.S. NGHGI (2018) Table 1-5; "Non-LULUCF CO_2" results are as listed in Table 1.5. "Forest carbon pools" (which includes tree biomass, soil, and litter) CI estimates are aggregated using error propagation to allow for comparison with NGHGI (2018) reported values. "Forest carbon pools" and "LULUCF" results show sensitivity to soil, litter, and tree biomass

volume coefficients uncertainty attribution (all uncertainty contribution values in MMT CO_2e: soil carbon stock change (CSC) = *255.7, **81.2, ***81.2; litter CSC = *33.2, **10.5, ***10.5; tree biomass volume coefficient = *77.7, **77.7, ***16.9).

Higher cropland and grassland Tier 3 uncertainty can be directly attributed to the expert elicitation, which directed respondents to identify the uncertainty contribution from elements not currently accounted for in reported U.S. NGHGI CIs, which ultimately included the two largest DayCent uncertainty elements (soil properties; leaching, runoff, and volatilization) (U.S. NGHGI 2018).

It is less clear whether higher forest carbon stock change uncertainty can be attributed to our choice of analytical region (eastern Texas), including a larger number of uncertainty elements in our analysis, or other assumptions made in our analysis (e.g. intertemporal covariance for litter and soil carbon pools). Accounting for sensitivity to uncertainty contributions from soil and litter carbon stock change and tree biomass volume coefficient assumptions, our high (low) end uncertainty estimates for these elements result in 27% (5%) higher forest carbon pool CI compared to U.S. NGHGI (2018) reported values.

A meaningful reduction in U.S. LULUCF uncertainty would require addressing many of the largest elements simultaneously. No single element or element group would reduce the LULUCF CI by more than 10% except for tree biomass sampling error (Figure 2.a). A 50% reduction in LULUCF CI magnitude would require reducing tree biomass sampling error by at least 15%, and reducing contributions of all other uncertainty elements by at least 50% (Figure 2.b). The optimal uncertainty reduction approach depends on availability and costs of alternative

methods, but this exercise illustrates the inevitable need to focus on forest sampling error, soil carbon modeling, and urban tree methods.

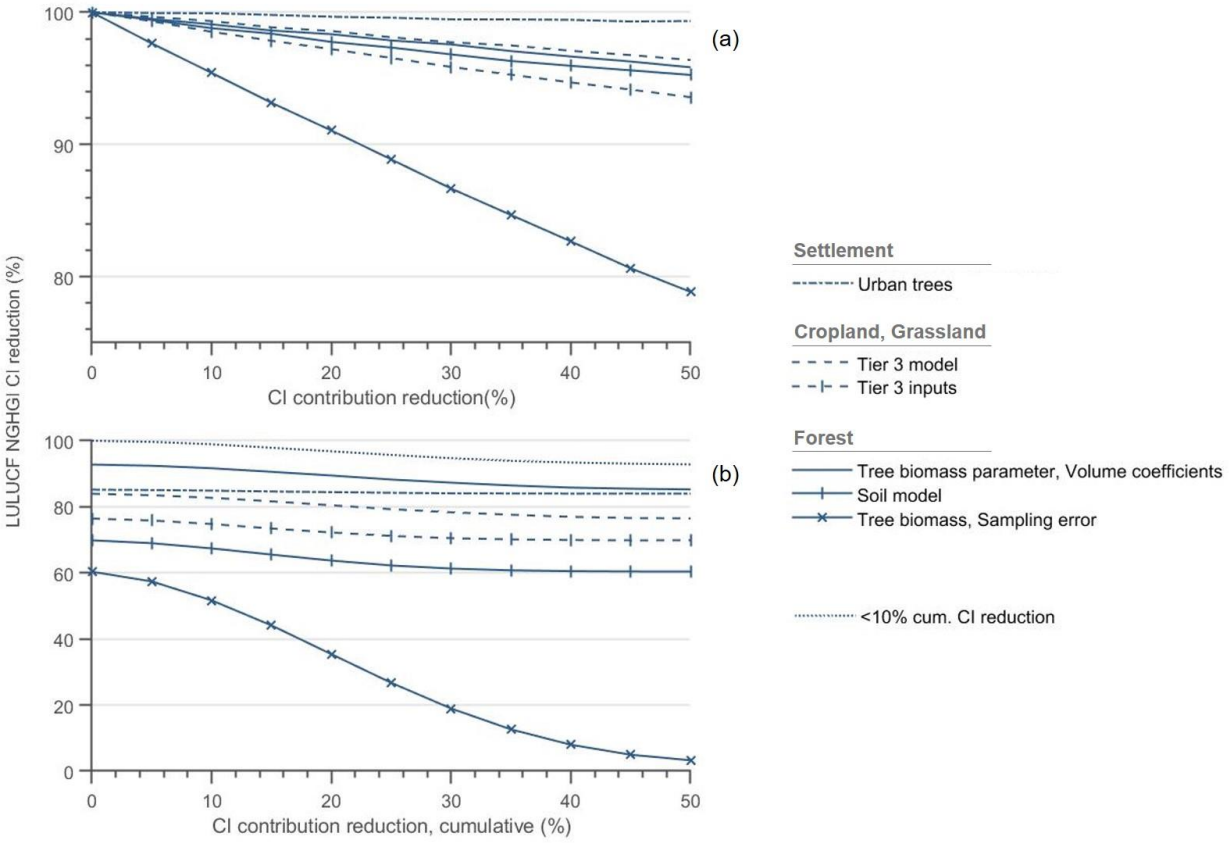

Fig. 2. Inventory uncertainty reduction potential. Percent reduction in LULUCF NGHGI 95% confidence interval (CI) magnitude (97.5% upper bound – 2.5% lower bound) given reduction in uncertainty contribution for each uncertainty element or element group. Panel (a): LULUCF uncertainty reduction for each uncertainty element, holding all other element contributions constant. Panel (b): Cumulative LULUCF NGHGI uncertainty reduction if element uncertainty contributions are sequentially reduced by 50%. "<10% cum. CI reduction" refers to uncertainty elements that, in aggregate, reduce LULUCF NGHGI CI magnitude by less than 10% if known with complete certainty. Forest soil model contribution is 255.7 MMT CO_2e.

3.5 Omitted fluxes

In total, we find net emissions of 123 MMT CO_2e could be omitted from the U.S. NGHGI, with the majority occurring on croplands and grasslands (Figure 3). The largest omissions are due

to data gaps in Alaska, where grassland soil carbon stock changes (31 MMT CO_2e) and wetland soil carbon and methane emissions (41 MMT CO_2e) are not currently estimated.

Emissions from settlement mineral soils are not included in the U.S. NGHGI due to a lack of activity data and emissions factors, a challenge that the IPCC acknowledges in allowing this omission as a Tier 1 method (IPCC 2006, 2019). We find settlement mineral soils could emit 35 MMT CO_2e, assuming they are managed similarly to low input cropland (IPCC 2006, 2019).[††] While the low input cropland emissions factor may reasonably reflect dynamics in undisturbed lawns and parks, settlement soils undergo intensive disturbance at irregular intervals, driven by landscaping and land grading, building development, and impervious surface cover, which are unlikely to be captured by cropland emissions factors. However, an emissions factor based on Boston mineral soil emissions suggests the omitted flux value could be much higher (Decina et al. 2016).

The U.S. NGHGI does not currently account for indirect and direct N_2O emissions from federally-owned croplands and grasslands with the exception of pasture, range, and paddock (PRP) sources. Assuming that federal croplands and grasslands emit direct and indirect N_2O at the same per-area rates as non-federal lands, net of PRP N_2O emissions, we find this omission could reach 22 MMT CO_2e.

The largest omitted sink category is microbial methane sequestration in cropland, grassland, and forest soils (-25 MMT CO_2e). However, we note that the soil methane sink is

[††] "Low input" refers to low carbon input management practices, including residue collection and low residue return, residue burning, frequent bare fallow, production of low-residue crops, and no or low mineral fertilization (IPCC 2006).

directly tied to methane's atmospheric lifetime, and is likely already incorporated to some extent in methane global warming potential (GWP) values. The IPCC (2006, 2019) does not yet provide guidance on these issues. If countries decide to include the soil microbial methane sink in NGHGIs, new methods may be needed to align inventory reporting with methane GWP estimates. We do not provide error bars for these estimates to avoid suggesting precision – as described above, these values are generated using highly simplified assumptions about average GHG fluxes over large areas. Our estimates are meant only to provide a basis for prioritizing research and data collection.

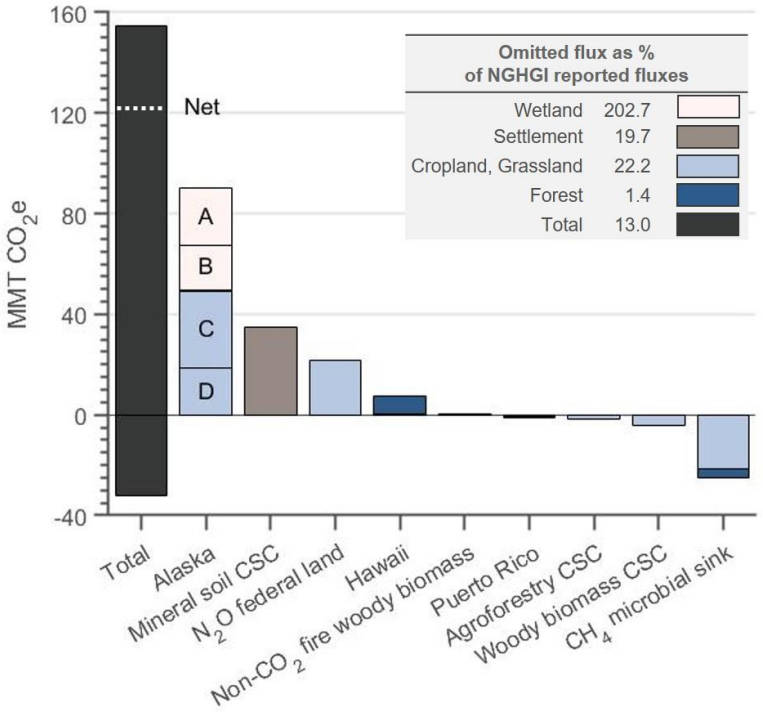

Fig. 3. U.S. NGHGI omitted GHG fluxes. "CSC" = carbon stock change. "Alaska" fluxes labeled as (A) wetland soil CH_4, (B) wetland soil CSC, (C) grassland soil CSC, and (D) agricultural soil management N_2O. "Omitted flux as % of NGHGI reported fluxes" is calculated by summing absolute values of all omitted fluxes by land use category and dividing result by sum of absolute values of all fluxes for that land use category as reported in U.S. NGHGI (2018).

4. Discussion

4.1 Comparison to other studies

Our results compare well with U.S. NGHGI Approach 2 key category analysis, which ranks source and sink categories, as defined by UNFCCC common reporting format (CRF) guidelines, by their one-direction 95% CI magnitude (IPCC 2006, 2019). The top five LULUCF key categories as identified using Approach 2 encompass the largest uncertainty elements identified in Figure 2 (U.S. NGHGI 2018).

However, our analysis provides important additional detail. For example, "Net CO_2 Emissions from Settlements Remaining Settlements" is the second ranked key category, while our analysis finds that addressing DayCent model uncertainty would have a larger impact than focusing on urban trees. This inconsistency is due to the fact that the DayCent model is used across nine different CRF key categories. Thus, uncertainty attribution analysis can usefully focus on highly ranked CRF key categories, as long as cross-cutting uncertainty elements are recognized. It is difficult to compare uncertainty attribution results across studies, since they vary widely in scope and structure. However, our findings are consistent with studies that suggest design-based sampling error outweighs allometric model uncertainty (Breidenbach et al. 2014, Ståhl et al. 2014, McRoberts et al. 2016), that forest soils are a large source of uncertainty (Peltoniemi et al. 2006, Monni et al. 2007b), and that N_2O emissions drive uncertainty in croplands and grasslands (Winiwarter and Muik 2010, Ramírez et al. 2008, Monni et al. 2007a, Petrescu et al. 2020).

4.2 Opportunities for inventory improvements

Countries looking to improve LULUCF GHG estimation methods can take advantage of existing research, data gathering, and model development targeting the largest uncertainty elements identified above.

Forest sampling error

Increasing the sampling rate or number of plots in existing forest inventories is a costly option for reducing sampling error. Rather, research has increasingly focused on using remote sensing data like LiDAR or radar to generate wall-to-wall forest biomass estimates (e.g., Blackard et al. 2008, McRoberts et al. 2016, Ma et al. 2021). Model-assisted estimators that utilize LiDAR and plot data have increased aboveground forest biomass precision by 2.5-6 times compared to plot-based simple random sample or post-stratified estimators (McRoberts et al. 2013, Gregoire et al. 2016, McRoberts et al. 2016). Historically, the necessary LiDAR and radar data has been costly to collect and only intermittently available over space and time, but new and planned global LiDAR and radar missions, including GEDI, ICE-Sat2, and NISAR, have the potential to greatly improve LULUCF monitoring precision and to help align aboveground biomass monitoring methods across countries (Duncanson et al. 2020, Babcock et al. 2018). Ongoing availability of LiDAR or radar data will be critical to ensure countries can sustain new LULUCF monitoring methods.

Care must be taken in comparing precision of plot-based and remote sensing-based methods. Countries with national forest inventories tend to use design-based or probability-based

statistical inference to estimate forest carbon fluxes, assuming that uncertainty is a function of the probability of selecting a given sample (observations are considered constant). When using remote sensing-based models, analysts may instead choose model-based inference, assuming that uncertainty is driven by a population probability distribution (observations are realizations of a random variable) (McRoberts 2010). It is not valid to rank precision across the two methods due to different assumptions about the source of randomness (McRoberts et al. 2013). Inventory compilers are therefore encouraged to clarify inference frameworks used to ensure uncertainty reporting transparency.

Annually-updated remote sensing data products can help address concerns that land cover and land use changes are not reflected in LULUCF flux estimates, a source of uncertainty that we were not able to evaluate in this paper due to data constraints. For example, the 2018 U.S. NGHGI uses the 2011 National Land Cover Database (NLCD) to stratify eastern Texas forest by canopy cover. Though individual plots could capture disturbance after 2011, spatial weights would reflect only area disturbed prior to 2011. As a result, large changes in U.S. forest GHG fluxes would not be reflected in the inventory for up to five years under current stratification methods. To address this issue, the United States has begun generating annual NLCD updates to more closely monitor land use change (LCMAP 2021, LCMS 2021).

Tree-level biomass estimation

We find a higher contribution from allometric model uncertainty compared to other studies (e.g., McRoberts et al. 2014, Breidenbach et al. 2014, Ståhl et al. 2014), possibly due to our assumption that allometric parameters are assigned by tree species or species group for each

Monte Carlo iterate rather than to individual trees. This approach was chosen for its computational efficiency and mimics a high degree of positive covariance between individual trees of the same species or species group, but results in higher variance of forest carbon stocks across Monte Carlo iterates than studies that assume independence at tree-level.

Tree-level biomass estimates are an important input to remote sensing models, and so will be key to inventory methods even as remote sensing data is increasingly utilized. Challenges to allometric model improvements include: inconsistent methods in biomass measurement field studies (Weiskittel et al. 2015); a dearth of data and models for estimating belowground biomass (Russell et al. 2015); a lack of accounting for impacts of climatic variables on tree density and other allometric parameters over time (Clough et al. 2016); and a lack of species-specific or region-specific data and incomplete or non-random samples across studies (Jenkins et al. 2003).
In an effort to address some of these challenges, the U.S. Forest Service has compiled the Legacy Tree Data platform, which contains over 15,000 individual tree biomass measurements (Radtke et al. 2015). However, to address the climatic dependency of tree variables and to fully address the data limitations described above, ongoing data collection and targeted research programs are required.

Cropland and grassland fluxes

Our expert elicitation survey asked respondents to rank research, modeling, and data priorities, as identified in the literature, for reducing uncertainty in cropland and grassland Tier 3 GHG flux estimates (SM Table 2-18).

Survey respondents noted that they were keen to have more empirical data in order to improve and validate existing soil models (Schmidt et al. 2011, Spencer et al. 2011). They acknowledged the difficulties in modeling such a complex system but noted that more data is the primary way to help reduce both input and structural uncertainty. For example, the NRI plot system, which provides key inputs to DayCent, could form the basis of a national soil carbon monitoring network, similar to FIA plots for forests. The U.S. NGHGI notes that the U.S. Department of Agriculture (USDA) is developing a national soil monitoring network (U.S. NGHGI 2018), but it is unclear the extent to which this framework will address limitations identified in this study – particularly, the input uncertainty driven by lacking model output (GHG fluxes) and model input observations at the same plots.

Survey respondents also indicated that increased collaboration among model developers would help refine soil carbon flux predictions (Paustian et al. 2016, Schmidt et al. 2011). Increased inter-model comparison, model validation, and collaboration were highly ranked as opportunities to reduce uncertainty (Brevik et al. 2015, Stockmann et al. 2013).

4.3 Application to other countries

Other countries with similar land cover and NGHGI methods can use U.S.-based uncertainty attribution to inform priorities for further analysis. For example, most of the world's forest area is now covered by strategic forest inventories, with many countries utilizing statistical sampling methods similar to the United States (McRoberts et al. 2010). Large forested countries continue to develop systems to increase precision and accuracy of forest carbon stock estimates, particularly in response to REDD+ financing programs (Brazil NC4 2020, Tewari et al. 2020,

Zeng et al. 2015). For example, as part of the Estimativa de biomassa na Amazonia (EBA) program, Brazilian researchers are working to integrate forest plot data, allometric models, and remote sensing (both LiDAR and Landsat) data to estimate landscape-scale aboveground forest biomass (INPE 2021). Many of the same uncertainty elements described above are relevant to countries developing such systems.

There is more international heterogeneity in non-forest flux estimation methods, with many non-Annex I countries omitting these inventory categories entirely (Smith et al. 2020). Other countries may use results from this paper to inform priorities for expanding inventory coverage. Several of the omitted fluxes identified here will be relevant for all other countries, given current IPCC (2006, 2019) inventory guidance, including the soil microbial CH_4 sink and settlement mineral soil fluxes.

5. Conclusion

Many countries have deprioritized NGHGI uncertainty estimation and reporting due to lack of data and programmatic resources, as well as the complexity of uncertainty methods. As Brazil indicated in their Third National Communication (2016), "Quantifying uncertainty for individual data items is as or more difficult to assess as the actual information sought." Countries are likely to prioritize improvements in LULUCF accuracy by increasing the use of Tier 3 methods and updating Tier 1 and 2 methods with the most recent science (Yona et al. 2020). However, investments in uncertainty estimation and transparency will also be required as more complex methods are adopted.

NGHGI LULUCF uncertainty is a challenge for many major-emitting countries, and for some, including the United States, is large enough that planned LULUCF emission reductions fall within the margin of estimation error. The analytical framework suggested here is one approach that governments can use to both transparently report uncertainty estimation methods and to identify opportunities for improving NGHGI accuracy and precision, with a view to increasing international confidence in NDC emissions reduction progress.

Using the United States as a case study, we detail the contribution of over 90 LULUCF uncertainty elements and omitted fluxes to uncertainty and bias in the U.S. NGHGI. Most inventory uncertainty is driven by a small set of elements distributed across forestry, cropland and grassland, and settlement land use categories. Omitted fluxes could account for up to 13% of the current LULUCF inventory on an absolute value basis, primarily driven by CO_2 and CH_4 emissions in Alaska and urban mineral soils. Other countries can use these results to inform initial priorities for further analysis, particularly those using similar NGHGI methods or those that plan to take up similar methods in the future.

References

"Third National Communication of Brazil to the UNFCCC (Brazil NC3)" 2016. Ministry of Science, Technology and Innovations. https://unfccc.int/documents/66129.

"Fourth National Communication of Brazil to the UNFCCC (Brazil NC4)" 2020. Ministry of Science, Technology and Innovations. https://unfccc.int/documents/267657.

Andersson, K. et al. 2008. "National Forest Carbon Inventories: Policy Needs and Assessment Capacity." *Climatic Change* 93 (1): 69.

Babcock, C. et al. 2018. "Geostatistical Estimation of Forest Biomass in Interior Alaska Combining Landsat-Derived Tree Cover, Sampled Airborne Lidar and Field Observations." *Remote Sensing of Environment* 212 (June): 212–30.

Blackard, J, et al. 2008. "Mapping U.S. Forest Biomass Using Nationwide Forest Inventory Data and Moderate Resolution Information." *Remote Sensing of Environment* 112 (4): 1658–77.

Breidenbach, J. et al. 2014. "Quantifying the Model-Related Variability of Biomass Stock and Change Estimates in the Norwegian National Forest Inventory." *Forest Science* 60 (1): 25–33.

Brevik, E.C., et al. 2015. The interdisciplinary nature of soil. *SOIL, 1*(1), 117-129.

Bun, R., et al. 2010. "Spatial GHG Inventory at the Regional Level: Accounting for Uncertainty." *Climatic Change* 103 (1): 227–44.

CAIT, WRI. 2021. "Climate Analysis Indicators Tool (CAIT): WRI's Climate Data Explorer." World Resources Institute. http://cait2.wri.org.

Chatfield, C. 1995. "Model Uncertainty, Data Mining and Statistical Inference." *Journal of the Royal Statistical Society.* 158 (3): 419.

Clough, B.J. et al. 2017. "Climate-Driven Trends in Stem Wood Density of Tree Species in the Eastern United States: Ecological Impact and Implications for National Forest Carbon Assessments." *Global Ecology and Biogeography* 26 (10): 1153–64.

Cruz, Florentino B. De la, and Morton A. Barlaz. 2010. "Estimation of Waste Component-Specific Landfill Decay Rates Using Laboratory-Scale Decomposition Data." *Environmental Science & Technology* 44 (12): 4722–28.

Decina, S.M., et al. 2016. "Soil Respiration Contributes Substantially to Urban Carbon Fluxes in the Greater Boston Area." *Environmental Pollution* 212 (May): 433–39.

Del Grosso, S.J, et al. 2000. "General CH_4 Oxidation Model and Comparisons of CH_4 Oxidation in Natural and Managed Systems." *Global Biogeochemical Cycles* 14: 999–1020.

Domke, G.M., et al. 2016. "Estimating Litter Carbon Stocks on Forest Land in the United States." *Science of The Total Environment* 557–558 (July): 469–78.

Domke, G.M., et al. 2017. "Toward Inventory-Based Estimates of Soil Organic Carbon in Forests of the United States." *Ecological Applications* 27 (4): 1223–35.

Duncanson, L., et al. 2020. "Biomass Estimation from Simulated GEDI, ICESat-2 and NISAR across Environmental Gradients in Sonoma County, California." *Remote Sensing of Environment* 242: 111779.

Dutaur, L., and Verchot, L.V. 2007. "A Global Inventory of the Soil CH4 Sink." *Global Biogeochemical Cycles* 21 (4).

Erb, K.H., et al. 2013. "Bias in the Attribution of Forest Carbon Sinks." *Nature Climate Change* 3 (10): 854–56.

Friedlingstein, P., et al. 2020. "Global Carbon Budget 2020." *Earth System Science Data* 12 (4): 3269–3340.

Grassi, G., et al. 2017. "The Key Role of Forests in Meeting Climate Targets Requires Science for Credible Mitigation." *Nature Climate Change* 7 (3): 220–26.

Grassi, G., et al. 2018. "Reconciling Global-Model Estimates and Country Reporting of Anthropogenic Forest CO2 Sinks." *Nature Climate Change* 8 (10): 914–20.

Gregoire, T.G., et al. 2016. "Statistical Rigor in LiDAR-Assisted Estimation of Aboveground Forest Biomass." *Remote Sensing of Environment* 173 (February): 98–108.

Hamal, K. 2010. Reporting GHG emissions: Change in uncertainty and its relevance for detection of emission changes. IIASA Interim Report IR-10-003.

Harmon, M.E., et al. 2015. "Uncertainty Analysis: An Evaluation Metric for Synthesis Science." *Ecosphere* 6 (4).

Harmon, M.E., et al. 2007. "Quantifying Uncertainty in Net Primary Production Measurements." In *Principles and Standards for Measuring Primary Production*. New York: Oxford University Press.

INPE. n.d. "EBA - Estimativa de Biomassa Na Amazônia - Divisão de Impactos, Adaptação e Vulnerabilidades." Accessed April 23, 2021. http://www.ccst.inpe.br/projetos/eba-estimativa-de-biomassa-na-amazonia/.

IPCC. 2006. *2006 IPCC Guidelines for National Greenhouse Gas Inventories*. Edited by H.S. Eggleston, L. Buendia, K. Miwa, T. Ngara, and K. Tanabe. Japan: IGES.

———. 2019. "2019 Refinement to the 2006 IPCC Guidelines for National Greenhouse Gas Inventories." Intergovernmental Panel on Climate Change. https://www.ipcc-nggip.iges.or.jp/public/2019rf/index.html.

Jenkins, J.C., et al. 2003. "National-Scale Biomass Estimators for United States Tree Species," *Forest Science* 49: 12-35.

Jonas, M. et al. 2010. "Comparison of Preparatory Signal Analysis Techniques for Consideration in the (Post-) Kyoto Policy Process." *Climatic Change* 103 (1–2): 175–213.

Jonas, M., et al. 2014. "Uncertainty in an Emissions-Constrained World." *Climatic Change* 124 (3): 459–76.

Larocque, G.R., et al. 2008. "Uncertainty Analysis in Carbon Cycle Models of Forest Ecosystems: Research Needs and Development of a Theoretical Framework to Estimate Error Propagation." *The Importance of Uncertainty and Sensitivity Analysis in Process-Based Models of Carbon and Nitrogen Cycling in Terrestrial Ecosystems with Particular Emphasis on Forest Ecosystems* 219 (3): 400–412.

Leip, A. 2010. "Quantitative Quality Assessment of the Greenhouse Gas Inventory for Agriculture in Europe." *Climatic Change* 103 (1–2): 245–61.

Lieberman, D., et al. 2007. *Accounting for Climate Change: Uncertainty in Greenhouse Gas Inventories - Verification, Compliance, and Trading*. Dordrecht: Springer.

Ma, L., et al. 2021. "High-Resolution Forest Carbon Modelling for Climate Mitigation Planning over the RGGI Region, USA." *Environmental Research Letters* 16 (4): 045014.

Magnussen, S., et al. 2014. "Error Propagation in Stock-Difference and Gain–Loss Estimates of a Forest Biomass Carbon Balance." *European Journal of Forest Research* 133 (6): 1137–55.

McRoberts, R.E., et al. 2013. "Inference for Lidar-Assisted Estimation of Forest Growing Stock Volume." *Remote Sensing of Environment* 128 (January): 268–75.

McRoberts, R.E. 2010. "Probability- and Model-Based Approaches to Inference for Proportion Forest Using Satellite Imagery as Ancillary Data." *Remote Sensing of Environment* 114 (5): 1017–25.

McRoberts, R.E., et al. 2010. "Advances and Emerging Issues in National Forest Inventories." *Scandinavian Journal of Forest Research* 25 (4): 368–81.

McRoberts, R.E., et al. 2014. "A General Method for Assessing the Effects of Uncertainty in Individual-Tree Volume Model Predictions on Large-Area Volume Estimates with a Subtropical Forest Illustration." *Canadian Journal of Forest Research* 45 (1): 44–51.

McRoberts, R.E., et al. 2016. "Hybrid Estimators for Mean Aboveground Carbon per Unit Area." *Forest Ecology and Management* 378 (October): 44–56.

Monni, S., et al. 2007a. "Uncertainty of Forest Carbon Stock Changes – Implications to the Total Uncertainty of GHG Inventory of Finland." *Climatic Change* 81 (3–4): 391–413.

Monni, S., et al. 2007b. "Uncertainty in Agricultural CH4 AND N2O Emissions from Finland – Possibilities to Increase Accuracy in Emission Estimates." *Mitigation and Adaptation Strategies for Global Change* 12 (4): 545–71.

Mooney, C. In press. *Washington Post.*

National Research Council. 2011. "Verifying Greenhouse Gas Emissions: Methods to Support International Climate Agreements." Washington, DC: The National Academies Press.

Nilsson, S., et al. 2007. "Uncertainties of a Regional Terrestrial Biota Full Carbon Account: A Systems Analysis." In *Accounting for Climate Change: Uncertainty in Greenhouse Gas Inventories — Verification, Compliance, and Trading*, edited by Lieberman, et al., 5–21. Dordrecht: Springer Netherlands.

Nowak, D.J., et al. 2008. "A Ground-Based Method of Assessing Urban Forest Structure and Ecosystem Services," 12.

Nowak, D. J., et al. 2013. Carbon storage and sequestration by trees in urban and community areas of the United States. *Environmental Pollution, 178*, 229-236.

Ogle, S.M., et al. 2006. "Bias and Variance in Model Results Associated with Spatial Scaling of Measurements for Parameterization in Regional Assessments." *Global Change Biology* 12 (3): 516–23.

Ogle, S.M., et al. 2010. "Scale and Uncertainty in Modeled Soil Organic Carbon Stock Changes for US Croplands Using a Process-Based Model." *Global Change Biology* 16 (2): 810–22.

Ogle, S.M., et al. 2003. "Uncertainty in Estimating Land Use and Management Impacts on Soil Organic Carbon Storage for US Agricultural Lands between 1982 and 1997." *Global Change Biology* 9 (11): 1521–42.

Paustian, K., et al. 2016. *Climate-smart soils.* Nature*, 532,* 49-57.

Peltoniemi, M., et al. 2006. "Factors Affecting the Uncertainty of Sinks and Stocks of Carbon in Finnish Forests Soils and Vegetation." *Forest Ecology and Management* 232 (1): 75–85.

Petrescu, A.M., et al. 2020. "European Anthropogenic AFOLU Greenhouse Gas Emissions: A Review and Benchmark Data." *Earth System Science Data* 12 (2): 961–1001.

Phillips, D.L., et al. 2000. "Toward Error Analysis of Large-Scale Forest Carbon Budgets." *Global Ecology and Biogeography* 9 (4): 305–13.

Pongratz, J., et al. 2014. "Terminology as a Key Uncertainty in Net Land Use and Land Cover Change Carbon Flux Estimates." *Earth System Dynamics* 5 (1): 177–95.

Pulles, T. 2017. "Did the UNFCCC Review Process Improve the National GHG Inventory Submissions?" *Carbon Management* 8 (1): 19–31.

Radtke, P.J., et al. 2015. "Legacy Tree Data: A National Database of Detailed Tree Measurements for Volume, Weight, and Physical Properties." In *Pushing Boundaries: New Directions in Inventory Techniques and Applications: Forest Inventory and Analysis (FIA) Symposium 2015.*

Ramírez, A., et al. 2008. "Monte Carlo Analysis of Uncertainties in the Netherlands Greenhouse Gas Emission Inventory for 1990–2004." *Atmospheric Environment* 42 (35): 8263–72.

Refsgaard, J.C., et al. 2007. "Uncertainty in the Environmental Modelling Process – A Framework and Guidance." *Environmental Modelling & Software* 22 (11): 1543–56.

Roe, S. et al. 2019. "Contribution of the Land Sector to a 1.5 °C World." *Nature Climate Change* 9 (11): 817–28.

Rogelj, J., et al. 2018. "Mitigation Pathways Compatible with 1.5°C in the Context of Sustainable Development. In: Global Warming of 1.5°C. An IPCC Special Report on the Impacts of Global Warming of 1.5°C above Pre-Industrial Levels and Related Global Greenhouse Gas Emission Pathways, in the Context of Strengthening the Global Response to the Threat of Climate Change, Sustainable Development, and Efforts to Eradicate Poverty."

Russell, M.B., et al. 2015. "Comparisons of Allometric and Climate-Derived Estimates of Tree Coarse Root Carbon Stocks in Forests of the United States." *Carbon Balance and Management* 10 (1): 20.

Rypdal, K. and K. Flugsrud. 2001. "Sensitivity Analysis as a Tool for Systematic Reductions in Greenhouse Gas Inventory Uncertainties." *Environmental Science & Policy* 4 (2–3): 117–35.

Rypdal, K. and W. Winiwarter. 2001. "Uncertainties in Greenhouse Gas Emission Inventories — Evaluation, Comparability and Implications." *Environmental Science & Policy* 4 (2): 107–16.

Schmidt, M.W., et al. 2011. Persistence of soil organic matter as an ecosystem property. *Nature, 478,* 49–56.

Shvidenko, A., et al. 2010. "Can the Uncertainty of Full Carbon Accounting of Forest Ecosystems Be Made Acceptable to Policymakers?" *Climatic Change* 103 (1): 137–57.

Skog, K.E. 2008. "Sequestration of Carbon in Harvested Wood Products for the United States." *FOREST PRODUCTS JOURNAL* 58 (6): 17.

Skog, K.E., et al. 2004. "A Method Countries Can Use to Estimate Changes in Carbon Stored in Harvested Wood Products and the Uncertainty of Such Estimates." *Environmental Management* 33 (S1).

Smith, J.E. and L.S. Heath. 2001. "Identifying Influences on Model Uncertainty: An Application Using a Forest Carbon Budget Model." *Environmental Management* 27 (2): 253–67.

Smith, P. et al. 2008. "Sectoral Approaches to Improve Regional Carbon Budgets." *Climatic Change* 88 (3): 209–49.

Smith, P., et al. 2020. "How to Measure, Report and Verify Soil Carbon Change to Realize the Potential of Soil Carbon Sequestration for Atmospheric Greenhouse Gas Removal." *Global Change Biology* 26 (1): 219–41.

Spencer, S., et al. 2011. Designing a national soil carbon monitoring network to support climate change policy: a case example for US agricultural lands. *Greenhouse Gas Measurement and Management, 1*(3-4), 167-178.

Ståhl, G., et al. 2014. "Sample-Based Estimation of Greenhouse Gas Emissions From Forests—A New Approach to Account for Both Sampling and Model Errors." *Forest Science* 60 (1): 3–13.

Stockmann, U., et al. 2013. The knowns, known unknowns and unknowns of sequestration of soil organic carbon. *Agriculture, Ecosystems and Environment, 164,* 80-99.

Tewari, V. P., et al. 2020. "National Forest Inventory in India: Developments Toward a New Design to Meet Emerging Challenges." In *Statistical Methods and Applications in Forestry and Environmental Sciences*, edited by Girish Chandra, Raman Nautiyal, and Hukum Chandra, 13–33. Singapore: Springer Singapore.

Udawatta, R. P., and Jose, S. 2011. "Carbon Sequestration Potential of Agroforestry Practices in Temperate North America." In *Carbon Sequestration Potential of Agroforestry Systems: Opportunities and Challenges*, edited by B. Mohan Kumar and P. K. Ramachandran Nair, 17–42. Dordrecht: Springer Netherlands.

U.S. Department of Agriculture. 2012. Agroforestry USDA Reports to America, Fiscal Years 201-2012 – Comprehensive Version. Retrieved December 20, 2018, https://www.usda.gov/sites/default/files/documents/usda-reports-to-america-comprehensive.pdf.

U.S. Forest Service. n.d. "Landscape Change Monitoring System (LCMS)." Accessed April 20, 2021. /rmrs/groups/landscape-change-monitoring-system-lcms-science-team.

U.S. Geological Survey. n.d. "Land Change Monitoring, Assessment, and Projection (LCMAP)." Accessed April 20, 2021. https://www.usgs.gov/core-science-systems/eros/lcmap.

UNFCCC. 2015. "Paris Agreement to the United Nations Framework Convention on Climate Change." T.I.A.S. No. 16-1104.

———. 2019a. "Decisions Adopted by the Conference of the Parties Serving as the Meeting of the Parties to the Paris Agreement." FCCC/PA/CMA/2018/3/Add.2.

———. 2019b. "Preparations for the Implementation of the Paris Agreement and the First Session of the Conference of the Parties Serving as the Meeting of the Parties to the Paris Agreement." FCCC/CP/2018/10/Add.1.

US EPA, OAR. 2002. "Quality Assurance/Quality Control and Uncertainty Management Plan for the U.S. Greenhouse Gas Inventory: Procedures Manual for Quality Assurance/Quality Control and Uncertainty Analysis." 430-R-02-007B.

———. 2018, 2019, 2020. "U.S. Greenhouse Gas Inventory Report Archive." https://www.epa.gov/ghgemissions/us-greenhouse-gas-inventory-report-archive.

———. 2021. "Inventory of U.S. Greenhouse Gas Emissions and Sinks: 1990-2019 (U.S. NGHGI 2021)." Reports and Assessments. https://www.epa.gov/ghgemissions/inventory-us-greenhouse-gas-emissions-and-sinks-1990-2019.

Walker, W.E., et al. 2003. "Defining Uncertainty: A Conceptual Basis for Uncertainty Management in Model-Based Decision Support." *Integrated Assessment* 4 (1): 5–17.

Weiskittel, A.R., et al. 2015. "A Call to Improve Methods for Estimating Tree Biomass for Regional and National Assessments." *Journal of Forestry* 113 (4): 414–24.

Winiwarter, W. and B. Muik. 2010. "Statistical Dependence in Input Data of National Greenhouse Gas Inventories: Effects on the Overall Inventory Uncertainty." *Climatic Change* 103 (1–2): 19–36.

Winiwarter, W. and K. Rypdal. 2001. "Assessing the Uncertainty Associated with National Greenhouse Gas Emission Inventories: A Case Study for Austria." *Atmospheric Environment*, 16.

Yanai, R.D., et al. 2019. "Uncertainty in Measurements of Trees in the US Forest Service Forest Inventory and Analysis (FIA) Program." https://agu.confex.com/agu/fm19/meetingapp.cgi/Paper/506321.

Yona, L., et al. 2020. "Refining National Greenhouse Gas Inventories." *Ambio* 49 (10): 1581–86.

Zeng, W., et al. 2015. "The National Forest Inventory in China: History - Results - International Context." *Forest Ecosystems* 2 (1): 23.

2. Conserving carbon: Evaluating term-limited conservation programs

Abstract

I develop a structural model of the landowner decision to participate in a voluntary, term-limited conservation program that constrains the timing of land use change. Allowing for re-enrollment addresses a key literature gap in the evaluation of climate and conservation policy in forestry and agricultural sectors. I focus on the policy objective of managing urban sprawl, a growing contributor to global land use change and greenhouse gas emissions. By accounting for important sources of stochasticity in landowner decision-making and assuming that program re-enrollment is possible, I show that term-limited programs can result in meaningful reductions in environmental impacts through two key mechanisms, (1) by subsidizing agricultural land use ("subsidy effect") and (2) by shielding agricultural parcels from spikes in real estate prices ("shield effect"). Parameterizing the model to agricultural profits and historical real estate prices in Santa Clara County, California, I show that the cost-minimizing conservation program, as defined by its incentive level and contract length, varies over time and balances the trade-off between conserving enrolled land for longer periods and reducing landowner willingness to enroll.

1. Introduction

Land use and land use change activities generate a large portion (11%) of global anthropogenic greenhouse gas (GHG) emissions, largely through conversion of forests and natural landscapes to higher carbon-intensity uses (IPCC 2022). Adjusting patterns of land use change is expected to contribute significantly to future GHG reductions: the first round of country pledges under the United Nations (U.N.) Paris Agreement indicates that land use, land use change, and forestry ac-

tivities would provide 25% of planned GHG reductions leading to 2030 (Grassi et al. 2017). Much of this mitigation potential is expected to result from preserving high carbon stock landscapes, such as primary forest, grasslands, and low-intensity agricultural use, from conversion to more intensively managed land uses like commodity row crop production or urban development. Policy that preserves high carbon landscapes and manages urban and agricultural land expansion is therefore often discussed or implemented as a complement to climate policy in fossil fuel-intensive sectors.

Yet much of the economics literature has not accounted for the political, administrative, and logistic realities of policies used to manage GHG emissions from land use and land use change. This paper addresses an important literature gap by developing a structural model of the landowner decision to participate in voluntary, term-limited incentive programs that constrain their land use choice, the primary approach to land sector climate policy used globally to date. In this study I focus on a particular category of land use change that is a growing contributor to global GHG emissions, urban sprawl (IPCC 2019).

Urban sprawl is referred to in the literature as low-density, non-contiguous development around an urban center (Irwin and Bockstael 2002). There is debate in the economic literature about whether such a development pattern might be socially optimal – after all, dynamic decision making by landowners may result in large areas around the urban center being held in reserve for future development even in efficient markets, creating scattered urban development over time (Mill 1981). However, many studies have identified the presence of spatial spillovers and environmental impacts that are external to land prices, including congestion, higher costs of delivering public services, loss of public environmental amenities, and higher GHG emissions compared to denser urban development, all of which suggests unmanaged urban expansion can result in socially suboptimal outcomes (Irwin and Bockstael 2002, Fujita 1976, Wheaton 1982, Mills 1981).

GHG emissions due to urban sprawl occur both at the land conversion event, during which carbon stocks in trees and soil can be emitted as CO_2 to the atmosphere (if combusted, non-CO_2 emissions may be emitted as well), and following the conversion event, as any additional emissions that occur on the developed parcel that would not have occurred if the land had been maintained in the previous use. As one might imagine, quantifying the amount of additional emissions due to urban sprawl compared to denser development is complex. For example, if an agricultural plot is converted to residential use, new emissions will result from electricity, natural gas, vehicle

miles traveled (VMT) and other residential activities, but these emissions must be compared to a counterfactual scenario in which that land conversion might occur in some other area which could result in greater or fewer GHG emissions. Given this complexity, I focus the analysis below simply on the amount of development avoided on agricultural parcels, and leave the analysis of a more complete set of social and private costs and benefits of avoided development to future research.

Permanent conservation easements have received significant theoretical and empirical attention in the environmental, agricultural, and land use economics literature, including with respect to their impact on urban development patterns, optimal timing of landowner development, and property values (Plantinga 2007, Towe et al. 2010), evaluation of how landowner and parcel characteristics influence the decision to enroll (Lynch and Lovell 2003), spatial spillovers in the decision to enroll (Zipp et al. 2017, Lawley and Yang 2015), the price of conservation as reflected in after-tax donation values of easements (Parker and Thurman 2019), and the amount of adverse selection (or protection of parcels at low risk of development) present in such programs (Stoms et al. 2009, Denning et al. 2010).

Term-limited conservation programs have also been evaluated in the literature, but only as applied to agriculture and forestry management choices. To the best of my knowledge, no paper has evaluated term-limited programs as a mechanism for managing land use change in general or urban sprawl in particular, likely because to date no programs have been implemented with this objective and because incentive levels in existing programs are too low to influence development rates in areas where residential rents are high. For example, in the United States, the Conservation Reserve Program (CRP) has been studied extensively as an agri-environmental program that enrolls landowners in 10-15 year contracts which prohibit intensive crop management or development. In exchange enrolled landowners receive incentive payments consistent with land rental rates in their county. Previous research has looked at supply curves for conserved acres using CRP incentive payments across counties (Plantinga et al. 2001), the performance of the CRP compared to a program that maximized the number of protected acres for the same budget (Feng et al. 2003), the effect of CRP enrollment on land values (Taylor et al. 2020), and landowner bidding behavior during iterations of the CRP that required landowners to indicate their required land rental payment (Kirwan et al. 2005). In a recent paper, Cramton et al. (2021) used a laboratory experiment to evaluate how caps on CRP bids impacts landowner enrollment and program efficiency.

Under the Williamson Act, California has a term-limited conservation program that allows landowners to encumber their land from development for rolling 10 year commitments in exchange for receiving a property tax evaluation consistent with agricultural use. Other than occasional case studies and statistical analysis (Stewart and Duane 2009), to my knowledge there has been no evaluation of the efficacy of the Williamson Act on avoiding agricultural land conversion.

Others have evaluated the theoretical efficacy of term-limited conservation contracts in the context of biodiversity protection (Lennox and Armsworth 2011, Juutinen et al. 2014, Dreschler et al. 2017), soil carbon payments (Gulati and Vercammen 2005), and in generic environmental protection settings (Glebe 2022, Ando and Chen 2011).

However, few studies to date have structurally motivated the landowner choice to participate in voluntary conservation programs or evaluated the effect of program design choices on both landowner behavior and net environmental impacts. Some have argued in passing that term-limited conservation programs would have limited effect on land use change patterns like urban development due to the ability for agents to enroll while they wait for the optimal development time (Parker and Thurman 2018). However, I show below that, by accounting for stochasticity in real estate markets and assuming that program re-enrollment is possible, term-limited programs can have meaningful reductions and delays in environmental impacts through two key mechanisms, by subsidizing agricultural land use and by shielding agricultural parcels from spikes in real estate prices.

There are several motivations for evaluating term-limited, voluntary conservation programs. First, conservation programs are a significant budgetary outlay for federal, state, and local governments, whether through direct payments to landowners through programs like CRP or local conservation easement programs that compensate landowners for forfeited development rights, or through reductions in tax revenue as compensation for donated easements. Conservation easements comprise one quarter of global conservation finance flows annually (NatureVest 2014). Given the large public financial commitment to land conservation, evaluating the performance of these programs and identifying opportunities for increasing cost-effectiveness should be policy priorities.

Second, many studies have identified contract length as a driver of landowner willingness to enroll. As I will describe in more detail below, the contract length represents the amount of time during which the enrolled landowner's land is encumbered. Mitani and Lindhjem (2022)

performed a meta-analysis of stated and revealed preference research on forest conservation program participation. They found 26 papers published over 1983-2018 that reported program contract length or evaluated the role of contract length on landowner enrollment, and show contract length significantly impacts program participation rates. Counterintuitively, permanent contracts exhibit higher participation rates than term-limited contracts. They do not provide an economic motivation for their findings.

Mamine et al. (2020) carried out a similar meta-analysis of survey-based discrete choice experiments applied to landowner's willingness to accept an agricultural preservation contract. They find 34 studies published between 2006-2019 that evaluate the effect of contract length on landowner enrollment choice while 117 studies evaluate the effect of incentive levels. While 20 of the 34 studies find that increasing contract length has a negative effect on enrollment, the remainder find positive (6 papers) or nonsignificant (5 papers) effects. Similarly, only 69% of reviewed studies find that increasing incentive levels has a significantly positive effect on enrollment, while 22% find a significantly negative effect.

Few studies provide a robust analytical motivation for the effect of contract length on landowner willingness to enroll. In a very informative paper for this exercise, Glebe (2022) derives a landowner's optimal sequences of bids in a repeated conservation auction, assuming a winning bid would enroll the landowner in a term-limited contract that results in annual operational and opportunity costs. These costs are assumed to be known by the landowner with certainty, but the landowner is uncertain about the maximum bid to be accepted in any given auction (cutoff bid). Through this model, Glebe (2022) shows that longer contract length (as exogenously set by the auctioneer) will increase the landowner's optimal bid, to compensate for increasing operational and opportunity costs. Through numerical analysis, they show that the cost-minimizing contract length for achieving some target area of enrollment depends on landowners' perceived uncertainty in the cutoff bid – for high (low) uncertainty, higher (lower) contract length is more cost-effective, conditional on the landowner belief that the cutoff bid follows a uniform distribution.

Ando and Chen (2011) develop a simple theoretical model of the landowner choice to enroll in a conservation program that prevents a landowner from earning farming income, and derive optimal contract length (such that the discounted present value of environmental benefits across all parcels is maximized, constrained by a conservation budget) through simulation. They find

a similar tradeoff to what I describe below: longer contract lengths require a higher lump sum payment to incentivize enrollment. For a given incentive level, increasing contract length will increase the total environmental benefits delivered for a single enrolled parcel, but total enrollment will be lower. They do not account for changing trends or non-stationarity in the expected value of farming or the possibility for alternative land uses, nor do they endogenously account for optimal timing of landowner enrollment – rather their setting assumes some landowners will optimally choose enrollment and others will not for all time periods.

To address limitations in this literature, I propose a dynamic programming model structure tailored to representing voluntary, term-limited conservation programs and that can predict program impacts under various incentive levels and contract lengths over policy-relevant regions. I focus on the policy case of a term-limited conservation program that pays landowners an incentive for every enrolled acre-year in exchange for committing to agricultural or non-developed land use. I assume that individual landowners are able to optimally choose, with respect to total net returns to land use, when and whether to enroll in the program, as well as when to optimally sell their parcel to a developer, assuming that real estate prices evolve stochastically over time.

I expand on the model structures in Glebe (2022) and Ando and Chen (2011) in a number of ways. First, I relax the assumption that enrolled landowners incur fixed annual costs and instead assume that the opportunity cost of conservation program enrollment occurs as constraint on land use change – this model setup is of interest for policymakers that seek to preserve agricultural land in the face of development pressure. I also assume that the opportunity cost is uncertain, consistent with volatile real estate markets.

I parameterize the agricultural profits and real estate market in this problem to a particular region of policy interest, Santa Clara County, California. Home to Silicon Valley, Santa Clara boasts the fifth largest county-level GDP in the United States (BEA 2020). Skyrocketing real estate values and suburban sprawl, driven by population and economic growth in the technology sector, put significant development pressure on the County's agricultural and open space land. Agriculture contributes $830 million annually to the County's economy (Santa Clara Valley Agricultural Plan 2018). Over 63,000 acres have been identified as at-risk of development in the next 30 years, or 26% of Santa Clara's active farmland and rangeland (Batker et al. 2014). County planners and agricultural and environmental stakeholders are concerned that rapid development will irreversibly

degrade local rural culture and make remaining agricultural operations more costly through disturbance restrictions, loss of agricultural infrastructure, and congestion (Towe 2010, Parker and Meretsky 2004, Irwin and Bockstael 2002). In the model developed below, parcel characteristics, landowner returns to agriculture and developed use, and real estate market trends and volatility are tailored to Santa Clara County data.

1.1 Economic models of land use change and conservation applications

A variety of economic models have been developed over the last several decades in an attempt to make predictions about how carbon prices and conservation policy might influence land use patterns, operating at different geographic scales and to accommodate different policy structures and spatial and market interactions. I briefly describe the main model structures employed in the literature and explain how the approach used in this paper is a useful and novel addition to existing economic land use models.

1.1.1 Partial equilibrium models

Partial equilibrium models covering large geographic areas have been frequently used by U.S. federal policymakers to evaluate the potential contribution of land use and land use change to future GHG reductions. For example, the Forest and Agricultural Sector Optimization Model-GHG (FASOM-GHG), the Global Timber Model (GTM), and the U.S. Agricultural Sector Model (USMP) have guided high-profile policy deliberations over the past two decades, including the Waxman-Markey cap-and-trade bill (Murray et al. 2005), the EPA Biogenic CO_2 Accounting Framework (U.S. EPA 2019), and the U.S. Mid-Century Strategy for Deep Decarbonization (White House 2016). These models optimize over welfare surplus in forestry and agriculture markets and include a variety of control variables for land use and management choices, including area of land devoted to commercial forestry or various crop types, timber rotation lengths, and reductions in GHG emissions due to fertilization, tillage, and other agricultural practices.

In a recent policy application, Hultman et al. (2021) finds that land use, land use change, and forestry (LULUCF) could sequester a net 1,000 MMT CO_2e by 2030, contributing approximately 6% of the GHG reductions needed to reduce U.S. emissions by 51%. This estimate is based on 15 studies published since the year 2000 that use agriculture and forestry partial equilibrium models

to estimate 106 scenarios of national LULUCF GHG reductions over 5-20 years. A large majority (78) of these scenarios assume a universal, compulsory price on GHG emissions can be applied to LULUCF activities, which in the context of these models assumes that every U.S. landowner would receive an incentive for every ton of CO_2e sequestered in soils or biomass and a fee exacted for every ton of CO_2e emitted (Murray et al. 2005, Schneider and McCarl 2002, Schneider and McCarl 2003, Alig 2010, Haim et al. 2014, Haim et al. 2015, Jackson and Baker 2010, Latta et al. 2011, Cai et al. 2018, Wade et al. 2021). The remainder of the scenarios (28) account for the voluntary nature of carbon incentive programs, assuming that landowners will only enroll in carbon incentive programs if it is profit maximizing (Lewandrowski et al. 2004, Latta et al. 2011, Dumortier 2013). However, there are several limitations in how voluntary programs are represented in partial equilibrium models to date; studies have either assumed that reversals (GHGs emitted due to conservation practice abandonment after the conclusion of the program contract) or breach of contract is impossible (Lewandrowski et al. 2004, Dumortier 2013) or they assume that reversals or breach of contract will be taxed at the carbon price, similar to the compulsory setting (Latta et al. 2011).

None of the studies discussed here account for the political reality that existing programs for incentivizing GHG reductions in agriculture and forestry sectors are structured as term-limited conservation programs, and that reversals are not penalized at the conclusion of the contract, consistent with programs like CRP and EQIP. In the model I present below, individual landowners across a given region choose whether or not to participate in a term-limited conservation program over time, and may reverse conservation practices at the conclusion of the contract or re-enroll.

1.1.2 Discrete choice models

Many studies have utilized a discrete choice modeling framework to predict the probability of land use change given returns to different land uses as well as regional, landowner, and plot-level characteristics. To represent climate policy, the value of a carbon incentive can be added or subtracted to the profits derived from each land use or management practice. For example, Lewis and Plantinga (2007) and Lubowski et al. (2006) train nested logit models of land use change on historical observations of land use and agricultural, forestry, and residential rental rates. They then calculate the increase in returns to forestry under a variety of carbon prices and use the estimated

logit parameters to predict total U.S. forest area and GHG reductions across policy scenarios. Other studies have used similar methods to evaluate conservation policies as represented by subsidies for agriculture and forestry (Plantinga and Ahn 2002), to evaluate the additionality of forest carbon offset policies compared to a business-as-usual case (Mason and Plantinga 2013), to predict the likelihood of landowner enrollment in conservation programs (Lynch and Lovell 2003, Langpap 2004), and to downscale the discrete choice model predictions to individual parcels, allowing for spatially-explicit results (Nelson et al. 2008).

Many of these discrete choice studies take an essentially static approach, assuming that landowners make land use choices based on current prices and profits or an infinite future flow of profits based on current prices, and will convert land uses as soon as the NPV of one exceeds another (usually conditional on some unobservable shock). In general, the model is cross-sectional, evaluating land use change between two historical time steps. De Pinto and Nelson (2009) note that this approach is likely to suffer from omitted variable bias, since landowners are likely to make land use decisions on a dynamic basis and so will care about future returns to land use. To address this problem, De Pinto and Nelson (2009) incorporate landowner expectations of prices into the discrete choice model, assuming agricultural prices are generated by a first order autoregressive process. They find that incorporating dynamics into the discrete choice structure strongly improves land use change predictions and, on balance, reduces the estimated likelihood of land use change compared to standard multinomial and mixed logit specifications, perhaps due to the fact that explicit representation of option value in the economic model better controls for landowner choices to delay land conversion.

The primary challenge with the discrete choice approach to modeling the effects of carbon pricing or environmental protection programs is that these programs generally do not take the form of a pure subsidy or increase in market returns to a given land use. Rather, carbon offsets or conservation programs will provide an incentive payment in exchange for some term-limited constraint on land use or management practices. These types of constraints are not easily represented in the discrete choice structure, particularly because time, and therefore contract length, is not explicitly represented in the model. In the methods I outline below, the term-limited constraint on enrolled landowner behavior can be explicitly represented. As a result, we might expect more pessimistic estimates of landowner responses to environmental incentives than what is found in the discrete

choice literature.

1.1.3 Real options, duration models

Land use change is also frequently modeled using a real options approach, recognizing that landowners have the option to convert an agriculture or forest parcel to developed use which can be postponed but, once exercised, is irreversible or comes with large sunk costs (Schatzki 2003, Power and Turvey 2010). The real options framework accounts for the value of this option, and its dynamics over time, in landowner choices. These methods are particularly useful in representing stochastic land markets or commodity prices, sources of uncertainty which encourage landowners to wait to gather more information before making irreversible investments.

The real options literature has found option value is likely to be a large driver of landowner decision-making. Schatzki (2003) indicates option value could account for up to 81% of expected agricultural land asset value in Georgia. Towe et al. (2008) use a duration model to find that the mere existence of a permanent conservation easement program can delay agricultural land conversion by an average of six years, by providing an alternative investment option to landowners. Wrenn et al. (2017) use similar methods to identify the effect of housing prices on the likelihood of agricultural parcel development, controlling for housing price endogeneity using an instrument of distant neighborhood characteristics. Vercammen (2019) argues that development value uncertainty can delay both the decision to develop as well as the decision to enroll in the easement.

The primary limitation of the real options literature is the focus on permanent as opposed to term-limited conservation programs, which greatly simplifies the modeling approach required because there is no need to account for the option to re-enroll or reverse land use decisions after the contract term. I show how the more flexible dynamic programming approach outlined below can fully account for more complex program structure.

1.1.4 Agent-based models

The fields of geography, urban planning, and land systems science have developed a variety of spatially-explicit land use change models, such as agent-based models (ABMs), to explain and predict land use change patterns under various ecological, policy, and economic scenarios (Kim et al. 2020, Verburg et al. 2019). ABMs are occasionally combined with a cellular automaton

model but prioritize the representation of individual economic actors (e.g., landowners, developers, households) through (sometimes heterogeneous) utility and profit functions, modeling agent-to-agent negotiations to derive emergent properties of regional real estate and land markets (Chen et al. 2011, Chen et al. 2021, Parker and Filatova 2008, Parker and Meretsky 2004, Filatova 2015, Magliocca et al. 2015). Given the flexibility to represent individual utility and profit functions, ABMs are able to represent equilibrium as well as non-equilibrium dynamics, spatially-explicit results, and spatial spillover effects. However, to date no ABM has represented the potential for landowners to choose timing of land conversion optimally given beliefs about future land prices – to the best of my knowledge, ABM studies have exclusively assumed that landowner reservation prices are calculated from current agricultural rents and that they will sell land to the developer with the highest bid as soon as the reservation price is exceeded.

In summary, I propose a model structure that can address gaps in the land use model literature by explicitly representing the landowner choice to participate in a term-limited, voluntary program, deriving landowner reservation prices from dynamic economic theory and accounting for important sources of stochasticity and heterogeneity across landowners. Allowing for the possibility to perpetually re-enroll in the conservation program, I derive important differences in total program effects compared to a one-shot enrollment setting.

2. Analytical Motivation

2.1 Agricultural landowner optimal stopping problem

Here I describe the landowner problem of whether to participate in a term-limited, voluntary conservation program. Starting with the simplest case, in the absence of the option to participate in a conservation program, I assume a risk-neutral agricultural landowner must decide when to stop receiving a constant stream of agricultural profits and sell their parcel to a developer, at which time they receive a lump sum payment for the parcel value and move away. The developer's willingness to pay evolves over time according to a stochastic process. I focus on the stochasticity of land prices rather than agricultural profits for analytical clarity and due to the noted volatility of land prices in the literature (2.8 times as volatile as real GDP) (Power and Turvey 2010).

As noted by Capozza and Helsley (1989) and Plantinga et al. (2002), this is a standard optimal

stopping problem, shown in Equation (1).

$$V(t) = \max_t E_t[\int_0^t \pi_A e^{-rs} ds + P(t)e^{-rt}] \tag{1}$$

where:

π_A = constant agricultural profit

r = risk-free interest rate

$P(t)$ = developer's willingness to pay for parcel

I assume $P(t)$ is exogenous to the landowner's decision and follows a geometric Brownian stochastic process, with $p(t) = ln(P(t))$ defined as a function of constant positive parameters g (drift) and σ^2 (variance) and standard Wiener process $W(t)$:*

$$p(t) = gt + \sigma W(t). \tag{2}$$

The solution to this problem is characterized by a constant optimal reserve price P^*, the price at or above which the landowner would optimally sell their parcel to the developer, which will be reached at some uncertain optimal stopping time, $t^* = \{min(t : P(t) \geq P^*)\}$, with expectation $E_t[t^*]$. Dixit and Pindyck (1994) show that the necessary assumptions for the existence of P^* are: (1) that $\pi_A - (r-g)P(t)$ is monotonically decreasing in $P(t)$, which holds if $r \geq g$, and (2) that the $P(t)$ process exhibits positive persistence of uncertainty, which we have by the normal distribution and constant variance of $W(t)$ increments.†

I solve for P^* explicitly using methods from Capozza and Helsley (1989). First I rewrite the expectation in Equation (1) as:

$$E_t[\frac{\pi_A}{r} + (P(t) - \frac{\pi_A}{r})e^{-rt}]. \tag{3}$$

Conditioning Equation (3) on P^* and initial value $P(0)$, both of which are deterministic, Equation (3) becomes:

*A Wiener process is the continuous-time analogue of a random walk, or the sum of infinitesimally small, independent, and normally distributed increments. A standard Wiener increment is distributed with mean 0 and variance equal to the length of the increment: $W(t+s) - W(t) \sim N(0, s)$ (Karlin and Taylor 1975).

†Equation (7) indicates an even stricter assumption on parameters r, g, and σ^2 is required for the existence of P^*.

$$\frac{\pi_A}{r} + (P^* - \frac{\pi_A}{r})E_t[e^{-rt^*}|P^*, P(0)]. \tag{4}$$

The distribution of t^* under Brownian motion is known, so the expectation can be written as (Karlin and Taylor 1975, pg. 364):

$$E_t[e^{-rt^*}|P^*, P(0)] = e^{-\alpha(ln(P^*)-ln(P(0)))} = \left(\frac{P(0)}{P^*}\right)^{\alpha}. \tag{5}$$

where:

$$\alpha = \frac{(g^2 + 2\sigma^2 r)^{\frac{1}{2}} - g}{\sigma^2}.$$

Now I rewrite Equation (1) as a maximization problem over P^* and use the first order condition to find P^* as a function of parameters.

$$V(P^*) = \max_{P^*} \frac{\pi_A}{r} + (P^* - \frac{\pi_A}{r})\left(\frac{P(0)}{P^*}\right)^{\alpha}, \tag{6}$$

$$P^* = \frac{\pi_A}{r}\frac{\alpha}{\alpha - 1}. \tag{7}$$

For P^* to exist, α must be greater than 1 and the interest rate must be larger than the price growth rate, such that $r > g + \frac{1}{2}\sigma^2$. The landowner will wait until the developer is willing to pay the value of an infinite stream of agricultural profits ($\frac{\pi_A}{r}$) multiplied by a term representing the additional value that can be accrued by waiting for the price to increase ($\alpha/(\alpha-1)$). This term, and therefore P^*, is increasing in price drift (g) and variance (σ^2). Equation (5) shows that, consistent with intuition, the expected time to reaching P^* increases with P^*.

2.2 Landowner conservation program enrollment choice, one-shot enrollment

In the next two sections I provide novel analysis by incorporating the choice to participate in a term-limited, voluntary conservation program. If the landowner chooses to enroll in the conservation contract, they receive a constant incentive value c, but in exchange they are not able to sell their parcel for the length of the contract J. In the one-shot setting, I assume that the landowner must decide whether to enroll at $t = 0$ and can only enroll once. The three choice variables in this

problem are δ, which determines whether the landowner enrolls or not; t_0, which is the optimal stopping time if the landowner is not enrolled; and t_1, which is the optimal stopping time if the landowner is enrolled. The problem becomes:

$$\begin{aligned} V(\delta, t_0, t_1) = \max_{\delta, t_0, t_1} (1-\delta) E_t[\int_0^{t_0} \pi_A e^{-rs} ds + P(t_0) e^{-rt_0}] \\ + \ \delta E_t[\int_0^{J} (\pi_A + c) e^{-rs} ds + \int_J^{t_1} \pi_A e^{-rs} ds + P(t_1) e^{-rt_1}] \\ \text{s.t.} \quad t_1 \geq J, \quad \delta \in \{0, 1\} \end{aligned} \tag{8}$$

If $\delta = 0$, the landowner has chosen to not enroll and the problem is equivalent to Equation (1). Therefore t_0^* and P_0^* are equivalent to t^* and P^* in the previous section.

If the landowner chooses $\delta = 1$, they will be enrolled in the conservation program from $t = 0$ to $t = J$ and their optimal parcel sale time t_1 will be constrained. Since the only change to problem structure is the constraint on t_1, P_1^* remains a single constant value. However, I must account for the possibility that P_1^* could occur prior to the end of the contract, or more specifically, that $P(J)$ is higher than P_1^*.

For this reason, I rewrite the second line of Equation (8) as a function of $P(J)$ and P_1^* (Equation (9)). From the perspective of $t = 0$, $p(J) = ln(P(J))$ is a normal random variable with the distribution $N(p(0) + gJ, \sigma^2 J)$, so I take the expectation over regions of the $p(J)$ distribution that are less than and greater than $p_1^* = ln(P_1^*)$:

$$\begin{aligned} \frac{\pi_A}{r} + \frac{c}{r}(1 - e^{-rJ}) \ + \ \int_{p_1^*}^{\infty} (e^{p(J)} - \frac{\pi_A}{r}) e^{-rJ} \ f_p(p(J)) dp(J) \\ + \ \int_{-\infty}^{p_1^*} (e^{p_1^*} - \frac{\pi_A}{r}) \ E_t[\ e^{-r(t_1 - J)} \mid p_1^*, p(J)] \ e^{-rJ} f_p(p(J)) dp(J) \\ \text{s.t.} \quad t_1 \geq J \end{aligned} \tag{9}$$

The last term of Equation (9) can be expressed as:

$$\left(\int_{p_1^*}^{\infty} e^{p(J)} \ f_p(p(J))dp(J) - \frac{\pi_A}{r}(1 - \ \Phi(\frac{p_1^* - p(0) - gJ}{\sigma\sqrt{J}}) \right) e^{-rJ} \ =$$

$$\left(\int_{(p_1^* - p(0) - gJ)/\sigma\sqrt{J}}^{\infty} e^{p(0)+gJ+\sigma\sqrt{J}z} \ \phi(z)dz - \frac{\pi_A}{r}(1 - \ \Phi(\frac{p_1^* - p(0) - gJ}{\sigma\sqrt{J}})) \right) e^{-rJ} \ =$$

$$\left(e^{p(0)+gJ+\frac{\sigma^2 J}{2}}(1 - \Phi(\frac{p_1^* - p(0) - gJ - \sigma^2 J}{\sigma\sqrt{J}})) - \frac{\pi_A}{r}(1 - \ \Phi(\frac{p_1^* - p(0) - gJ}{\sigma\sqrt{J}})) \right) e^{-rJ} \tag{10}$$

where:

$\phi(\cdot) =$ standard normal probability density

$\Phi(\cdot) =$ standard normal cumulative distribution function

The second line uses a change of variable from $p(J)$ to standard normal variable z. The expected value of $e^{p(J)}$ is weighted by a value greater than the probability that $p(J) \geq p_1^*$ to account for the fact that the expectation is over the region above p_1^*.

The fourth term of Equation (9) can be expressed as:

$$(e^{p_1^*} - \frac{\pi_A}{r}) \ \int_{-\infty}^{p_1^*} e^{-\alpha(p_1^* - p(J)) - rJ} f_p(p(J))dp(J) =$$

$$(e^{p_1^*} - \frac{\pi_A}{r}) e^{-\alpha p_1^* - rJ} \ \int_{-\infty}^{p_1^*} e^{\alpha p(J)} f_p(p(J))dp(J) =$$

$$(e^{p_1^*} - \frac{\pi_A}{r}) e^{-\alpha p_1^* - rJ} \int_{-\infty}^{(p_1^* - p(0) - gJ)/\sigma\sqrt{J}} e^{\alpha(p(0)+gJ+\sigma\sqrt{J}z)} \phi(z)dz =$$

$$(e^{p_1^*} - \frac{\pi_A}{r}) \ e^{-\alpha(p_1^* - p(0) - gJ - \frac{\alpha\sigma^2 J}{2}) - rJ} \ \Phi(\frac{p_1^* - p(0) - gJ - \alpha\sigma^2 J}{\sigma\sqrt{J}}) \tag{11}$$

Again, the expected value of $e^{-\alpha(p_1^* - p(J))}$ is weighted by a value less than the probability that $p(J) \leq p_1^*$ to account for the fact that the expectation is over the region below p_1^*.

With $p(J)$ integrated out of the problem, I write Equation (9) as a function of only p_1^*:

$$
\begin{aligned}
V(p_1^*) \;=\; & \frac{\pi_A}{r} + \frac{c}{r}(1 - e^{-rJ}) \\
& + \; e^{-rJ}\left(e^{p(0)+gJ+\frac{\sigma^2 J}{2}}(1 - \Phi(\frac{p_1^* - p(0) - gJ - \sigma^2 J}{\sigma\sqrt{J}})) - \frac{\pi_A}{r}(1 - \; \Phi(\frac{p_1^* - p(0) - gJ}{\sigma\sqrt{J}}))\right) \\
& + \; e^{-\alpha(p_1^* - p(0) - gJ - \frac{\alpha\sigma^2 J}{2}) - rJ} \; (e^{p_1^*} - \frac{\pi_A}{r}) \; \Phi(\frac{p_1^* - p(0) - gJ - \alpha\sigma^2 J}{\sigma\sqrt{J}})
\end{aligned}
\tag{12}
$$

I find an expression for p_1^* using the first order condition for maximizing $V(p_1^*)$:

$$
\begin{aligned}
\frac{dV(P_1^*)}{dP_1^*} = & \frac{-e^{-rJ}}{\sigma\sqrt{J}}(e^{p(0)+gJ+\frac{\sigma^2 J}{2}}\phi(\frac{p_1^* - p(0) - gJ - \sigma^2 J}{\sigma\sqrt{J}}) - \frac{\pi_A}{r}\phi(\frac{p_1^* - p(0) - gJ}{\sigma\sqrt{J}})) \\
& + \; e^{-\alpha(p_1^* - p(0) - gJ - \frac{\alpha\sigma^2 J}{2}) - rJ}\Bigg[(e^{p_1^*} - \alpha(e^{p_1^*} - \frac{\pi_A}{r}))\Phi(\frac{p_1^* - p(0) - gJ - \alpha\sigma^2 J}{\sigma\sqrt{J}}) \\
& + \; \frac{1}{\sigma\sqrt{J}}(e^{p_1^*} - \frac{\pi_A}{r})\phi(\frac{p_1^* - p(0) - gJ - \alpha\sigma^2 J}{\sigma\sqrt{J}})\Bigg] \equiv 0
\end{aligned}
\tag{13}
$$

Equation (13) simplifies to:

$$
e^{p_1^*} = P_1^* = \frac{\pi_A}{r}\frac{\alpha}{\alpha - 1} \tag{14}
$$

Therefore, $P_1^* = P_0^* = P^*$, and the conservation program does not affect the landowner's optimal reservation price. Inserting Equations (12) and (14) into Equation (8), it is optimal for the landowner to choose enrollment ($\delta^* = 1$) if and only if the sum of the conservation incentive (first term on left hand side) and the expected value of the constrained developer price (term in square brackets) exceeds the expected value of the unconstrained developer price (right hand side) (Equation 15):

$$
\begin{aligned}
&\frac{c}{r}(1-e^{-rJ}) \\
&+\Bigg[\; e^{-rJ}\Bigg(e^{p(0)+gJ+\frac{\sigma^2 J}{2}}(1-\Phi(\frac{ln(\frac{\pi_A}{r}\frac{\alpha}{\alpha-1})-p(0)-gJ-\sigma^2 J}{\sigma\sqrt{J}})) \\
&\qquad -\frac{\pi_A}{r}(1-\;\Phi(\frac{ln(\frac{\pi_A}{r}\frac{\alpha}{\alpha-1})-p(0)-gJ}{\sigma\sqrt{J}}))\Bigg) \qquad (15) \\
&\qquad +\; e^{-\alpha(ln(\frac{\pi_A}{r}\frac{\alpha}{\alpha-1})-p(0)-gJ-\frac{\alpha\sigma^2 J}{2})-rJ}\;(\frac{\pi_A}{r}\frac{1}{\alpha-1})\;\Phi(\frac{ln(\frac{\pi_A}{r}\frac{\alpha}{\alpha-1})-p(0)-gJ-\alpha\sigma^2 J}{\sigma\sqrt{J}})\Bigg] \\
&\geq \quad \frac{\pi_A}{r}\frac{1}{\alpha-1}e^{-\alpha(ln(\frac{\pi_A}{r}\frac{\alpha}{\alpha-1})-p(0))}
\end{aligned}
$$

As J approaches 0, left and right hand sides of Equation (15) become equal, indicating the one-shot conservation program has no value when the contract length is zero.

I use numerical analysis to evaluate the effect of J on landowner willingness to enroll by fixing all parameters in Equation (15) except contract length (J) and incentive level (c). Brownian motion parameters $g = 0.035$ and $\sigma^2 = 0.083$ are calculated following Pachamove and Fabozzi (2011) as the average and variance, respectively, of the first differences of a Santa Clara County annual agricultural parcel price index, described in detail in the Methods section. Given these values and the constraint on parameter values derived from Equation (7), the discount rate is set to $r = 0.087$. As described in more detail in the Methods section, I assume parcel prices can be decomposed into additively separable temporal (varying at county-level over time) and spatial (varying at parcel-level) factors. Therefore, initial parcel price $p(0) = 12.7$ is the 2020 value of the parcel price index plus the estimated median parcel-specific value across all Santa Clara County agricultural parcels. The 2020 level price of the parcel is \$340,550. Agricultural profit π_A is the product of the 2020 California average annual cropland rental rate (\$439 per acre, USDA NASS 2022) and the median developable agricultural parcel size in Santa Clara County, 28 acres.

Figure 1 shows the effect of J and c on expected net present value of the landowner enrollment payoff. The figure plots the difference between the left and right hand sides of Equation (15), so any region of the curve that lies above zero indicates that the landowner is willing to enroll for

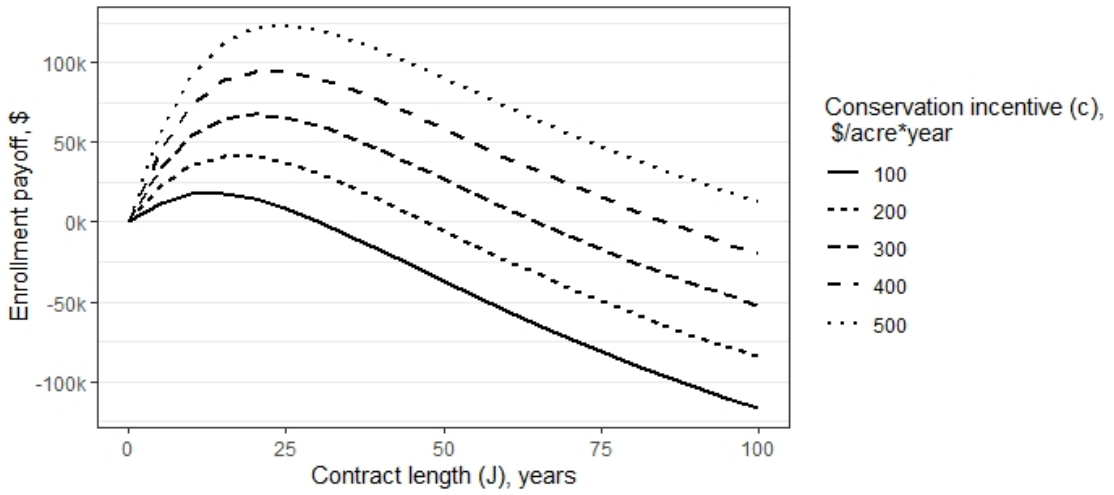

Figure 1: Landowner is willing to enroll in term-limited conservation incentive program when "enrollment payoff" values are positive, indicating net present value of conservative payments and constrained parcel sale price exceeds unconstrained parcel sale price (see Equation (15)). For a given conservation incentive level, some intermediate contract length J maximizes expected net present enrollment value.

those values of c and J. For each c, there is an intermediate J that maximizes the expected net present value of enrollment, balancing the total conservation incentive (increasing in J) and the expected net present value of the constrained parcel price (decreasing in J). As c increases, the maximizing J increases. Importantly for the policy maker, as c increases the maximum value of J for which the landowner is willing to enroll also increases. For example, at $c = \$100$/acre, the landowner will not enroll for J higher than 30 years, while at $c = \$400$ per acre contracts up to 85 years would be feasible.

I also evaluate the effect of contract length on the expected time of development. The time at which a Brownian process reaches fixed value p^* follows an inverse Gaussian distribution, such that the conditional expected value of t^* is:

$$E_t[t^*|p^*, p(0)] = \frac{p^* - p(0)}{g}. \tag{16}$$

Given the estimated parameters above, the business as usual expected time of development for a representative undeveloped agricultural parcel in Santa Clara is 2068 (48 years after 2020). Under a term-limited voluntary conservation program, development time will be J if $p(J)$ exceeds

p^*, otherwise it will be some expected time after J depending on the value of $p(J)$:

$$\begin{aligned} E_t[\, t^* \mid p^*, p(0), J] &= J \times Prob(p(J) \geq p^*) \\ &\quad + \int_{-\infty}^{p^*} \left(\frac{p^* - p(J)}{g} + J\right) f_p(p(J)) dp(J) \\ &= J + \int_{-\infty}^{p^*} \left(\frac{p^* - p(J)}{g}\right) \phi\left(\frac{p(J) - p(0) - gJ}{\sigma\sqrt{J}}\right) dp(J). \end{aligned} \tag{17}$$

Therefore, the expected time of development will be no lower than the contract length (first term of Equation (17)), but will also provide some expected additional delay beyond J (second term). Figure 2 shows that the second term is decreasing in J, consistent with the fact that as J increases, the contract is more likely to be binding in determining optimal development time (it is more likely that $p(J)$ is higher than p^*).

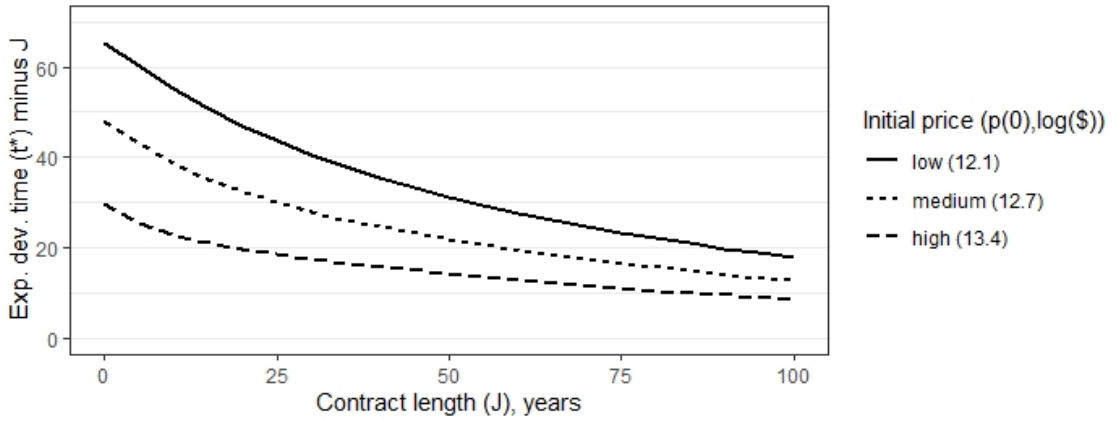

Figure 2: Expected optimal time of development, net of contract length (J). The term-limited conservation program delays development beyond the contract length, but the additional delay is decreasing in J.

2.3 Landowner conservation program enrollment choice, unlimited re-enrollment

Now I assume it is possible for the landowner to re-enroll in the conservation program after the contract ends. This case is important to evaluate because it is consistent with the reality of existing term-limited programs (e.g. USDA's CRP, EQIP, or CSP) and because there are important differences in optimal landowner and policymaker choices.

In the re-enrollment setting, the landowner chooses the optimal number of times to enroll in the program (x), given some exogenous contract length J and incentive level c. Non-enrollment occurs when $x = 0$. For simplicity I assume that once the landowner decides to stop re-enrolling they cannot start again at some later point (this assumption will be relaxed in the numerical analysis discussed in Section 5). Therefore the landowner problem is:

$$\begin{aligned} V(x,t) \;=\; \max_{x,t} \sum_{i=1}^{x} \int_{J(i-1)}^{Ji} (\pi_A + c) e^{-rs} ds \;+\; E_t[\int_{Jx}^{t} \pi_A e^{-rs} ds + P(t) e^{-rt}] \\ \text{s.t.} \quad t \geq Jx, \quad x \in \mathbb{N}_0 \end{aligned} \tag{18}$$

where x is restricted to the set of nonnegative integer values $\mathbb{N}_0$.

It is helpful to rewrite Equation (18) as a quasi-discrete time optimal stopping problem (Equation (19)), wherein at the end of the x^{th} contract the landowner must choose to either re-enroll in contract for the $x+1^{th}$ time (the term in braces in Equation (19)) or to stop enrolling and sell their parcel at the optimal reserve price, which could occur immediately at price $P(xJ)$ if $P(xJ) \geq P^*(x)$ (the second line of Equation (19)), or at some point after xJ if $P(xJ) < P^*(x)$ (the third line in Equation (19)). The optimal x^* occurs when the second term exceeds the first term:

$$\begin{aligned} V(P^*(x), x) \;=\; \max \Bigg[\Big\{ \frac{\pi_A + c}{r} \left(1 - e^{-rJ}\right) + e^{-rJ} V(P^*(x+1), x+1) \Big\} \;, \\ P(xJ) \;\mathbb{1}(P(xJ) > P^*(x)) \\ +\; \left(\frac{\pi_A}{r} + (P^*(x) - \frac{\pi_A}{r}) \big(\frac{P(xJ)}{P^*(x)} \big)^{\alpha} \right) \mathbb{1}(P(xJ) \leq P^*(x)) \Bigg], \end{aligned} \tag{19}$$

where:

$$\mathbb{1}(A) = \begin{cases} 0, & \text{if A is false} \\ 1, & \text{if A is true.} \end{cases}$$

I use the term "quasi-discrete" to acknowledge that discounting still occurs in continuous time in this problem, but the stochastic variable $P(xJ)$ evolves in discrete time increments of length J. Price increments are independent and normally distributed, such that $e^{P((x+1)J)} - e^{P(xJ)} \sim N(gJ, \sigma^2 J)$. Note the change in notation which allows for the land sale reserve price $P^*(x)$ to change with x.

I would like to find the optimal stopping value $P^*(xJ)$ at which point the landowner will stop re-enrolling (also referred to as the enrollment reserve price hereafter). First I must demonstrate that such a value exists, which requires that the marginal value of waiting to stop monotonically decreases as $P(xJ)$ increases (Dixit and Pindyck 1994). Formally, Equation (20) must be decreasing in $p(xJ)$.

$$
\begin{aligned}
&\frac{\pi_A + c}{r}(1 - e^{-rJ}) \\
&+ e^{-rJ}\Bigg[\int_{p^*(x+1)}^{\infty} e^{p((x+1)J)} f_p(p((x+1)J))dp((x+1)J) \\
&\qquad + \int_{-\infty}^{p^*(x+1)} (\frac{\pi_A}{r} + (e^{p^*(x+1)} - \frac{\pi_A}{r})e^{\alpha(p((x+1)J) - p^*(x+1))}) f_p(p((x+1)J))dp((x+1)J)\Bigg] \\
&- \left[e^{p(xJ)}\ \mathbb{1}(p(xJ) > p^*(x)) + \left(\frac{\pi_A}{r} + (e^{p^*(x)} - \frac{\pi_A}{r})e^{\alpha(p(xJ) - p^*(x))}\right)\ \mathbb{1}(p(xJ) \leq p^*(x))\right]
\end{aligned}
\tag{20}
$$

Using similar methods for rewriting Equation (9), I express Equation (20) in a form that allows for taking the derivative with respect to $p(xJ)$:

$$
\begin{aligned}
&\frac{\pi_A + c}{r}(1 - e^{-rJ}) \\
&\quad + e^{-rJ+p(xJ)+gJ+\frac{1}{2}\sigma^2 J}\left(1 - \Phi\big(\frac{p^*(x+1) - p(xJ) - gJ - \sigma^2 J}{\sigma\sqrt{J}}\big)\right) \\
&\quad + e^{-rJ}\ \frac{\pi_A}{r}\ \Phi\big(\frac{p^*(x+1) - p(xJ) - gJ}{\sigma\sqrt{J}}\big) \\
&\quad + e^{-rJ-\alpha(p^*(x+1)-p(xJ)-gJ-\frac{1}{2}\alpha\sigma^2 J)}(e^{p^*(x+1)} - \frac{\pi_A}{r})\Phi\big(\frac{p^*(x+1) - p(xJ) - gJ - \alpha\sigma^2 J}{\sigma\sqrt{J}}\big) \\
&- \left[e^{p(xJ)}\ \mathbb{1}(p(xJ) > p^*(x)) + \left(\frac{\pi_A}{r} + (e^{p^*(x)} - \frac{\pi_A}{r})e^{\alpha(p(xJ)-p^*(x))}\right)\ \mathbb{1}(p(xJ) \leq p^*(x))\right]
\end{aligned}
\tag{21}
$$

Using numerical analysis, I find no cases with reasonable parameter values in which the derivative of Equation (21) with respect to $p(xJ)$ is positive. Therefore, I proceed assuming $P^*(xJ)$ exists.

By visual inspection, it is clear there is no optimal contract length for the landowner, an important distinction from the one-shot enrollment setting. When re-enrollment is possible, value to the landowner continually increases as J approaches zero, such that the conservation incentive program becomes a pure agricultural subsidy without development constraint. Landowner willingness to enroll is monotonically decreasing in J.

However, as J decreases, any environmental benefits that depend on the amount of conserved acres and length of conservation period will also decrease, since the landowner has more frequent opportunities to develop at the end of each contract. Therefore, while there is no optimal J for the landowner, the conservation program administrator will want to identify the contract length that optimizes the trade-off between conserving enrolled land for a longer period of time and reducing landowner willingness to enroll, similar to the trade-off identified in Ando and Chen (2011). The optimal J is a function of conservation incentive c, since the continuation term in Equation (19) is monotonically increasing in c.

For the remainder of the analysis I assume that the administrator must choose values for J and c that both (1) maintain total conservation spending below program budget and (2) maximize

conservation outcomes (here, the only outcome I assess is expected area of avoided development) with respect to J and c.

Such an analysis requires predicting the solution to Equation (19), $P^*(xJ)$, and therefore willingness to enroll over time, for all parcels of interest. Given the difficulty of deriving an analytical solution to a discrete optimal stopping problem, as well as the need for numerical analysis for any comparative statics around J and c, I use numerical analysis to identify optimal values of J and c in Santa Clara County, California.

3. Numerical methods

To undertake the numerical analysis, I make several adjustments to model structure. I discretize time into annual time steps. Developer offers follow a random walk approximated using a first order autoregressive model, parameterized using methods discussed below. To enhance the realism of the model, I relax the assumption that landowners cannot wait to re-enroll between contract periods. This change introduces analytical complexity but is easily assessed using numerical dynamic programming methods.

The problem therefore becomes a flexible Markov Decision Process (MDP) model in which the landowner must decide the optimal action a (wait to enroll, enroll, or develop) in each state x, defined by their current state of enrollment and the developer's current offer, given the expectation of future developer offers. The Bellman equation for this problem is shown in Equation (22).

$$V(x(j, P(t), t)) = V(x) = \max_a E[R_a(x)|q_a(x, x')] + \beta E[V(x')|x] \tag{22}$$

where:

t = time index, $t \in \{0, 1, ..., T\}$

j = conservation enrollment index, $j \in \{0, 1, 2, ..., J\}$; $j = 0$ indicates the parcel is not enrolled, $j > 1$ indicates the parcel has been enrolled for j time steps

$P(t)$ = developer offer, a continuous variable that follows a random walk

$x = x(j, P(t), t)$ = state at time t, defined by current enrollment status and developer offer

$x' = x(j', P(t+1), t+1)$ = state at time $t+1$, defined by the next period's enrollment status and developer offer

a = action chosen at state x, where a is an element of a set of possible actions defined at each x, $\mathcal{A}(x)$; if $j = 0$ or $j = J$ (parcel is not currently enrolled or has reached end of contract), $\mathcal{A}(x) = \{wait, enroll, develop\}$; if $0 < j < J$ (parcel is currently enrolled), then $\mathcal{A}(x) = \{enroll\}$

$R_a(x)$ = payoff received from choosing action a at state x; if $a = wait$, $R_a(x) = \pi_A$ (agricultural profit); if $a = enroll$, $R_a(x) = \pi_A + c$ (agricultural profit plus conservation incentive); if $a = develop$, $R_a(x) = P(t)$ (developer offer at state x)

$q_a(x, x')$ = conditional on choosing action a, probability of transitioning from state x to x'; a function of developer offer $P(t)$ transition probabilities as well as deterministic transitions with respect to time and enrollment status

β = discrete time discount factor

I use data from Santa Clara County to parameterize MDP rewards, transition probabilities, and developer offers. Given these model fundamentals, the MDP can be solved using value iteration, starting with an initial guess at the value of being located at state x, $V_0(x(j, P(t), t)$, for all x, choosing the optimal sequence of actions given this guess, and recalculating a new iteration of state values $V_1(x(j, P(t), t)$. Iteration continues until the change in state values for all x fall below some acceptable error.

The model is solved for a subset of agricultural parcels in unincorporated Santa Clara County, CA where at least one additional primary residence could be created through subdivision, as indicated by the County of Santa Clara Zoning Ordinance (2003) (hereafter, developable agricultural parcels - shown as all parcels with estimated agricultural profits in Figure 3.A). Parcels of interest were further limited to areas with higher value agricultural production (Figure 3.A), higher risk of development due to proximity to cities and parcel slope (Figure 3.C), and are not currently protected by easements or other existing conservation programs, e.g. the Williamson Act (Figure 3.D). Santa Clara County planners used these variables to define the Agricultural Resource Area (ARA), shown in dark red outline in each panel of Figure 3. Going forward analysis is limited to ARA parcels, which range in size from less than an acre to over 2,500 acres and are at highest risk of conversion from agricultural to developed use due to residential expansion surrounding Morgan Hill and Gilroy.

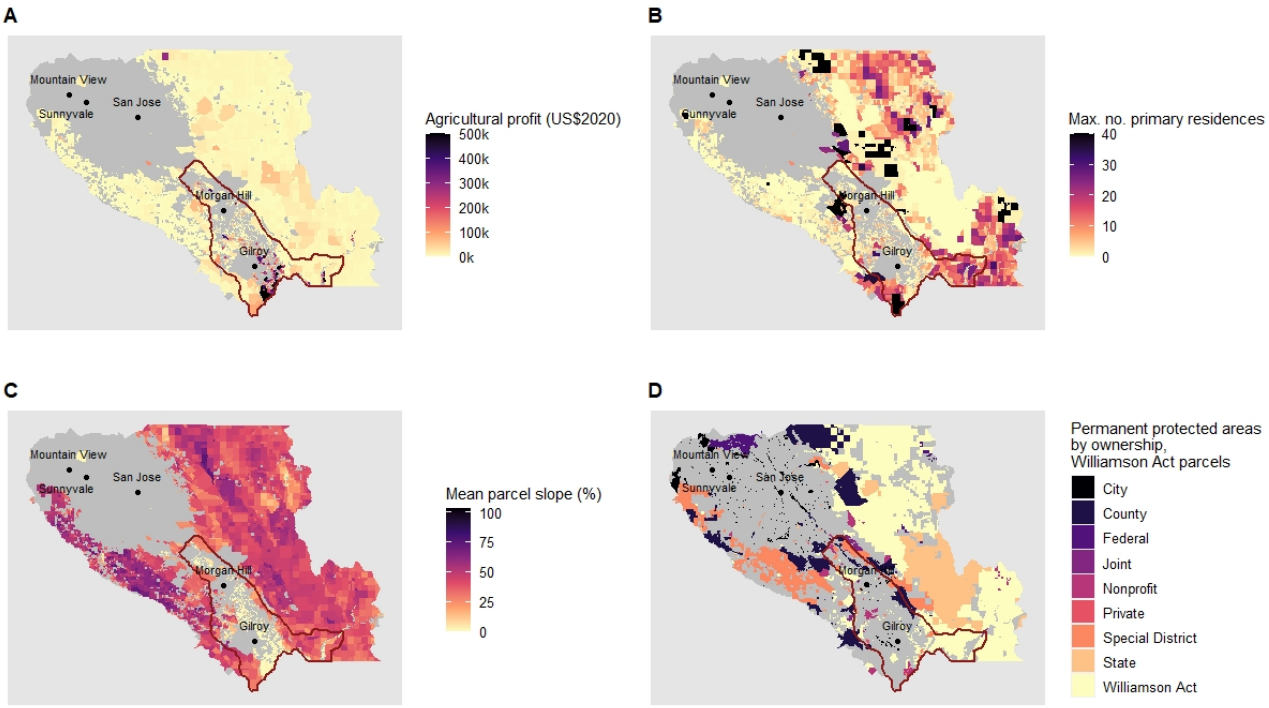

Figure 3: Developable agricultural parcels in unincorporated Santa Clara County, CA. Agricultural Resource Area (ARA) outlined in dark red in each panel. Dark gray areas do not meet the definition of "developable" (at least one additional primary residence can be created through subdivision).

I use the MDP model to find each ARA landowner's decision to wait, enroll, or develop in each state, given contract length J, conservation incentive c, and stochastic sequence of developer

offers $P(t)$. The developer offers are generated for each parcel using a price prediction model that accounts for both county-wide time-dependent factors and parcel-level characteristics. Given the landowner's optimal sequence of actions, I find the probability of the landowner choosing a given action in each time step between 2020 and 2050. By comparing a business as usual case without a conservation program ($c = 0$) to conservation program scenarios with varying J and c, I identify the values of J and c that achieve the highest area of avoided development while maintaining a county-wide conservation program budget.

For the remainder of this section I describe how model fundamentals are parameterized using Santa Clara County data.

3.1 Agricultural profit estimation

I estimate annual agricultural profits for each developable Santa Clara parcel using the USDA Crop Data Layer (CDL), an annual 30m raster dataset of U.S. crop cover derived from LandSat satellite imagery, the National Land Cover Dataset (NLCD), and USDA sample plot observations (USDA NASS 2022). Agricultural profits are estimated by major agricultural land use (mixed forest, shrubland, grassland/pasture, evergreen forest) and for the most common high value crop types in Santa Clara County (tomatoes, grapes, cherries, lettuce/greens, corn, walnuts, beans).

Given the large variety of California crop types, CDL user accuracy (the likelihood that a pixel's designated crop type matches ground observation) in this region can be low, ranging from 25% for sweet corn to 90% for walnuts, with a total area-weighted user accuracy of 63% in Santa Clara County (USDA NASS 2022). To reduce the impact of annual, pixel-level uncertainty, I use 10 years of CDL data and aggregate pixel data to the parcel level. I create a composite raster layer of the maximum agricultural profit earned in each pixel between 2010 and 2020. Each developable parcel's assumed future agricultural profits is the sum of composite layer profit values for all intersecting pixels. This method assumes that future agricultural rents will be the maximum potential agricultural value as reflected by recent historical land use.

Agricultural profits are estimated from several sources. Pixels designated as mixed forest, shrubland, grassland/pasture, evergreen forest, winter wheat, alfalfa, hay, oat, lettuce, and greens are assumed to have profits of $13 per acre, which is the average California pastureland rent for 2020 (USDA NASS 2020). Santa Clara County forested areas are likely to earn lower annual rents

on average, based on estimates from the County of Santa Clara 2020 Crop Report (SCC 2020), however I assume landowners have the option to remove tree cover and lease land as pasture. Cost studies find lettuce and greens may generate negative returns, so I make a similar assumption for this crop type (Tourte et al. 2019).

For major high value crops, I estimate per acre revenue from per acre yields and unit prices reported in SCC 2020 and per acre operational costs from crop-specific cost studies produced by the University of California Davis. All cost estimates are inflated to 2020 dollars. I ignore capital and overhead costs, assuming these are sunk for agricultural landowners. Remaining crop types cover 0.01% of Santa Clara developable land on average over 2010-2020 and are assigned profits of $439 per acre, the average 2020 California cropland rent (USDA NASS 2020).

3.2 Developer offer estimation

My goal is to estimate the expectation of future developer offers that an agricultural parcel owner would reasonably expect, for any future time step, given historical parcel sale observations. To do this, I use an autoregressive econometric model, drawing on the economic literature for deriving unbiased real estate price indices. Since I will use the model to predict future developer offers for individual parcels, in addition to estimating a historical price index, I also seek high model prediction accuracy conditional on hedonic parcel characteristics.

The primary dataset used in this section is proprietary CoreLogic data encompassing all sales of developable agricultural parcels in Santa Clara County from 1985 to 2020, including observed price and and a parcel identifier, assessor's parcel number (APN). Additional geospatial data made available by the Santa Clara County Department of Planning and Development and Open Space Authority were used to allocate parcel hedonic variables to the CoreLogic observations, including: parcel size; zoning designation; number of allowable primary residences; parcel slope; distance to amenities like major road types and public open space; the portion of parcel protected by permanent easement; level of farmland quality as measured by the California Farmland Mapping and Monitoring Program; and dummy variables indicating whether or not the parcel is enrolled in the Williamson Act program; location in urban service area, urban growth boundary, or urban sphere of influence; flood zone; and high or very high fire risk.

To motivate the econometric model, I assume that if the landowner of parcel i were to receive

a developer offer in any time step t, it would be a multiplicative function of parcel characteristics X_i and time varying component Z_t:

$$P_{it} = \prod_j X_{ij}^{\alpha_j} \prod_t Z_t^{\beta_t} e^{\epsilon_{it}} \tag{23}$$

where:

P_{it} = developer offer for parcel i at time t

X_{ij} = hedonic characteristic j of parcel i

Z_t = time-varying fixed effect (annual time dummy)

ϵ_{it} = normally distributed error term, independent over time and space, such that $\epsilon_{it} \sim N(0, \sigma_\epsilon^2)$

$\alpha, \beta, \sigma_\epsilon^2$ = parameters to be estimated

Equation (23) admits a log-linear function which, lacking a complete panel, I estimate using pooled ordinary least squares, representing the time-varying component Z_t with annual time dummy variables (Equation (24)):

$$p_{it} = \beta_0 + \sum_j \alpha_j X_{ij} + \sum_{t=1986}^{2020} \beta_t Z_t + \epsilon_{it} \tag{24}$$

The intercept of the log-linear model (β_0) is the county quality-adjusted parcel price index for 1985, where parcel quality is measured by hedonic variables X_{ij}. Summing β_0 with each year dummy parameter ($\beta_{1986}, ..., \beta_{2020}$) provides the county index for the historical time frame, referred to hereafter as I_t for all t. Hedonic parameter estimates $\hat{\alpha}_j$ are assumed to stay constant over time and are saved for estimating future parcel prices.

One would expect volatility in the historical county price index I_t for a number of reasons. Developer willingness to pay for a unit of parcel quality, as measured by parcel-level covariates X_{ij}, may change as new information arrives in the market about the per unit value, for example about residential homeowner willingness to pay for being located in Santa Clara County. The developer population may also change, with opinions about parcel value shifting as individuals enter and exit the market. While these market drivers are also likely to impact hedonic parameters, I simplify the model by assuming that the only time-vary component of parcel prices is the county-wide index

value. This reduces the number of assumptions needed for forecasting future parcel prices.

To enable forecasting, county index estimates are fit to a first order autoregressive model:

$$\Delta I_t = \rho \Delta I_{t-1} + \sum_k \gamma_k \Delta C_{kt} + u_t \tag{25}$$

where:

ΔI_t = first difference of index I_t

C_{kt} = county-wide covariate: population, personal income (income from wages, government benefits, dividends and interest, business ownership, measured by place of residence), and construction cost index

u_t = normally distributed error term, independent over time, such that $u_t \sim N(0, \sigma_u^2)$

$\rho, \gamma_k, \sigma_u^2$ = parameters to be estimated

Including county-wide covariates (population, personal income, and construction costs) in Equation (25) necessitates assumptions about future values for these variables when creating expectations of future parcel prices. Therefore, economic and population growth scenarios are required. The results reported below focus on a scenario in which county population, personal income, and construction costs grow at a constant annual rate equal to the average annual growth from 1985 to 2020.

Since individual parcels are infrequently traded, there is a structural bias towards negative serial correlation between proximate estimates of I_t, especially for indices created over small regions. That is, there are unobservable characteristics of parcels sold in one time step that may be captured in time dummies and that, since they are unlikely to appear in nearby time steps, result in spurious negative serial correlation between index values. This would bias $\hat{\rho}$ away from zero and create noisier forecasts, a key application for the index estimates here.

To address this issue, I follow methods from Case and Shiller (1989) and Kuo (1996), who recommend a bootstrap approach to estimating Equation (25) parameters. For each iteration, the historical parcel sales data is randomly divided into two samples. Equation (24) is estimated for each sample and Equation (25) is estimated using one set of index results for the left hand side and the other for the lagged index values.

I also want to ensure that Equation (24) admits an unbiased estimate of developer willingness

to pay. Fisher, Geltner, and Pollajowski (FGP 2007) note that a naive regression of Equation (24) will result in a biased estimate of mean buyer willingness to pay, since sales are only observed when buyer willingness to pay exceeds seller willingness to accept. For this reason, I use FGP (2007) methods to isolate buyer-side parameters, using a two-stage Heckman procedure to control for the likelihood that any given transaction would be observed on the market. This is an important consideration, since 1,118 out of 5,314 total developable agricultural parcels in Santa Clara County have not been transacted since 1985.

In the real estate economics literature, controlling for likelihood of sale in a hedonic price model generates a "constant liquidity index." Real estate markets are characterized by variable liquidity over time, or changes in the ease of selling an asset reflected through variables like number of days on the market or number of transactions. A constant liquidity index controls for the fact that it is more difficult to sell a property during a down market and therefore reflect that the true value of a property may be lower than the transactions observed on the market (FGP 2007).

The constant liquidity index can also be interpreted as a buyer willingness to pay index. This is because controlling for the probability of sale is, by definition, controlling for the probability that the buyer willingness to pay exceeds the seller willingness to accept. The first stage probit results of the Heckman procedure can therefore be used to identify price parameters specific to buyer and seller populations. FGP (2007) and Fisher, Gatlaff, Geltner, and Haurin (2003) describe the procedure to derive the buyer parameters from the two stage Heckman regression parameters, which requires adding together the variable liquidity index parameters estimated from the sample selection-controlled second stage Heckman regression and a term that is a function of the coefficients on time dummies in the first stage probit regression, which removes the effect of market liquidity from the index.

Buyer-side parameter estimates for Equation (24) are shown in Figure 4 and parameter estimates for Equation (25) are reported in Table 1. The variables with the largest positive influence on parcel price include being located in an urban service area, which indicates that the parcel is sufficiently close to one of Santa Clara's cities to receive waste removal, water, sewer, and other municipal services. Being located in a "design review" special district, which indicates proximity to visual and environmental amenities protected by the County zoning ordinance, is associated with an increase in parcel value. Conversely, being located in zones with large minimum lot sizes (5, 20,

and 40 acres) is associated with lower parcel values, likely because these zoning designations reduce the total number of primary residences that could be created through subdivision.

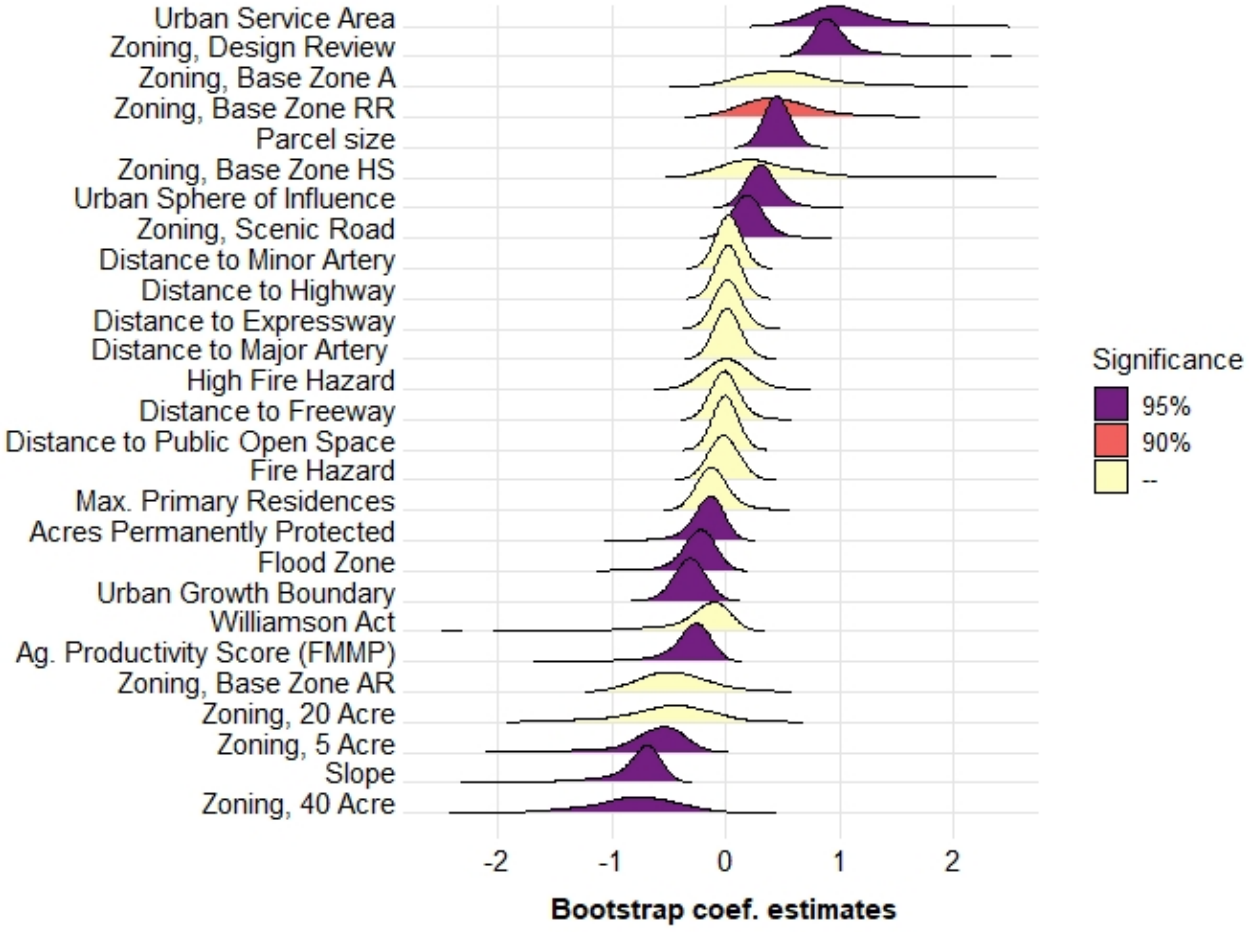

Figure 4: Buyer-side, sample selection-corrected parameter estimates ($\hat{\alpha}_j$) for log-linear parcel price model (Equation (24)). Average model $R^2 = 0.30$. "Zoning, Design Review" is a dummy variable for parcels located in a special district requiring review of the impact of any development on local visual and environmental amenities. "Zoning, Scenic Roads" is a dummy variable for parcels subject to special development and sign regulations protecting the visual character of scenic roads. "Zoning, X Acres" refers to parcel zone's minimum lot size restriction. "Zoning, Base Zone X" refers to parcel base zone, which defines allowable uses; "A" = "Exclusive Agriculture", "AR" = "Agricultural Ranchlands", "HS" = "Hillside", "RR" = "Rural Residential".

Using Monte Carlo analysis, I draw many realizations of the county index error term u_t for all forecasted years, given estimated $\hat{\sigma}_u^2$. With the resulting iterations of future county index paths (Figure 5), I discretize the space of possible future index values into bins for each time step and calculate the probability of transitioning from one price bin to another. The expected index values within each bin, summed with each parcel's hedonic value as estimated from Equation (24),

Table 1: County index autoregressive parameter estimates, Equation (25)

Parameter	Bootstrap Average	2.5th pc	97.5th pc
ρ (ΔI_{t-1})	-0.103	-0.410	0.163
γ_{PI} (ΔC_{PI}, Personal income)	2.00	1.09	2.98
γ_P (ΔC_P, Population)	-1.36	-9.45	9.95
γ_C (ΔC_C, Constr. costs)	-3.15	-9.64	-0.347
σ_u^2	0.136	0.066	0.433

are used as the rewards to choosing development ($R_{develop}(x)$) and the estimated index transition probabilities serve as $q_a(x, x')$ in the MDP model.

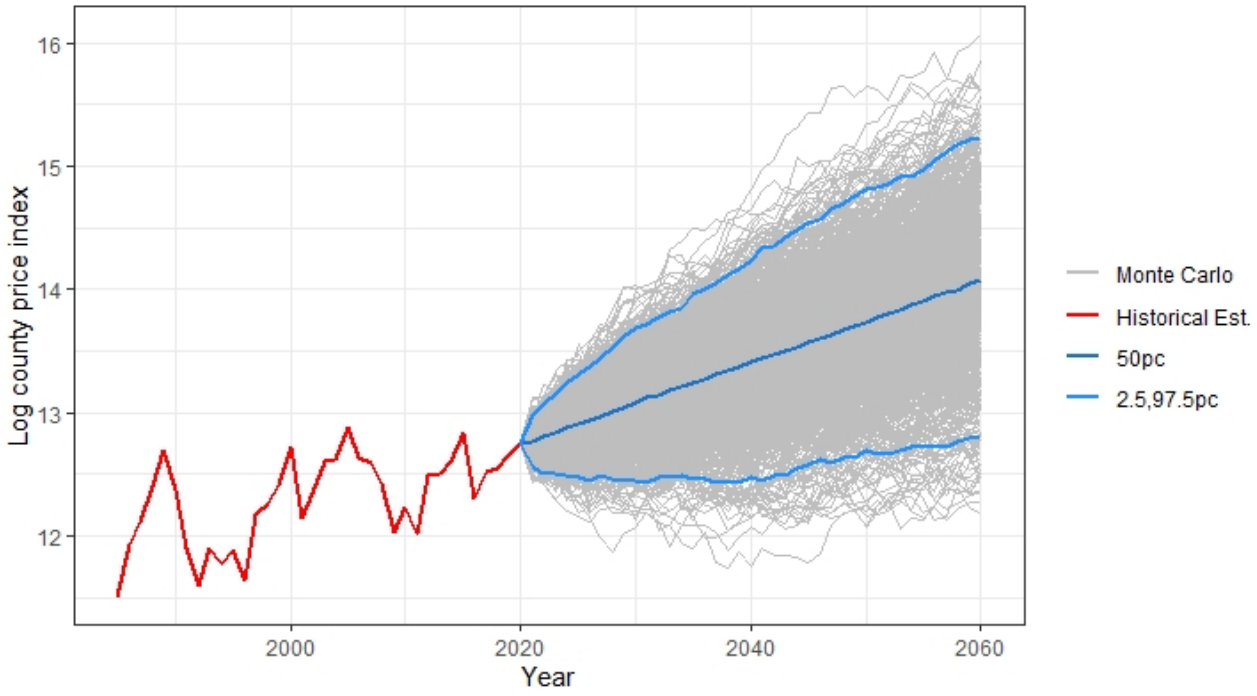

Figure 5: County-wide agricultural parcel price index (estimated 1985-2020, in red), and forecasted future price indices, assuming constant future growth in county population, personal income, and construction costs (forecast 2021-2060, in gray).

Some of the model assumptions used here are usefully relaxed in the real estate economics literature, but since the focus of this exercise is to evaluate the likelihood of landowner participation

in conservation programs, I do not pursue more elaborate analysis of real estate market structure. For example, a number of past studies find that real estate prices follow a random walk, identified through autoregressive models on differenced prices (Case and Shiller 1989, Kuo 1996, Plazzi et al. 2011) while others demonstrate the presence of more complex market cycles, including regime switching (Crawford and Fratantoni 2003, Gu 2002, Ghysels et al. 2013). While I assume hedonic parameters are constant over time to simplify forecasting, similar to FGP (2007) and other applications in conservation literature (Cho et al. 2014), other studies have relaxed this assumption (Wallace 1996, Ghysels et al. 2013, Glumac et al. 2019), for example separately estimating Equation (24) in each time step (Murphy 2018). Other studies have been able to exploit complete panels, for example using real estate investment trust data that provide asset value estimates in every time step, to use a Kalman Filter approach to jointly estimate Equations (24) and (25) (Brown et al. 1997, Guirguis et al. 2005). Applying these methods in my setting would provide a useful sensitivity but would require evaluating tradeoffs between spatial and temporal error variance. Finally, while I assume homoskedasticity in estimating parcel price parameters, through Breusch-Pagan analysis I find that parcel size significantly affects estimated error variance. Future refinements to this analysis could account for higher price uncertainty for larger parcels.

3.3 Calculating county-wide expected development

This analysis seeks to inform conservation program design choices. A simple measure that county planners could use to compare choices of J and c is expected area of development across all eligible parcels, with a programmatic objective of minimizing expected developed area for a given budget. Using parcel-level MDP solutions, I calculate expected county-wide developed area, from the perspective of $t = 2020$, for a chosen policy evaluation year $\bar{t}$:

$$E[D_{\bar{t}}] = \sum_{s} \left\{ \sum_{i} \left(\sum_{k_i} \sum_{t}^{\bar{t}} \mathbb{1}(a_{ik_i st} = develop)\ p(k_i) \right)\ Ac_i \right\} p(s) \tag{26}$$

where:

$E[\cdot]$ = expectation over realizations of county price index I_t, indexed by s, and parcel-shocks, indexed by k_i for all parcels i, for all $t = 2020, ..., \bar{t}$

$D_{\bar{t}}$ = cumulative area of developable agricultural land sold to developer between $t = 2020$ and $\bar{t}$

$\mathbb{1}(a_{ik_ist} = develop)$ = 1 if it is optimal for landowner i to accept developer offer at time t, given county index realization s and parcel shock realization k_i, 0 otherwise

$p(k_i)$ = probability that parcel shock realization k_i occurs

$p(s)$ = probability that county index realization s occurs

Ac_i = size of parcel i in acres

Equation (26) can be interpreted as each parcel's cumulative probability of development (the term within the round brackets), conditional on a given county index realization, weighted by each parcel's area and summed over all parcels. This value (the term in the braces) is then summed over the probabilities of all possible county index realizations (experienced simultaneously by all parcels). The equation can be rearranged for ease of calculation such that the MDP model solves for each parcel's cumulative probability of development separately, over all possible county index realizations, then parcel results are weighted by parcel area and summed:

$$E[D_{\bar{t}}] = \sum_i Ac_i \sum_s \sum_{k_i} \sum_t^{\bar{t}} \mathbb{1}(a_{ik_ist} = develop)\ p(k_i)\ p(s) \tag{27}$$

4. Results

All results reported here assume a future scenario in which annual county population, personal income, and construction costs increase at the same average annual rate over 2050-2080 as observed 1985-2020.

4.1 Business as usual development in Santa Clara

In the absence of a conservation program, the model predicts high likelihood of development for most parcels in the Santa Clara County ARA region: over 72,000 acres out of 153,000 total ARA developable acres have a greater than 50% probability of developing before 2050 (Figure 6.A). Using Equation (27), the expected area of development in the ARA increases from 22% to 33%

to 43% of developable ARA area in 2030, 2040, and 2050, respectively. The areas with highest development risk are found within Gilroy and Morgan Hill spheres of influence, or areas closest to existing urban and suburban development (Figure 6.B). Visual and environmental amenities protected by "design review" and "scenic road" zoning provisions also drive higher predicted real estate values and therefore development risk.

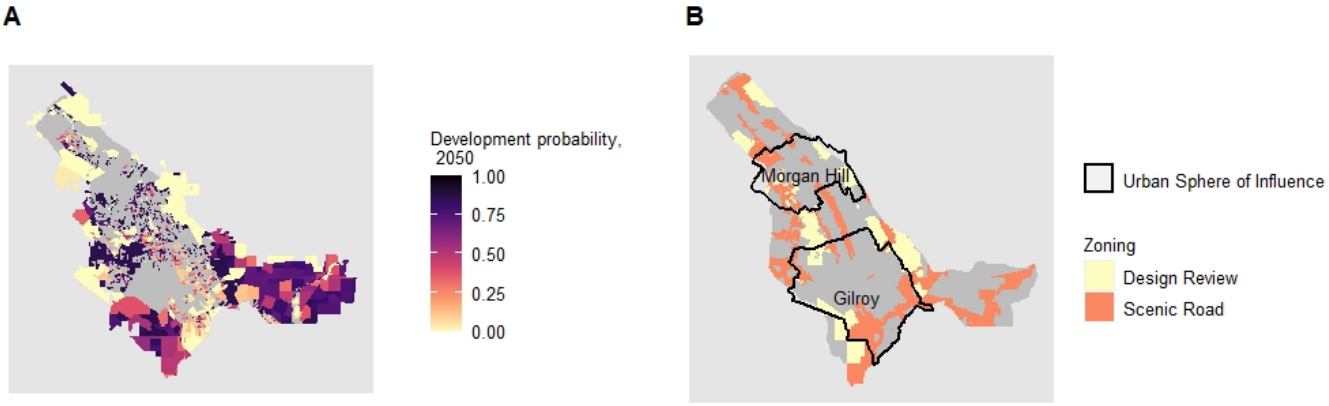

Figure 6: Probability and drivers of development in the Santa Clara County Agricultural Resource Area (ARA), business as usual scenario.

To evaluate the performance of the MDP and price prediction models, I compare the business as usual results to an independent, qualitative study of open space development risk in the San Francisco Bay region carried out by the Greenbelt Alliance (GBA 2017). The GBA analysis primarily focuses on spatially-varying drivers of development risk, including city and county general plans and zoning ordinances, urban service areas, spheres of influence, proximity to roads, land slope, and environmental, habitat, and agricultural protection policies. They also use information on planned development projects from county websites, news, and local interviews. They then attribute qualitative "development pressure factors" to the range of possible values for each variable assessed, and use the union of all spatial layers to identify regions that are (1) high risk (urban development likely within 10 years), (2) medium risk (urban development likely from 10 to 30 years) and (3) low risk (development unlikely within 30 years).

Overlaying this study's business as usual development predictions for all of Santa Clara County with the GBA risk assessment, the findings are largely consistent. Table 2 shows that, for example, out of the 28,874 acres identified as "high risk" in the GBA analysis, this study finds that expected

development reaches 39.4% of that area by 2050. Conversely, only 8.5% of the area identified as "low risk" is predicted to be developed by 2050 in this analysis. The modeling approach used here therefore broadly aligns with analysis that benefited from even more detailed data on project-level announced and planned development in the region.

Table 2: Greenbelt Alliance comparison

GBA analysis		This study, expected developed area (% of GBA acres)		
Risk categories	**Santa Clara acres**	**2030**	**2040**	**2050**
High risk	28,874	8.0	21.4	39.4
Medium risk	105,895	4.7	13.3	29.5
Low risk	571,836	0.5	2.0	8.5

4.2 Conservation program effect on a single parcel

As shown in Equation (19), landowner behavior in the conservation program re-enrollment setting simplifies to two reservation prices, one the developer offer price at which they will stop enrolling in the conservation program (enrollment reserve price, $p^*(xJ)$ in log form) and the other the developer offer price at which they will sell their parcel to the developer (sale reserve price, $p^*(x)$ in log form). Solving for landowner reserve prices using numerical analysis provides several findings (Figure 7). For this exercise, I report results for a single parcel with annual agricultural profits of approximately $150,000 and the median parcel-specific (hedonic) component of developed land value across all ARA parcels. The numerical analysis throughout this section operates on 5 year time steps.

First, $p^*(x)$ is substantially larger than $p^*(xJ)$ for all scenarios assessed, suggesting that landowners will stop enrolling in the conservation program even if market prices are substantially lower than their ultimate sale reserve price. The difference between $p^*(x)$ and $p^*(xJ)$ depends on, in addition to other problem parameters, the landowner's discount rate and their beliefs about future real estate prices.

Second, the reserve price series $p^*(x)$ is essentially constant across contract length J for all time steps, consistent with the single-shot enrollment setting - that is, the length of the contract does not influence the landowner's sale reserve price. However, $p^*(x)$ increases as the conservation incentive c increases, a departure from the single-shot enrollment setting. When the landowner can only enroll once, the value of the conservation program is not accounted for in the landowner's value of the property (Equation (7)). However, when repeated enrollment is possible, the landowner increases their reservation price to reflect the ability to permanently increase agricultural land rents. Across scenarios assessed here, for each increase in c of \$100 per enrolled acre, the landowner's sale reserve price (in levels) increases between 3% and 9%. The rate of increase in reserve price for a given increase in incentive level is higher for shorter contracts, which provide more flexibility and therefore value to the landowner.

Third, the enrollment reserve price $p^*(xJ)$ does not follow the same patterns as the sale reserve price. First, the enrollment reserve price is not estimated for time steps in which the landowner is certain to be enrolled (there are no states for that time step in which waiting to enroll is optimal) (Figure 7). This is more prevalent for scenarios with higher enrollment incentives, as well as scenarios where the contract length is equal to the temporal resolution of the model and therefore not a constraint on development (here, 5 years).

Enrollment reserve price is influenced by both contract length and incentive level. For every 5-year increase in contract length, enrollment reserve price decreases between 5 and 25% (in levels), for two reasons. First, holding incentive level constant, increasing contract length decreases the value of the conservation program to the landowner and therefore reduces the sale reserve price. Second, a longer contract length increases the probability that the sale reserve price is reached at some point during the contract. Both effects increase the range of states over which it is optimal to wait rather than enroll.

Similar to sale reserve price, enrollment reserve price is increasing in incentive level. For each \$100 increase in c, enrollment reserve price increases between 8% and 25% (in levels), more rapidly than sale reserve price. By increasing the sale reserve price, higher incentive levels increase the range of developer offers over which it is optimal to enroll, pushing up enrollment reserve price.

For states where the landowner is not enrolled and where the developer offer is less than $p^*(xJ)$, the landowner will choose to enroll and will be enrolled for the length of the contract J. For

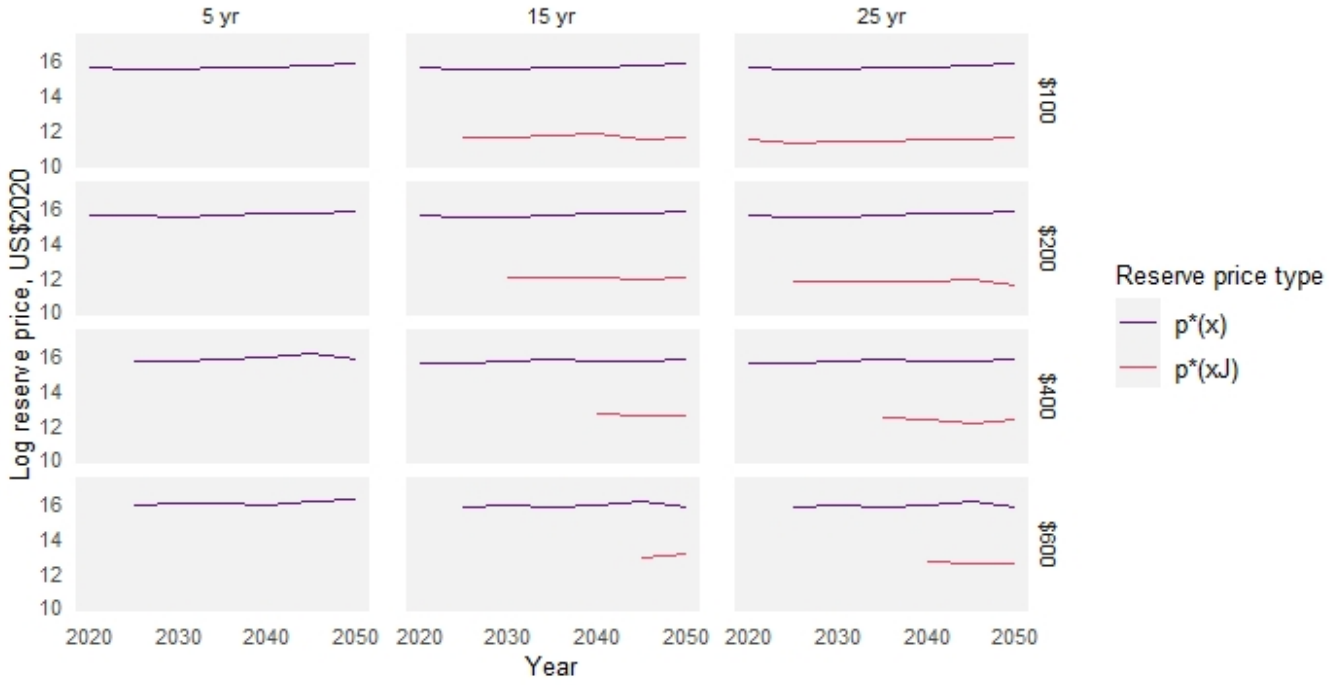

Figure 7: Representative landowner reservation prices for sale of parcel to developer ($p^*(x)$) and for conservation program enrollment ($p^*(xJ)$). Contract length J varies in panels from left to right (5 years to 25 years) and conservation incentive c varies from top to bottom ($100-$600 per enrolled acre).

example, a 5 year contract allows the representative parcel in this analysis to develop whenever the developer offer exceeds $p^*(x)$ (Figure 8). That is, the conservation incentive acts as an agricultural subsidy, and it will always be optimal to either enroll or develop in each (5 year) time step. As the contract length extends to greater than one time step (10 years and above), the landowner will only enroll if the developer offer is less than $p^*(xJ)$, which is a function of both J and c. Finally, for instances where the landowner is not enrolled but the developer offer is between $p^*(xJ)$ and $p^*(x)$, the landowner will wait to decide whether to sell or re-enroll at a later point. For example, see the conservation program scenario where $c = \$100$ and $J = 20$ years (Figure 9). The landowner will not enroll in 2020 because the developer offer exceeds $p^*(xJ)$, but there are some states where the developer offer has decreased below $p^*(xJ)$ in 2025 and 2030, increasing the probability of enrollment in those years.

To estimate the expected area of development for each parcel, the metric of interest is cumulative probability of development for each time step (Figure 9). It is instructive to attribute

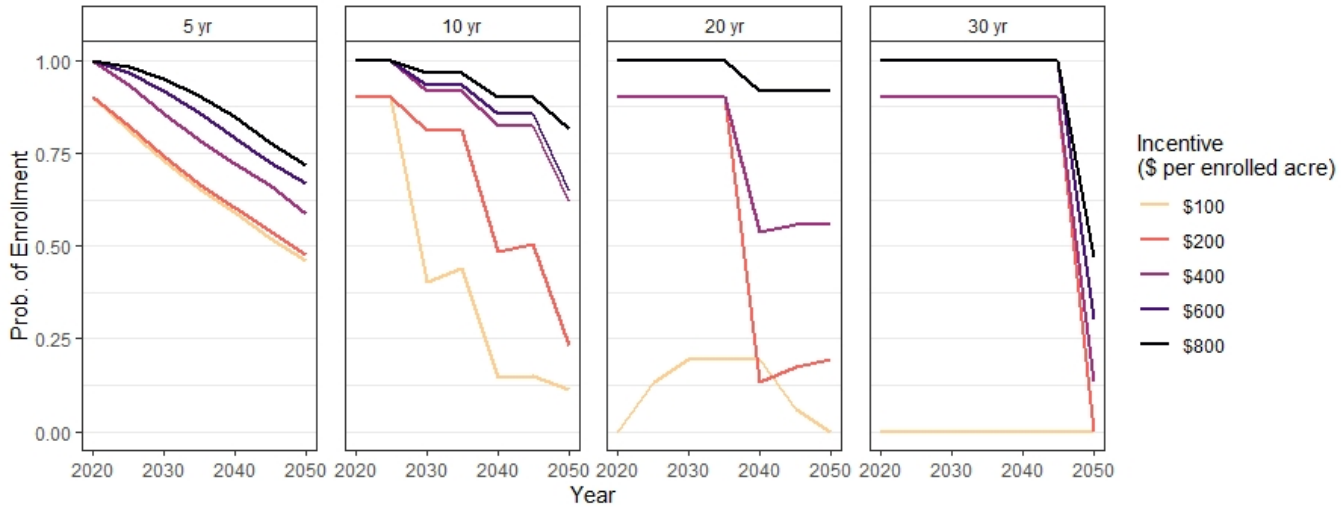

Figure 8: Probability that representative landowner is enrolled in the conservation program, 2020-2050. Contract length J is shown by panel (5 years to 30 years, left to right).

cumulative development results to two drivers: first, the incentive c increases the value of agricultural land use, and through the ability to re-enroll, increases $p^*(x)$ and delays the expected time to development. This so-called "subsidy effect" is isolated in the 5-year contract scenarios (Figure 9), where increasing the subsidy decreases the cumulative development probability for all time steps but there is no lasting conservation protection.

Second, extending the term of the contract ensures the landowner cannot choose to develop even if there is a transitory surge in the developer offer higher than $p^*(x)$. This so-called "shield effect" can be seen by comparing the same incentive level across increasing contract lengths in Figure 9. Conditional on the landowner being willing to enroll, a longer contract length will shield parcels from price spikes in the real estate market over longer periods, delaying the expected time of development (Table 3). As a result, for sufficiently high incentive levels (e.g. $c = \$800$), a long contract period (e.g. $J = 30$ years) can significantly reduce cumulative probability of development (equivalently, increase expected time of development) from the business as usual scenario. However, if the incentive is too low (e.g., $c = \$100$, $J = 30$ years), the landowner will not enroll and the program will have no effect on timing of development (Table 3).

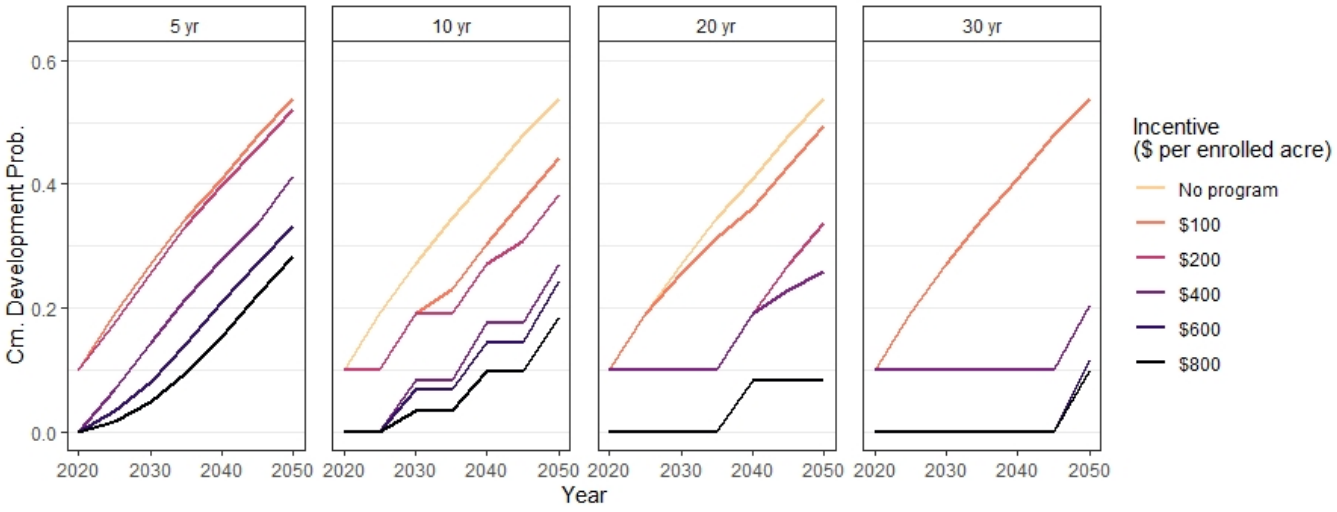

Figure 9: Cumulative probability of development for representative landowner, 2020-2050. Contract length J is shown by panel (5 years to 30 years, left to right).

Table 3: Single parcel expected time of development

	Contract length, J			
Incentive, c	5 years	10 years	20 years	30 years
Business as usual	2050			
\$100	2050	2055	2051	2050
\$200	2051	2057	2059	2062
\$400	2057	2064	2062	2064
\$600	2061	2066	2071	2070
\$800	2063	2069	2071	2072

4.3 Agricultural Resource Area conservation program effect

Given spatial heterogeneity in agricultural profits and real estate values, a given conservation program will have a wide variety of impacts on development across parcels (Figure 10). The program administrator will be interested in total conservation program performance in a given region.

I assume the Santa Clara County program administrator's objective is to minimize the expected area of development within the ARA for a given budget level. The budget-constrained development-minimizing program will manage the trade-off between attracting landowner enrollment (which increases as J decreases and as c increases) and protecting enrolled acres from development (which

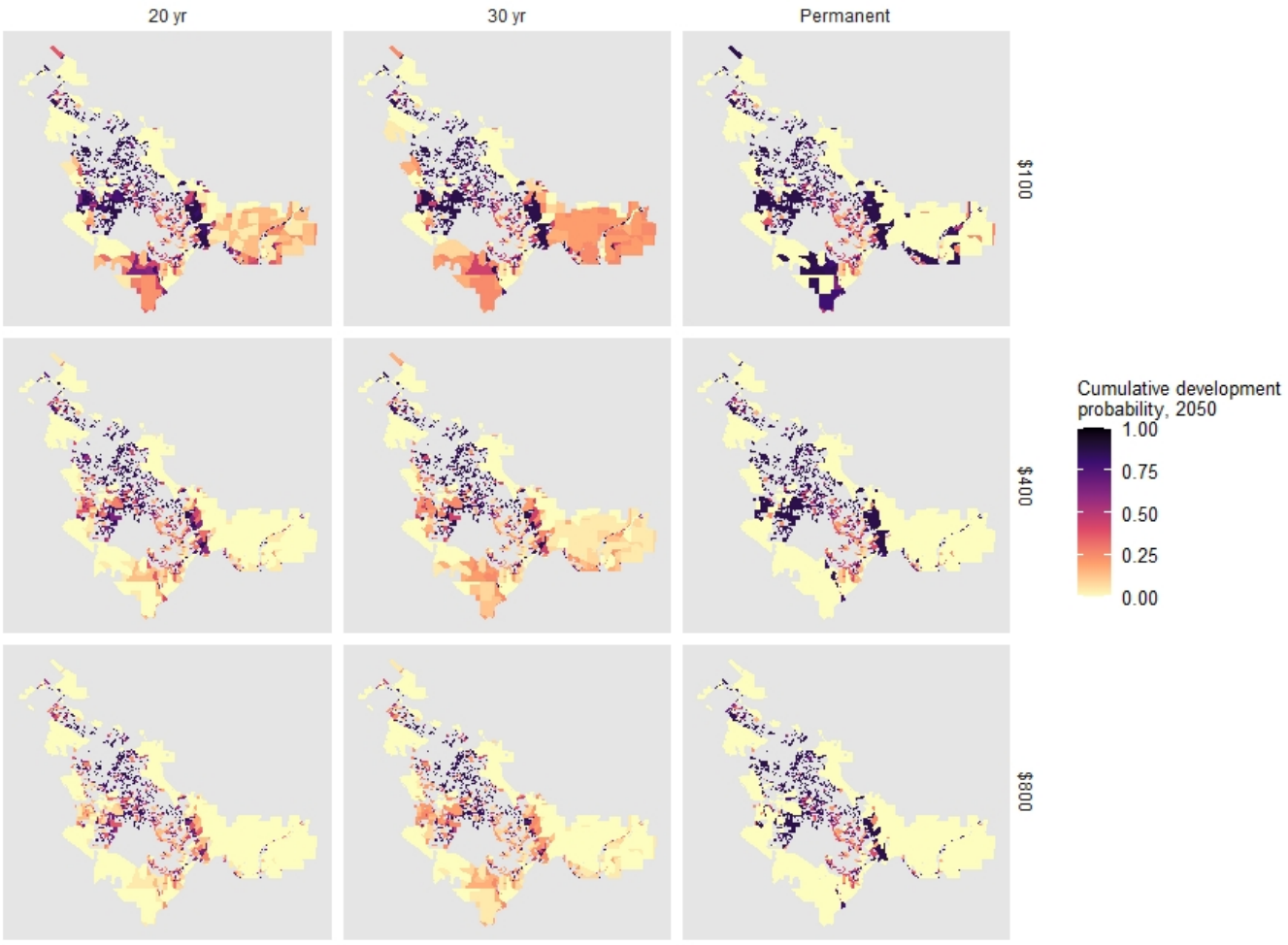

Figure 10: Cumulative probability of development in 2050 for Agricultural Resource Area (ARA) parcels. Contract length J is shown left to right (20 years, 30 years, and permanent easement) and incentive level is shown top to bottom ($100, $400, and $800 per enrolled acre).

increases as J increases). As the county budget increases, the program is able to protect more acres by increasing the per acre enrollment incentive (c), which also allows for increasing contract length J without impacting enrollment rates. Evaluating a range of annual county budgets ($10-30

million), this study predicts upwards of 40,000 acres of development could be avoided by 2050 compared to the business as usual scenario, on an expected value basis (Figure 11).

Figure 11 makes clear that the development-minimizing conservation program is not consistent across time steps. For example, in 2030, the 20-year contract length achieves the most avoided development for all incentive levels, whereas in 2040 the 30-year contract performs best. Since many parcels are predicted to enroll in 2020, the performance of each contract length declines following the end of the first enrollment cycle, and so by 2050 the 30-year contract falls behind both the permanent easement program and the 20-year contract.

Using these results, the program administrator would choose their preferred evaluation year and budget level, which would allow them to identify the contract length J that delivers the maximum avoided development for that year, and the incentive level c that ensures the budget constraint is met. For example, having chosen a budget of $20 million and evaluation year of 2050, the administrator would use results in Figure 11 to choose a contract length of 20 years and an incentive of slightly greater than $200 per acre.

5. Discussion and Conclusion

This study highlights important structural differences between a single-shot enrollment conservation program and a program in which re-enrollment is possible. First, re-enrollment allows for the conservation incentive to be capitalized into agricultural land value and therefore increases the landowner's reserve price at which they are willing to sell to a developer. The effect of the incentive on reserve price depends on contract length, with longer contracts resulting in stronger protection but lower capitalization effect. Second, unlike the single-shot enrollment setting, under the re-enrollment setting there is no optimal contract length from the perspective of the landowner because as contract length approaches zero the conservation program approaches a pure agricultural subsidy without constraint on land use change. However, program administrators will want to identify the conservation program, defined by a contract length and incentive level, that minimizes expected area of development for a given budget. The choice of optimal conservation program depends strongly on the evaluation year, particularly when evaluating a small region where the contract length can cause large swings in the amount of protection provided year to year.

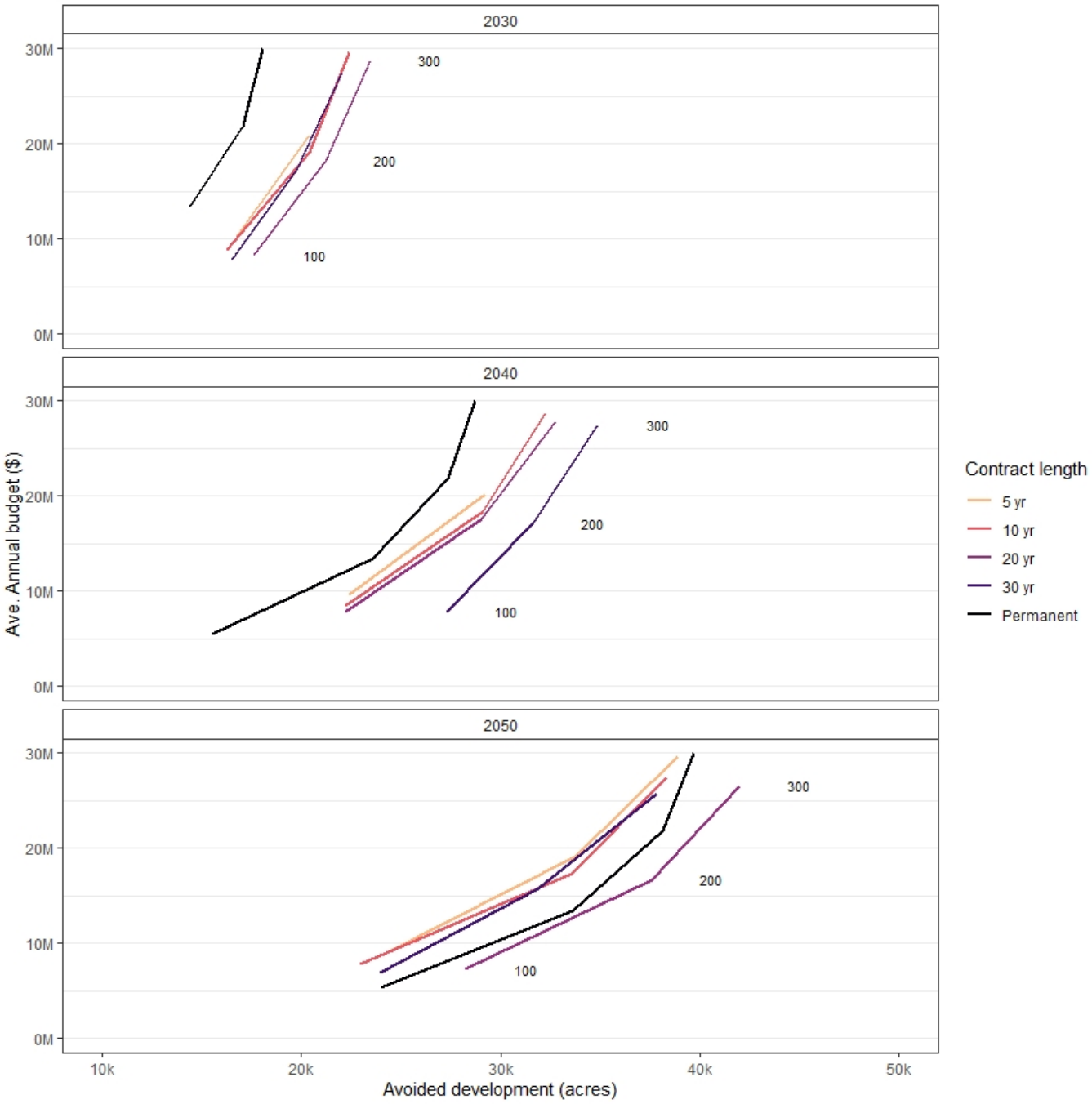

Figure 11: Conservation program performance by average annual budget. "Avoided development (acres)" is the difference in cumulative development between conservation program scenarios and business as usual for all ARA parcels, in 2030, 2040, and 2050. "Average annual budget ($)" is the average annual total program expenditure for all enrolled parcels between 2020 and 2030, 2040, and 2050. Incentive levels ($/acre-year) are shown in annotations for the leading contract length in each panel.

This study demonstrates that term-limited conservation programs may be able to reduce development rates by (1) subsidizing agricultural use and (2) "shielding" parcel from unanticipated real estate price shocks. However, unmanaged, long term market trends can drive suboptimal development as contracts end. Therefore, the term-limited program should be viewed as only one tool in the arsenal for managing land conservation. Options for long-term protection include changes to zoning ordinances, although any changes to allowable land uses may reduce land value and therefore agricultural landowner welfare.

There are a number of future avenues for research building on the results of this study. As with many dynamic and predictive models, it's difficult to validate model structure and to test historical predictions, due to limited time series availability. In this application, it is rare to find programs that implement a variety of contract lengths and incentive levels that would allow for testing the comparative statics described above. Future research could identify empirical settings that allow for testing key model predictions.

In estimating program effects over larger regions, the methods would need to account for the impacts of constraining agricultural land supply on real estate markets. Accounting for real estate market complexities is not trivial, markets are highly regionalized, and both locating and characterizing regional supply and demand elasticities can be confounded by business cycles. This work would also usefully account for regional preferences for alternative residential development options like urban in-fill.

The results presented here focus on a single scenario, where average county-wide parcel value grows constantly at the historical rate observed from 1985 to 2020. Scenario analysis should be employed to evaluate program performance over a broader range of possible futures.

Here I focused on a single measure of program benefit, expected area of development. Program performance should be evaluated across a suite of benefits, including avoided greenhouse gas emissions, avoided water runoff, and other development impacts. Accounting more fully for program benefits would allow for designing a conservation program that increases social welfare rather than simply minimizing programmatic costs.

There are many complications in landowner decision making for which this study's model structure does not account. In addition to landowner risk neutrality, I assume the landowner's objective is only influenced by agricultural profits and land asset value, while many landowners value non-

market amenities like open space and family tradition that are not fully priced into land markets. Hedonic valuation methods could therefore usefully be paired with this modeling approach. Furthermore, landowners are likely to be influenced by demographic and generational dynamics, with agricultural parcel sales more likely when a parent passes. Lacking data on parcel ownership age or landowner age distribution, it is difficult to predict about how this structural omission would impact results.

The modeling approach demonstrated in this study could be usefully applied in any setting where we seek to predict voluntary landowner decisions over a limited term, given some stochastic component. In particular, this approach could be used in evaluating the effect of voluntary carbon offset and conservation programs on net greenhouse gas emissions, a literature which currently abstracts many of the nuances of both realistic policy and landowner decision-making. Structural representation of landowner decisions to participate in term-limited programs can help determine the true costs of attracting enrollment as well as the effects of limited contract length on environmental gains and reversals over time.

References

Alig, Ralph, Greg Latta, Darius Adams, and Bruce McCarl. 2010. "Mitigating Greenhouse Gases: The Importance of Land Base Interactions between Forests, Agriculture, and Residential Development in the Face of Changes in Bioenergy and Carbon Prices." Forest Sector Models and Their Application 12 (1): 67–75. https://doi.org/10.1016/j.forpol.2009.09.012.

Ando, Amy W., and Xiaoxuan Chen. 2011. "Optimal Contract Lengths for Voluntary Ecosystem Service Provision with Varied Dynamic Benefit Functions." Conservation Letters 4 (3): 207–18. https://doi.org/10.1111/j.1755-263X.2010.00160.x.

Batker, David, Aaron Schwartz, Rowan Schmidt, Andrea MacKenzie, Jake Smith, and Jim Robins. 2014. "Nature's Value in Santa Clara County." Earth Economics and Santa Clara Valley Open Space Authority. http://www.openspaceauthority.org/about/pdf/NaturesValue$_SCC_int.pdf$.

Cai, Yongxia, Christopher M. Wade, Justin S. Baker, Jason P. H. Jones, Gregory S. Latta, Sara B. Ohrel, Shaun A. Ragnauth, and Jared R. Creason. 2018. "Implications of Alternative Land Conversion Cost Specifications on Projected Afforestation Potential in the United States." RTI Press. https://doi.org/10.3768/rtipress.2018.op.0057.1811.

Capozza, Dennis R., and Robert W. Helsley. 1989. "The Fundamentals of Land Prices and Urban Growth." Journal of Urban Economics 26 (3): 295–306. https://doi.org/10.1016/0094-1190(89)90003-X.

Case, Karl E., and Robert J. Shiller. 1989. "The Efficiency of the Market for Single-Family Homes." The American Economic Review 79 (1): 125–37.

Chen, Yong, Elena Irwin, and Ciriyam Jayaprakash. 2011. "An Agent-Based Model of Exurban Land Development."

Chen, Yong, Elena Irwin, Ciriyam Jayaprakash, and Kyoung Jin Park. 2021. "An Agent Based

Model of a Thinly Traded Land Market in an Urbanizing Region." Journal of Artificial Societies and Social Simulation 24 (2): 1. https://doi.org/10.18564/jasss.4518.

Cho, Seong-Hoon, Roland K. Roberts, Taeyoung Kim, Sae Woon Park, and Heeho Kim. 2014. "Chapter 6 - Varying Implicit Prices of Housing Attributes: Testing Tiebout Theory." In Handbook of Asian Finance, edited by Greg N. Gregoriou and David Lee Kuo Chuen, 117–29. San Diego: Academic Press. https://doi.org/10.1016/B978-0-12-800986-4.00006-6.

Cramton, Peter, Daniel Hellerstein, Nathaniel Higgins, Richard Iovanna, Kristian López-Vargas, and Steven Wallander. 2021. "Improving the Cost-Effectiveness of the Conservation Reserve Program: A Laboratory Study." Journal of Environmental Economics and Management 108 (July): 102439. https://doi.org/10.1016/j.jeem.2021.102439.

Crawford, Gordon W., and Michael C. Fratantoni. 2003. "Assessing the Forecasting Performance of Regime-Switching, ARIMA and GARCH Models of House Prices." Real Estate Economics 31 (2): 223–43. https://doi.org/10.1111/1540-6229.00064.

De Pinto, Alessandro, and Gerald C. Nelson. 2009. "Land Use Change with Spatially Explicit Data: A Dynamic Approach." Environmental and Resource Economics 43 (2): 209–29. https://doi.org/10.1007/s10640-008-9232-x.

Denning, Carrie A., Robert I. Mcdonald, and Jon Christensen. 2010. "Did Land Protection in Silicon Valley Reduce the Housing Stock?" Biological Conservation 143 (5): 1087–93. https://doi.org/10.1016/j.biocon.2010.01.025.

Dixit, Avinash, and Robert Pindyck. 1994. Investment under Uncertainty. Princeton University Press.

Drechsler, Martin, Karin Johst, and Frank Wätzold. 2017. "The Cost-Effective Length of Contracts for Payments to Compensate Land Owners for Biodiversity Conservation Measures." Biological Conservation 207 (March): 72–79. https://doi.org/10.1016/j.biocon.2017.01.014.

Dumortier, Jerome. 2013. "The Effects of Uncertainty under a Cap-and-Trade Policy on Afforestation in the United States." Environmental Research Letters 8 (4): 044020. https://doi.org/10.1088/1748-9326/8/4/044020.

Feng, Yongjiu, Yan Liu, and Michael Batty. 2016. "Modeling Urban Growth with GIS Based Cellular Automata and Least Squares SVM Rules: A Case Study in Qingpu–Songjiang Area of Shanghai, China." Stochastic Environmental Research and Risk Assessment 30 (5): 1387–1400. https://doi.org/10.1007/s00477-015-1128-z.

Filatova, Tatiana. 2015. "Empirical Agent-Based Land Market: Integrating Adaptive Economic Behavior in Urban Land-Use Models." Computers, Environment and Urban Systems 54 (November): 397–413. https://doi.org/10.1016/j.compenvurbsys.2014.06.007.

Fisher, Jeff, David Geltner, and Henry Pollakowski. 2007. "A Quarterly Transactions-Based Index of Institutional Real Estate Investment Performance and Movements in Supply and Demand." The Journal of Real Estate Finance and Economics 34 (1): 5–33. https://doi.org/10.1007/s11146-007-9001-6.

Fisher, Jeffrey, Dean Gatzlaff, David Geltner, and Donald Haurin. 2003. "Controlling for the Impact of Variable Liquidity in Commercial Real Estate Price Indices." Real Estate Economics 31 (2): 269–303. https://doi.org/10.1111/1540-6229.00066.

Fujita, Masahisa. 1976. "Spatial Patterns of Urban Growth: Optimum and Market." Journal of Urban Economics 3 (3): 209–41. https://doi.org/10.1016/0094-1190(76)90041-3.

Ghysels, Eric, Alberto Plazzi, Rossen Valkanov, and Walter Torous. 2013. "Chapter 9 - Forecasting Real Estate Prices." In Handbook of Economic Forecasting, edited by Graham Elliott and Allan Timmermann, 2:509–80. Elsevier. https://doi.org/10.1016/B978-0-444-53683-9.00009-8.

Glebe, Thilo W. 2022. "The Influence of Contract Length on the Performance of Sequential Conservation Auctions." American Journal of Agricultural Economics 104 (2): 739–64. https://doi.org/

10.1111/ajae.12247.

Glumac, Brano, Marcos Herrera-Gomez, and Julien Licheron. 2019. "A Hedonic Urban Land Price Index." Land Use Policy 81 (February): 802–12. https://doi.org/10.1016/j.landusepol.2018.11.032.

Grassi, Giacomo, Jo House, Frank Dentener, Sandro Federici, Michel den Elzen, and Jim Penman. 2017. "The Key Role of Forests in Meeting Climate Targets Requires Science for Credible Mitigation." Nature Climate Change 7 (3): 220–26. https://doi.org/10.1038/nclimate3227.

Gu, Anthony. 2002. "The Predictability of House Prices." Journal of Real Estate Research 24 (3): 213–34. https://doi.org/10.1080/10835547.2002.12091099.

Guirguis, Hany S., Christos I. Giannikos, and Randy I. Anderson. 2005. "The US Housing Market: Asset Pricing Forecasts Using Time Varying Coefficients." The Journal of Real Estate Finance and Economics 30 (1): 33–53. https://doi.org/10.1007/s11146-004-4830-z.

Gulati, Sumeet, and James Vercammen. 2005. "The Optimal Length of an Agricultural Carbon Contract." University of British Columbia, Food and Resource Economics. https://EconPapers.repec.org/RePEc:ags:ubcwps:15843.

Haim, David, Eric M. White, and Ralph J. Alig. 2014. "Permanence of Agricultural Afforestation for Carbon Sequestration under Stylized Carbon Markets in the U.S." Forest Policy and Economics 41 (April): 12–21. https://doi.org/10.1016/j.forpol.2013.12.008.

———. 2016. "Agriculture Afforestation for Carbon Sequestration Under Carbon Markets in the United States: Leakage Behavior from Regional Allowance Programs." Applied Economic Perspectives and Policy 38 (1): 132–51. https://doi.org/10.1093/aepp/ppv010.

Hultman, Nathan, Leon Clarke, Haewon McJeon, Ryna Cui, Pete Hansel, Emily McGlynn, Kowan O'Keefe, John O'Neill, Celeste Wanner, and Alicia Zhao. 2021. "Working Paper: Charting an Ambitious U.S. NDC of 51% Reductions by 2030." Center for Global Sustainability, University of Maryland. https://cgs.umd.edu/research-impact/publications/working-paper-charting-ambitious-us-ndc-51-reductions-2030.

IPCC. 2019. "Climate Change and Land: An IPCC Special Report on Climate Change, Desertification, Land Degradation, Sustainable Land Management, Food Security, and Greenhouse Gas Fluxes in Terrestrial Ecosystems. [P.R. Shukla, J. Skea, E. Calvo Buendia, V. Masson-Delmotte, H.-O. Pörtner, D. C. Roberts, P. Zhai, R. Slade, S. Connors, R. van Diemen, M. Ferrat, E. Haughey, S. Luz, S. Neogi, M. Pathak, J. Petzold, J. Portugal Pereira, P. Vyas, E. Huntley, K. Kissick, M. Belkacemi, J. Malley, (Eds.)]."

———. 2022. "Summary for Policymakers." In Climate Change 2022: Mitigation of Climate Change. Contribution of Working Group III to the Sixth Assessment Report of the Intergovernmental Panel on Climate Change. [P.R. Shukla, J. Skea, R. Slade, A. Al Khourdajie, R. van Diemen, D. McCollum, M. Pathak, S. Some, P. Vyas, R. Fradera, M. Belkacemi, A. Hasija, G. Lisboa, S. Luz, J. Malley, (Eds.)]. Cambridge, UK and New York, NY, USA: Cambridge University Press. doi: 10.1017/9781009157926.001.

Irwin, Elena G., and Nancy E. Bockstael. 2002. "Interacting Agents, Spatial Externalities and the Evolution of Residential Land Use Patterns." Journal of Economic Geography 2 (1): 31–54.

Jackson, Robert B., and Justin S. Baker. 2010. "Opportunities and Constraints for Forest Climate Mitigation." BioScience 60 (9): 698–707. https://doi.org/10.1525/bio.2010.60.9.7.

Juutinen, Artti, Markku Ollikainen, Mikko Mönkkönen, Pasi Reunanen, Olli-Pekka Tikkanen, and Jari Kouki. 2014. "Optimal Contract Length for Biodiversity Conservation under Conservation Budget Constraint." Forest Policy and Economics 47: 14–24. https://doi.org/10.1016/j.forpol.2013.11.008.

Karlin, Samuel, and Howard Taylor. 1975. "Chapter 7 - Brownian Motion." In A First Course in Stochastic Processes (Second Edition), edited by Samuel Karlin and Howard Taylor, Second

Edition, 340–91. Boston: Academic Press. https://doi.org/10.1016/B978-0-08-057041-9.50011-8.

Kim, Youjung, Galen Newman, and Burak Güneralp. 2020. "A Review of Driving Factors, Scenarios, and Topics in Urban Land Change Models." Land 9 (8). https://doi.org/10.3390/land9080246.

Kirwan, Barrett, Ruben N. Lubowski, and Michael J. Roberts. 2005. "How Cost-Effective Are Land Retirement Auctions? Estimating the Difference between Payments and Willingness to Accept in the Conservation Reserve Program." American Journal of Agricultural Economics 87 (5): 1239–47. https://doi.org/10.1111/j.1467-8276.2005.00813.x.

Kuo, Chiong-Long. 1996. "Serial Correlation and Seasonality in the Real Estate Market." The Journal of Real Estate Finance and Economics 12 (2): 139–62. https://doi.org/10.1007/BF00132264.

Langpap, Christian. 2004. "Conservation Incentives Programs for Endangered Species: An Analysis of Landowner Participation." Land Economics 80 (3): 375–88. https://doi.org/10.2307/3654727.

Latta, Gregory, Darius M. Adams, Ralph J. Alig, and Eric White. 2011. "Simulated Effects of Mandatory versus Voluntary Participation in Private Forest Carbon Offset Markets in the United States." Journal of Forest Economics 17 (2): 127–41. https://doi.org/10.1016/j.jfe.2011.02.006.

Lawley, Chad, and Wanhong Yang. 2015. "Spatial Interactions in Habitat Conservation: Evidence from Prairie Pothole Easements." Journal of Environmental Economics and Management 71 (May): 71–89. https://doi.org/10.1016/j.jeem.2015.02.003.

Lennox, Gareth D., and Paul R. Armsworth. 2011. "Suitability of Short or Long Conservation Contracts under Ecological and Socio-Economic Uncertainty." Ecological Modelling 222 (15): 2856–66. https://doi.org/10.1016/j.ecolmodel.2011.04.033.

Lewandrowski, Jan, Mark Peters, Carol Jones, Robert House, Mark Sperow, Marlen Eve, and Keith Paustian. 2004. "Economics of Sequestering Carbon in the U.S. Agricultural Sector." Technical Bulletin No. (TB-1909). United States Department of Agriculture.

Lewis, David J., and Andrew J. Plantinga. 2007. "Policies for Habitat Fragmentation: Combining Econometrics with GIS-Based Landscape Simulations." Land Economics 83 (2): 109–27.

Lubowski, Ruben N., Andrew J. Plantinga, and Robert N. Stavins. 2006. "Land-Use Change and Carbon Sinks: Econometric Estimation of the Carbon Sequestration Supply Function." Journal of Environmental Economics and Management 51 (2): 135–52.

Lynch, Lori, and Sabrina J. Lovell. 2003. "Combining Spatial and Survey Data to Explain Participation in Agricultural Land Reservation Programs." Land Economics 79 (2): 259–76. https://doi.org/10.2307/3146870.

Magliocca, Nicholas, Virginia McConnell, and Margaret Walls. 2015. "Exploring Sprawl: Results from an Economic Agent-Based Model of Land and Housing Markets." Ecological Economics 113 (May): 114–25. https://doi.org/10.1016/j.ecolecon.2015.02.020.

Mamine, Fateh, M'hand Fares, and Jean Joseph Minviel. 2020. "Contract Design for Adoption of Agrienvironmental Practices: A Meta-Analysis of Discrete Choice Experiments." Ecological Economics 176 (October): 106721. https://doi.org/10.1016/j.ecolecon.2020.106721.

Mason, Charles F., and Andrew J. Plantinga. 2013. "The Additionality Problem with Offsets: Optimal Contracts for Carbon Sequestration in Forests." Journal of Environmental Economics and Management 66 (1): 1–14. https://doi.org/10.1016/j.jeem.2013.02.003.

Mills, David. 1981. "Growth, Speculation and Sprawl in a Monocentric City." Journal of Urban Economics 10 (2): 201–26.

Mitani, Yohei, and Henrik Lindhjem. 2022. "Meta-Analysis of Landowner Participation in Voluntary Incentive Programs for Provision of Forest Ecosystem Services." Conservation Biology 36 (1): e13729. https://doi.org/10.1111/cobi.13729.

Murphy, Alvin. 2018. "A Dynamic Model of Housing Supply." American Economic Journal: Economic Policy 10 (4): 243–67. https://doi.org/10.1257/pol.20150297.

Murray, Brian C., Brent Sohngen, Allan J. Sommer, Brooks Depro, Kelly Jones, Bruce A. McCarl, Dhazn Gillig, Benjamin DeAngelo, and Kenneth Andrasko. 2005. "Greenhouse Gas Mitigation Potential in U.S. Forestry and Agriculture." EPA 430-R-05-006. United States Environmental Protection Agency.

NatureVest. 2014. "Investing in Conservation: A Landscape Assessment of an Emerging Market." https://thegiin.org/research/publication/investing-in-conservation-a-landscape-assessment-of-an-emerging-market.

Nelson, Erik, Stephen Polasky, David Lewis, Andrew Plantinga, Eric Lonsdorf, Denis White, David Bael, and Joshua Lawler. 2008. "Efficiency of Incentives to Jointly Increase Carbon Sequestration and Species Conservation on a Landscape." Proceedings of the National Academy of Sciences 105 (28): 9471–76. https://doi.org/10.1073/pnas.0706178105.

Pachamanova, Dessislava A., and Frank J. Fabozzi. 2011. "Modeling Asset Price Dynamics." In The Theory and Practice of Investment Management, 125–58. John Wiley Sons, Ltd. https://doi.org/10.1002/9781118267028.ch6.

Parker, Dawn C., and Vicky Meretsky. 2004. "Measuring Pattern Outcomes in an Agent-Based Model of Edge-Effect Externalities Using Spatial Metrics." From Pattern to Process: Landscape Fragmentation and the Analysis of Land Use/Land Cover Change 101 (2): 233–50. https://doi.org/10.1016/j.agee.2003.09.007.

Parker, Dawn Cassandra, and Tatiana Filatova. 2008. "A Conceptual Design for a Bilateral Agent-Based Land Market with Heterogeneous Economic Agents." GeoComputation: Modeling with Spatial Agents 32 (6): 454–63. https://doi.org/ 10.1016/j.compenvurbsys.2008.09.012.

Parker, Dominic P., and Walter N. Thurman. 2018. "Tax Incentives and the Price of Conservation." Journal of the Association of Environmental and Resource Economists 5 (2): 331–69. https://doi.org/10.1086/695615.

———. 2019. "Private Land Conservation and Public Policy: Land Trusts, Land Owners, and Conservation Easements." Annual Review of Resource Economics 11 (1): 337–54. https://doi.org/10.1146/annurev-resource-100518-094121.

Plantinga, Andrew. 2007. "The Economics of Conservation Easements." In Essay 5 In Land Policies and Their Outcomes, Proceedings Of 2006 Land Policy Conference. Lincoln Institute of Land Policy.

Plantinga, Andrew J., and SoEun Ahn. 2002. "Efficient Policies for Environmental Protection: An Econometric Analysis of Incentives for Land Conversion and Retention." Journal of Agricultural and Resource Economics 27 (1): 128–45.

Plantinga, Andrew J, Ralph Alig, and Hsiang-tai Cheng. 2001. "The Supply of Land for Conservation Uses: Evidence from the Conservation Reserve Program." Resources, Conservation and Recycling 31 (3): 199–215. https://doi.org/10.1016/S0921-3449(00)00085-9.

Plantinga, Andrew J., Ruben N. Lubowski, and Robert N. Stavins. 2002. "The Effects of Potential Land Development on Agricultural Land Prices." Journal of Urban Economics 52 (3): 561–81. https://doi.org/10.1016/S0094-1190(02)00503-X.

Plazzi, Alberto, Walter Torous, and Rossen Valkanov. 2011. "Exploiting Property Characteristics in Commercial Real Estate Portfolio Allocation." The Journal of Portfolio Management 37 (5): 39–50. https://doi.org/10.3905/jpm.2011.37.5.039.

Power, Gabriel J., and Calum G. Turvey. 2010. "U.S. Rural Land Value Bubbles." Applied Economics Letters 17 (7): 649–56. https://doi.org/10.1080/13504850802297970.

Santa Clara County. 2020. "Santa Clara 2020 Crop Report." https://ag.sccgov.org/2020-crop-report.

Santa Clara County Open Space Authority. 2018. "Santa Clara Valley Agricultural Plan."

Schatzki, Todd. 2003. "Options, Uncertainty and Sunk Costs: An Empirical Analysis of Land Use Change." Journal of Environmental Economics and Management 46 (1): 86–105. https://doi.org/10.1016/S0095-0696(02)00030-X.

Schneider, Uwe A, and Bruce A McCarl. 2002. "The Potential of U.S. Agriculture and Forestry to Mitigate Greenhouse Gas Emissions: An Agricultural Sector Analysis." Working Paper 02-WP 300, 26.

———. 2003. "Economic Potential of Biomass Based Fuels for Greenhouse Gas Emission Mitigation." Environmental and Resource Economics 24: 291–312.

Stewart, Brendan, and Timothy P. Duane. 2009. "Easement Exchanges for Agricultural Conservation: A Case Study Under the Williamson Act in California." Landscape Journal 28 (2): 181–97. https://doi.org/10.3368/lj.28.2.181.

Stoms, David, Patrick Jantz, Frank Davis, and Gregory DeAngelo. 2009. "Strategic Targeting of Agricultural Conservation Easements as a Growth Management Tool." Land Use Policy 26 (October): 1149–61. https://doi.org/10.1016/j.landusepol.2009.02.004.

Taylor, Mykel R., Nathan P. Hendricks, Gabriel S. Sampson, and Dillon Garr. 2021. "The Opportunity Cost of the Conservation Reserve Program: A Kansas Land Example." Applied Economic Perspectives and Policy 43 (2): 849–65. https://doi.org/10.1002/aepp.13040.

Tourte, Laura, Richard Smith, Jeremy Murdock, and Daniel Sumner. 2019. "Sample Costs to Produce and Harvest Romaine Hearts." University of California Agriculture and Natural Resources Cooperative Extension and Agricultural Issues Center, UC Davis Department of Agricultural and Resource Economics.

Towe, Charles A. 2010. "Testing the Effect of Neighboring Open Space on Development Using Propensity Score Matching." 2010 Annual Meeting, July 25-27, 2010, Denver, Colorado. Agricultural and Applied Economics Association. https://ideas.repec.org/p/ags/aaea10/61512.html.

Towe, Charles A., Cynthia J. Nickerson, and Nancy Bockstael. 2008. "An Empirical Examination of the Timing of Land Conversions in the Presence of Farmland Preservation Programs." American Journal of Agricultural Economics 90 (3): 613–26. https://doi.org/10.1111/j.1467-8276.2007.01131.x.

U.S. BEA. 2020. "GDP by County, Metro, and Other Areas." U.S. Bureau of Economic Analysis (BEA). 2020.

U.S. EPA. 2019. "SAB Review of Framework for Assessing Biogenic CO2 Emissions from Stationary Sources (2014), Tech. Rep. U.S. EPA Science Advisory Board, Biogenic Carbon Emissions Panel."

USDA NASS. 2020. "USDA/NASS QuickStats Ad-Hoc Query Tool." 2020.

———. 2022. "2020 California Cropland Data Layer — NASS/USDA." Data.raster digital data. Cropland Data Layer - California 2020. USDA, NASS, Spatial Analysis Research Section. February 1, 2022.

Verburg, Peter H, Peter Alexander, Tom Evans, Nicholas R Magliocca, Ziga Malek, Mark DA Rounsevell, and Jasper van Vliet. 2019. "Beyond Land Cover Change: Towards a New Generation of Land Use Models." Sustainability Governance and Transformation 38 (June): 77–85. https://doi.org/10.1016/j.cosust.2019.05.002.

Vercammen, James. 2019. "A Welfare Analysis of Conservation Easement Tax Credits." Journal of the Association of Environmental and Resource Economists 6 (1): 43–71. https://doi.org/10.1086/700721.

Wade, Christopher M., Jason P.H. Jones, Justin S. Baker, Kemen Austin, Yongxia Cai, Alison Bean, Greg Latta, et al. 2021. "Projecting the Impact of Socioeconomic and Policy Factors on Greenhouse Gas Emissions and Carbon Sequestration in U.S. Forestry and Agriculture."

Wallace, Nancy. 1996. "Hedonic-Based Price Indexes for Housing: Theory, Estimation, and Index Construction." Economic Review - Federal Reserve Bank of San Francisco, no. 3: 34–48.

Wheaton, William C. 1982. "Urban Residential Growth under Perfect Foresight." Journal of Urban Economics 12 (1): 1–21. https://doi.org/10.1016/0094-1190(82)90002-X.

White House. 2016. "United States Mid-Century Strategy for Deep Decarbonization." November 2016.

Wrenn, Douglas, Henry Klaiber, and David Newburn. 2017. "Confronting Price Endogeneity in a Duration Model of Residential Subdivision Development." Journal of Applied Econometrics 32 (3): 661–82.

Zipp, Katherine Y., David J. Lewis, and Bill Provencher. 2017. "Does the Conservation of Land Reduce Development? An Econometric-Based Landscape Simulation with Land Market Feedbacks." Journal of Environmental Economics and Management 81 (January): 19–37. https://doi.org/10.1016/j.jeem.2016.08.006.

3. The problem with pricing "carbon": exploring forest-driven albedo effects in DICELAND*

Abstract

Climate change policies encouraging up to a billion hectares of new forest this century focus only on CO_2 sequestration, ignoring other drivers of radiative forcing and risking inefficient outcomes. Increasing forest area, stand age, and carbon density removes CO_2 from the atmosphere, but may also decrease Earth's albedo, which increases radiative forcing and thus global surface temperatures. We build on the literature exploring this trade-off by directly quantifying the impact of forest-driven albedo change on global climate damages, carbon prices, and industrial vs. forest sector mitigation levels using the Dynamic Integrated model of Climate and the Economy (DICE) and the Global Timber Model (GTM), dubbing the new model DICELAND. Under policy limiting global warming below 2 degrees Celsius, the unexpected damages from ignoring albedo reach 22% of 2100 climate damages, with unexpected temperature change reaching 0.27 degrees Celsius. Accounting for albedo effects increases 2100 carbon prices by 36%, and requires the

* Co-authored with Alice Favero (Georgia Institute of Technology) and Bernardo Adolfo Bastien Olvera (University of California Davis). Emily McGlynn (lead author) developed the research design, developed the DICELAND model and methods, wrote DICELAND code and results calculations, and drafted the manuscript. Alice Favero produced all Global Timber Model outputs and provided guidance on methods, results, and discussion. Bernardo Adolfo Bastien Olvera provided guidance on the DICE model and supported DICELAND development.

industrial sector to reach zero greenhouse gas emissions a decade earlier (2050 rather than 2060). We suggest policymakers account for albedo effects to minimize climate mitigation costs.

1. Introduction

Economists have long dealt with the problem of environmental and natural resource externalities, most simply identified by Pigou as "incidental uncharged disservices" (1920). To efficiently address externalities, policy makers must (1) identify the problem (what is the phenomenon resulting in "uncharged" costs or benefits?), (2) quantify the resulting marginal costs or benefits, and (3) ultimately use regulation or pricing structure to manage economic activities such that the marginal cost of mitigation equals the marginal benefit of reducing the externality. Much of the economic literature has focused on steps (2) and (3), pointing to the efficiency of using taxes or market-based mechanisms to price the externality in accordance with marginal conditions of efficiency (e.g., Freeman 1982, Lyon and Farrow 1995, Muller and Mendelsohn 2009, Hsueh 2017). Yet inadequately or incompletely specifying the scope of the problem in step (1), whether purposefully or not, can create its own potential for economic inefficiency, even if steps (2) and (3) are executed to perfection.

A case in point is climate change policy, which has largely focused on the need to directly regulate or price greenhouse gas (GHG) emissions (Stern 2008, Weitzman 2009, Dasgupta 2014, Linn et al. 2014). GHG emissions are in fact a proxy for the primary externality driving climate change, which is radiative forcing in the Earth's atmosphere. The Intergovernmental Panel on Climate Change (IPCC) uses the concept of radiative forcing, measured as "the net change in the

energy balance of the Earth system due to some imposed perturbation" to quantify and compare how a variety of physical drivers contribute to anthropogenic climate change (Myhre et al. 2013). The largest of these drivers are increasing atmospheric concentrations of GHGs like CO_2, CH_4, and N_2O, making emissions of these gases a prime target for climate change policy. But other radiative forcing drivers include the effects of land use change on global albedo—the percent of incoming solar radiation reflected by the Earth's surface—and a host of other atmospheric dynamics (e.g. indirect formation of ozone and stratospheric water vapor; direct emissions of aerosols and their interactions with clouds). In this paper, we identify the economic inefficiency of focusing climate change policy solely on GHG emissions, particularly at the expense of ignoring land-driven albedo changes under global climate policy, even when GHG pollution is managed efficiently.

Radiative forcing due to anthropogenic GHG emissions over the Industrial Era (post 1750) is 2.83 Wm^{-2}, while the albedo effects of anthropogenic land use change over this period, largely characterized by conversion of forests to agriculture and settlement, has decreased radiative forcing by 0.15 Wm^{-2} (Myhre et al. 2013). To date, therefore, the "surface lightening" impact of land use change has had a cooling effect. But current policy proposals to expand and recover global forests are likely to reverse this trend.

Governments indicate forests will deliver 25% of GHG reductions pledged to date under the UN Paris Agreement (Grassi et al. 2017). Under scenarios to keep global warming below 1.5 °C above pre-industrial levels, global forest area could expand by up to 1.2 billion ha (Rogelj et al. 2018), an area greater than the size of China (World Bank 2018), with an upper bound of approximately 1.9 billion ha of new forestland (IIASA 2019, Riahi et al. 2017).

The challenge is that forests have one of the lowest albedos of any land surface cover, so converting agriculture or grasslands to forest can have a significant increase in radiative forcing at the Earth's surface (Myhre et al. 2013, Gibbard et al. 2005, Bala et al. 2007, Bonan 2008, Kirschbaum et al. 2011, Jones et al. 2013, Jones et al. 2015) and this effect is particularly pronounced in snow and ice-covered areas (Betts 2000, Gibbard et al. 2005, Bonan 2008, Arora and Montenegro 2011). Even if forest area is kept constant, extending forest stand age and tree density to increase carbon storage can result in land darkening and lower global albedo (Mykleby et al. 2017; Favero et al. 2018).

The albedo effect can be substantial in counteracting forest carbon sequestration benefits. Favero et al. (2018) found that, under a 2100 carbon price of US$147 tCO_2^{-1}, albedo effects reduce global forest climate mitigation potential by 46 percent. They further found that pricing albedo changes on a CO_2-equivalent basis encourages optimal location of forest area expansion, lower levels of forest expansion, decreases forest optimal rotation, and increases in forest carbon-equivalent density (again, with albedo change measured on a CO_2 equivalent basis and counted against forest carbon stock).

A significant contraction in forest climate mitigation potential for a given carbon price is equivalent to higher forest climate mitigation costs and therefore higher global climate mitigation costs overall. As a result, economic analysis suggests that efficient global carbon prices (that is, carbon prices that correspond to optimal global welfare when considering both climate damages and climate mitigation costs) will increase. More costly mitigation results in lower levels of efficient global climate mitigation, and more mitigation will come from the industrial sector rather

than the forest sector. We motivate these results using a simple economic model in the Theory section below.

To quantify the economy-wide climate policy implications of albedo change, we incorporate the global forest sector as an endogenous mitigation option into the Dynamic Integrated model for Climate and the Economy (DICE), a global model that maximizes net economic output with respect to climate mitigation costs, climate damages, and capital investment (Nordhaus 1992, Nordhaus 2014, Nordhaus 2018). We use the Global Timber Model (GTM) to parameterize the DICE forest sector mitigation costs, branding our new model DICELAND. DICE considers the land sector to be exogenous while GTM considers carbon prices exogenous, so pairing these models can answer the dynamic economy-wide questions posed here. With DICELAND we assess carbon prices, mitigation activity in the industrial and forestry sectors, and total climate damages across scenarios that both account for and ignore forest-driven albedo changes. We detail these models and scenarios in the Methods section.

Our work builds on previous research assessing the forest sector's role in global climate mitigation. Sohngen and Mendelsohn (2003) solved iteratively between GTM and DICE for carbon rental rates that are consistent across both models, finding that forest carbon sequestration could account for one third of future CO_2 abatement. Favero et al. (2017) similarly solved iteratively between the integrated assessment model WITCH and GTM to assess scenarios of using forests for bioenergy production versus carbon storage. However, neither paper includes a control variable for mitigating land sector radiative forcing in the general equilibrium model as we do in this paper, so their carbon prices do not reflect optimal mitigation across both industrial and forest sectors, nor

does either paper reflect albedo interactions. Eriksson (2015) included three new control variables in DICE to optimize over roundwood harvest, bioenergy harvest, and deforestation to achieve optimal global climate mitigation in both the industrial and forest sectors, but does not include the option of forest management intensification, as GTM does, nor are albedo effects included. Increasing forest management intensity is an important carbon sequestration alternative to forest expansion, particularly when assessing albedo effects.

We also benefit from literature that identifies trade-offs between forest carbon sequestration and albedo change through dynamic optimization. Thompson et al. (2009) first looked at the effects of albedo on optimal forest age under climate policy for a single stand. Mykleby et al. (2017) estimated these trade-offs with respect to optimal forest rotation age in different climatic and vegetation regions in North America, identifying a latitudinal dividing line between areas that resulted in net climate benefits of expanding forest area vs. net climate damages. We build on this literature by incorporating forest albedo effects into a global integrated assessment model and exploring effects on optimal mitigation levels in forests and other sectors, carbon prices, and climate damages.

A number of integrated assessment models, such as GCAM (JGCRI 2019), IMAGE (Stehfest et al. 2010), MESSAGE-GLOBIOM, and REMIND-MAgPIE (IAMC 2018), already have endogenous land modules and could perform these types of analyses. For example, Jones et al. (2015) incorporated albedo impacts from land use change into GCAM to identify potential effects on energy sector GHG reductions and carbon prices. However, their carbon price is not applied to albedo effects directly, so they do not allow for increasing efficiency of land use in response to

pricing albedo effects, nor are they able to estimate efficient mitigation levels across both land and industrial sectors. Furthermore, Jones et al. (2015) only considers the albedo effects of changes in forest area, not due to changes in forest management, for example the additional darkening that occurs due to increasing forest stand age. Finally, GCAM, like many other integrated assessment models, does not include the potential to increase forest management intensity, other than shifting forest land to more productive regions.

Albedo considerations have been built into GTM by Favero et al. (2018), allowing for directly pricing the radiative forcing effects from albedo change due to changes in forest area and forest management. We take advantage of the simplicity and transparency of the DICE model, as well as Favero et al.'s (2018) work to incorporate albedo into GTM, to complete our analysis efficiently. Similar analysis using other integrated assessment models is welcome. Given that other integrated assessment models do not include potential for forest management intensity, and thus rely more heavily on forest area expansion to increase carbon sequestration, we expect they may find greater economic effects of accounting for albedo.

Our analysis accounts for forest impacts on global surface temperature through albedo changes and carbon sequestration. However, other factors can influence the net effect of forests on global surface temperature. For instance, forests increase evapotranspiration, contributing to cloud formation (Spracklen et al. 2008) and lowering surface temperatures (Duveiller et al. 2018). Duveiller et al. found that observed global land use change over 2000-2015, largely driven by agricultural expansion and forest loss in lower latitudes, resulted in a net increase in local surface temperatures, with effects of lower evapotranspiration more than compensating for increased

albedo (2018). Furthermore, incorporating more trees into urban and settlement areas can reduce energy needs for heating and cooling (Wang et al. 2018). Any albedo effect from changes in forest area or management might be tempered or exacerbated by these other factors, which our model does not account for. Future research would usefully expand the model scope to estimate the total impact of land use and land management changes in a given region on global average surface temperature.

2. Theory

We introduce here a simple economic model to motivate how accounting for albedo might affect mitigation levels across sectors, total economy-wide mitigation levels, and mitigation shadow prices. The model is based on Cropper and Oates (1992) basic theory of environmental policy.

Consider a static system in which there is a phenomenon (here, radiative forcing) that results in negative impacts to society's utility. In this example, for simplicity, radiative forcing can occur through CO_2 emissions or through changes in albedo. CO_2 emissions result from production of some good that enhances social utility, thus we risk inefficient levels of production that do not account for the negative impacts of the radiative forcing without some mitigating policy. There are two options for mitigating radiative forcing, other than reducing production: (1) reduce the CO_2 intensity of good production, and (2) absorb CO_2 in forests, but this option can also increase radiative forcing by reducing albedo.

Assume social utility is strictly increasing in good consumption and strictly decreasing in radiative forcing, and twice continuously differentiable and strictly quasiconcave in its inputs. Good production and radiative forcing are defined by strictly convex production sets and are twice differentiable in their inputs. These assumptions allow for a unique solution that exists and is interior. For simplicity, we assume the options to mitigate CO_2 in either the goods producing sector or the forest sector are equivalent in terms of effectiveness (i.e. the marginal reduction in radiative forcing from absorbing one unit of CO_2 in forests is equal to the marginal reduction in radiative forcing from reducing one unit of CO_2 from goods production).

Let social utility be represented by equation (1):

$$W = U\big[X(E, I, Q), Q\big(E, M_E, M_{FC}, M_{FD}(M_{FC})\big)\big] \quad (1)$$

Where $U[\ \bullet\ ]$ represents social utility as a function of consumption of good X, which is increasing in investment I and in CO_2 emissions E through the production process, and is negatively impacted by radiative forcing Q. Utility is also directly decreasing in radiative forcing Q, which is increasing in CO_2 emissions E, and can be mitigated at levels M_E (reducing CO_2 intensity of good production) and M_{FC} (absorbing CO_2 in forests). Land darkening M_{FD} will increase radiative forcing as a function of forest CO_2 mitigation levels M_{FC}.

Investment in good production and total productive activity required for radiative forcing mitigation ($f(M_E)$, $f(M_{FC})$) must fall below some budget constraint R, so by strict monotonicity of W we can assume $I + f(M_E) + f(M_F) = R$. Therefore, production of good X is a function of

mitigation activity through the resource constraint R, such that $X(E,I,Q) = X(E,M_E,M_{FC},Q)$ – there are input tradeoffs between CO_2 mitigation and good production. We assume R is exogenous and unchanging and so do not include this as an input to good X production for the remainder of the analysis. To summarize the relationships in W:

$$\frac{\partial U}{\partial X} = U_X > 0, \qquad U_Q < 0$$

$$X_E > 0, \qquad X_{M_E} < 0, \qquad X_{M_{FC}} < 0, \qquad X_Q < 0$$

$$Q_E > 0, \qquad Q_{M_E} < 0, \qquad Q_{M_{FC}} < 0, \qquad Q_{M_{FD}} > 0$$

$$Q_{M_E} = Q_{M_{FC}} \text{ by equivalence of mitigation options}$$

$$\frac{dM_{FD}}{dM_{FC}} > 0$$

Second derivatives of radiative forcing Q with respect to CO_2 mitigation (M_E, M_{FC}) are positive, consistent with decreasing marginal benefit of mitigation. Second derivatives of X with respect to mitigation are also positive, consistent with increasing marginal costs of mitigation.

We want to maximize social welfare W with respect to CO_2 emissions E (as an "input" to production of good X), CO_2 mitigation in good production M_E, and CO_2 mitigation in the forest sector M_{FC}. First, let's ignore the land darkening term ($\frac{dM_{FD}}{dM_{FC}} = 0$ for all M_{FC}). By first order conditions we find the solution is characterized by the marginal cost of mitigation equaling the marginal benefit of mitigation, for M_k representing M_E or M_{FC}:

$$X_{M_k} = -\left[\frac{U_Q Q_{M_k}}{U_X} + X_Q Q_{M_k}\right] \quad (2)$$

The marginal cost of mitigation is represented by the reduction in good consumption (left hand side of equation (2)) and the marginal benefit represented by the increase in utility due to lower radiative forcing (first term on the right hand side of equation (2)) and the increase in good production due to lower radiative forcing (second term on the right hand side of equation (2)).

By the fact that $Q_{M_E} = Q_{M_{FC}}$, the marginal benefit of CO_2 mitigation is equivalent in both good production and forestry for any quantity of CO_2 mitigation. Thus the solution is also characterized by the marginal cost of mitigation being equal across consumption good and forest sectors, as we would expect.

Now we include the albedo term. The solution to good production CO_2 mitigation remains the same as equation (2), but the solution to forest CO_2 mitigation changes from equation (2) to:

$$X_{M_{FC}} + \left(\frac{U_Q}{U_X} + X_Q\right)\left(Q_{M_{FD}} \frac{dM_{FD}}{dM_{FC}}\right) = -\left[\frac{U_Q Q_{M_{FC}}}{U_X} + X_Q Q_{M_{FC}}\right] \quad (3)$$

Accounting for albedo increases the marginal cost of CO_2 mitigation from forests, on the left hand side of equation (3), which is now represented by the marginal cost with respect to good consumption (first term), and the marginal cost of higher radiative forcing from land darkening (second term). The marginal benefit remains the same on the right hand side of equation (3), thus we retain equality of marginal mitigation costs across good producing and forest sectors.

Since any given quantity of forest CO_2 mitigation is now characterized by higher marginal costs (a leftward shift in the mitigation supply curve), optimal forest CO_2 mitigation quantity M_{FC} will decrease. With the shadow price of CO_2 mitigation occurring where marginal cost equals marginal benefit, accounting for albedo effects will raise shadow prices. The unchanged mitigation supply curve of the goods sector, combined with a higher solution shadow price, results in higher mitigation from the goods sector.

This example simplifies these questions in a static, general model. To fully quantify these effects, and given the complexity of both the climate system and forestry sector, we require dynamic models and numerical analysis, which we undertake next.

3. Models and Methods

For the discussion of methods and results below, we use the term "carbon price" throughout, but for certain scenarios our carbon price also reflects marginal damages from albedo effects. A more appropriate term would be "radiative forcing price" but we use carbon price throughout for ease of policy communication. We make clear where albedo is and is not considered.

Our analysis uses DICE and GTM to assess the effects of considering forest-driven albedo changes on efficient global climate policy. We modify DICE to include an additional control variable representing the level of CO_2 mitigation in the forest sector and use GTM to parameterize the costs of forest sector CO_2 mitigation within DICE. The resulting model is called DICELAND. We describe DICELAND and GTM in more detail below.

With DICELAND we assess carbon prices, mitigation activity in the industrial and forestry sectors, and total climate damages across two radiative forcing accounting (*Traditional*, *Integrated*) and two global climate policy (*Optimal*, *2 Degree*) scenario components (Table 1). We also present *Traditional, Net Albedo* (*TNA*) results, wherein albedo effects are accounted for *ex post* under the *Traditional* accounting scenario, as well as a *No Land* scenario, wherein GHG mitigation can only be provided by the industrial sector. Table 1 shows how we use these scenario components to build eight different scenarios, with each scenario represented by one radiative forcing accounting component and one global climate policy component.

Scenario components		*Description*	*Scenarios*							
			Opt Trad	Opt TNA	Opt Int	Opt No Land	2 Deg Trad	2 Deg TNA	2 Deg Int	2 Deg No Land
Forest carbon accounting, policy	*Traditional*	DICELAND considers only forest CO_2 sequestration impacts on radiative forcing when optimizing forest sector mitigation	✓				✓			
	Integrated	*DICELAND* accounts for both albedo and CO_2 sequestration impacts, converting any forest-driven albedo change into carbon-equivalents on a radiative forcing basis (Favero et al. 2018)			✓				✓	
	Traditional, net albedo	DICELAND uses *Traditional* forest carbon accounting. Albedo effects on net forest CO_2 sequestration, global temperature, and climate damages are calculated *ex post*		✓				✓		

	No Land	DICELAND only allows mitigation from the industrial sector				✓				✓
Global climate policy	*Optimal*	DICELAND optimizes global welfare over 2015-2520 unconstrained	✓	✓	✓	✓				
	2 Degree	DICELAND optimizes global welfare such that global temperature increase stays below 2 degree Celsius following 2110					✓	✓	✓	✓

Table 1. DICELAND Scenarios

The Global Timber Model (GTM) is a detailed partial equilibrium economic model that accounts for spatially-explicit global forest stocks and growth rates and optimizes the net present value of consumer and producer surplus in timber markets, originally developed by Sohngen et al. (1999). The model covers 200 forest types, 16 global regions, and three carbon pools (aboveground biomass, soil carbon, and wood products). Forest carbon stock at a given point in time is a function of historical changes in forest land area, forest growth rates, and management intensity choices (e.g. planting, fertilization, and other management inputs like thinning). GTM uses exogenous carbon prices to predict changes in forest management behavior and forest area under climate policy scenarios. For more discussion of GTM's structure, see Favero et al. (2018) and Tian et al. (2018).

Favero et al. (2018) used GTM to assess the effect of accounting for albedo on optimal forest carbon sequestration. They used MODIS satellite imagery and the MODIS white-sky albedo dataset to estimate the difference in mean annual albedo between mature forests and cropland or

bareland by dominant forest type for each climatic region. The difference in albedo between land cover types is converted into surface radiative forcing, which is then converted into an equivalent change in atmospheric CO_2 concentration. Finally, the change in atmospheric CO_2 concentration is converted into an equivalent CO_2 emission per hectare, or the amount of CO_2-equivalent emissions that would result in the same radiative forcing as that attributable to albedo changes from a hectare of cropland or bareland being converted to mature forest. They also calculated albedo 'decay' as forest matures, interpolating albedo between bare land and mature forest. The result is regional- and forest type-specific empirical estimates of the albedo impacts of converting land to forest and increasing forest stand age. Favero et al. (2018) incorporated these estimates into GTM by subtracting any albedo changes from forest carbon stock on the radiative forcing basis described above. Thus as the model seeks to optimize producer surplus under a carbon pricing regime, inefficient albedo change is avoided to achieve higher carbon payments. We use this version of GTM for our analysis below.

The Dynamic Integrated model of Climate and the Economy (DICE) is a well-studied model originally developed by Nordhaus (1992). It is a global optimal control model that optimizes social welfare with respect to climate damages and climate mitigation costs. We use a version of DICE coded for MATLAB by Faulwasser, Kellett, and Weller (2016); conventional DICE is coded in GAMS. The DICE-2013R manual provides additional information about model structure and code (Nordhaus and Sztorc 2013), but the equations listed below conform to the 2016 MATLAB version. We use parameter values consistent with Nordhaus (2016), except when

otherwise specified. In particular, we use DICE 2016 default pure rate of time preference (1.5%) and default elasticity of marginal utility of consumption (1.45) for all scenarios.

The two DICE control variables are savings rate of global economic output (s) and CO_2 mitigation rate in the industrial sector (μ). Three state variables are global average surface temperature (T), atmospheric CO_2 concentration (M), and capital (K). Global population is exogenous and acts as the labor input to a Cobb-Douglas global economic output function (equation (4)).

The conventional DICE industrial CO_2 mitigation control variable (μ) enters the system of equations as a percent reduction of global emissions (equation (5)), and the mitigation cost enters as a proportional reduction of global economic output (equations (6) and (8)). In conventional DICE, the land sector emits CO_2 at exogenously determined levels which decline to zero over time. Global welfare is a function of per capita consumption c_t (equation (9)).

$$G_t = A_t^{TFP} K_t^{\gamma} L_t^{1-\gamma} \quad (4)$$

$$E_t = \sigma_t(1-\mu_t)G_t + E_t^{Land} \quad (5)$$

$$\Lambda_t = \theta_{1,t}\mu_t^{\theta_2} \quad (6)$$

$$D_t = a_2(T_t^{AT}(E_t))^{a_3} \quad (7)$$

$$N_t = (1 - D_t - \Lambda_t)G_t \quad (8)$$

$$c_t = (1 - s_t)\frac{N_t}{L_t} \quad (9)$$

Where, in time t G_t = Gross global economic output, US$ trillion;

A_t^{TFP} = Total factor productivity, exogenous;

K_t = Capital, a function of net economic output and saving rate, function not shown;

L_t = Population, exogenous;

E_t = Total global GHG emissions, Gt CO_2e (DICE includes exogenous non-CO_2 climate forcing);

σ_t = GHG emissions intensity of gross global output, declines over time at exogenous rate;

E_t^{Land} = GHG emissions from land, exogenous in conventional DICE, starting at 2.6 Gt CO_2 per year in 2015 and declining by 11.5% every 5-year time step;

Λ_t = Cost of GHG mitigation, proportion of gross global economic output;

$\theta_{1,t}, \theta_2$ = GHG mitigation cost parameters, $\theta_{1,t}$ declines over time at exogenous rate;

D_t = Climate damages due to GHG emissions, proportion of gross global economic output;

T_t^{AT} = Global average surface temperature change from 1900, degrees Celsius, a function of the state variable atmospheric CO_2 concentration (M), which is a function of emissions (E_t);

a_2, a_3 = Climate damage parameters;

N_t = Global net economic output;

c_t = Per capita consumption, input to the social welfare function;

s_t = Saving rate, control variable; and

μ_t = GHG mitigation rate, control variable.

Furthermore, $\theta_{1,t}$ is a function of the industrial sector mitigation "backstop price" and the change in backstop price over time (θ_2 is an exogenous constant):

$$\theta_{1,t} = \sigma_t \left(\frac{PB}{\theta_2}\right)(1 - \Delta PB)^{t-1} \qquad (10)$$

Where PB = backstop price; and

ΔPB = annual percent change in backstop price

A backstop price is required to identify a unique carbon price path. By defining $\theta_{1,t}$ in this way, the marginal cost of mitigation will equal the backstop price when $\mu_t = 1$, or 100% mitigation of all industrial emissions.

3.1 DICELAND

To make the global forest sector endogenous within DICE, we removed the exogenous land sector emissions E_t^{Land} and added a control variable $\mu_{2.t}$ to indicate absolute emissions reduced in the forest sector (Gt CO_2), as well as a parameter indicating maximum mitigation potential from the land sector, μ_{2MAX} (Gt CO_2). We also include two additional parameters to reflect the cost of land sector mitigation ($\theta_{3,t}$, θ_4) which are analogous to parameters $\theta_{1,t}$ and θ_2 in the industrial sector. We incorporate these new variables into equations (5) and (6) to create equations (11) and (12):

$$E_t = \sigma_t(1-\mu_t)G_t + (E_t^{F-base} - \mu_{2.t}) \qquad (11)$$

$$\Lambda_t = \theta_{1,t}\mu_t^{\theta_2} + \theta_{3,t}\left(\frac{\mu_{2,t}}{\mu_{2MAX}}\right)^{\theta_4} \qquad (12)$$

Where E_t^{F-base} = exogenous baseline forest sector GHG emissions, reflects GTM baseline scenario with no carbon price

$\theta_{3,t}$, θ_4 = Forest sector GHG mitigation cost parameters

$\mu_{2,t}$ = Forest sector GHG mitigation control, $GtCO_2$

μ_{2MAX} = Maximum land GHG mitigation, $GtCO_2$

We also designate backstop price and change in backstop price parameters for the land sector in order to specify $\theta_{3,t}$ (θ_4 is a constant):

$$\theta_{3,t} = \left(\frac{PB_L}{\theta_4}\right)(1-\Delta PB_L)^{t-1} \qquad (13)$$

Where PB_L = Land sector mitigation backstop price; and

ΔPB_L = Land sector annual percent change in backstop price

The forest sector mitigation control variable $\mu_{2.t}$ is specified as an absolute reduction rather than a proportional reduction like in the industrial sector because the industrial sector is characterized by rapidly increasing marginal costs as emissions approach zero. This is not appropriate for the forest sector. While there are increasing marginal costs, there is no asymptote for forest CO_2 emissions levels around zero, because the forest sector can readily sequester CO_2 (i.e., negative CO_2 emissions). Thus, representing total net emissions in equation (11) requires subtracting $\mu_{2.t}$ from baseline land sector emissions E_t^{F-base}. Further, representing mitigation costs in terms of proportional reduction in equation (12) requires introducing the μ_{2MAX} term.

We introduce four new DICELAND parameters (PB_L, ΔPB_L, θ_4, and μ_{2MAX}), as well as the E_t^{F-base} exogenous time series. To set these parameter values, we use GTM. E_t^{F-base} is derived by first running conventional DICE without mitigation (setting the upper bound of μ_t to zero for all t), recording c_t (per capita consumption) and real interest rate for all t, and feeding these two series into GTM to derive a baseline series of forest sector GHG emissions under a "no carbon price" scenario. The GTM baseline series is fit to a fourth-order polynomial which is then coded into DICELAND as the exogenous forest sector GHG baseline.

μ_{2MAX} is readily defined by the maximum GTM mitigation level found through eight carbon price scenarios assessed by Favero et al. (2018) and is set at 25 Gt CO_2 for all t. Griscom et al. found maximum global land sector mitigation potential of 23.8 Gt CO_2 by 2030, with cost-

effective mitigation potential limited to 11.3 Gt CO_2 (achievable at less than \$100 tCO_2e^{-1}) (2017). Smith et al. identifies annual demand side land sector mitigation potential at 15.6 Gt CO_2e by 2050 for carbon prices less than \$100 tCO_2e^{-1} (2013). Ultimately the μ_{2MAX} value is arbitrary, and the other forest sector mitigation cost parameters are defined with respect to this assumed value.

The three forest mitigation cost parameters (PB_L, ΔPB_L, θ_4) are determined through a convergence process between DICELAND and GTM (Figure 1).

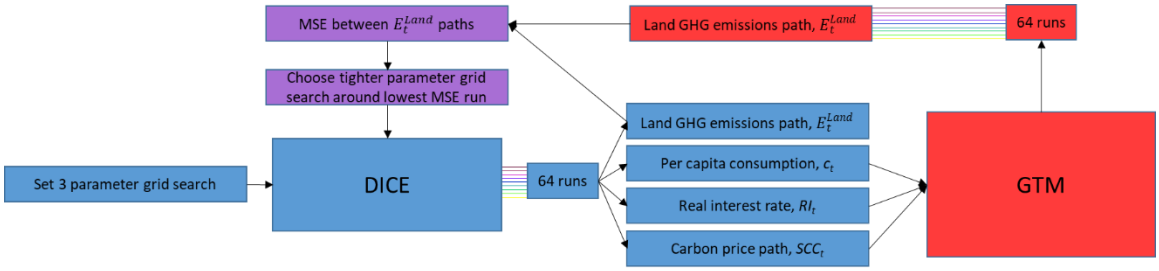

Figure 1. DICELAND-GTM forest sector cost parameter convergence process.

The convergence process requires (1) setting a grid search of 4 values for each of the three cost parameters, resulting in 64 total DICELAND runs for every combination of the 3 parameters' 4 values; (2) generating DICELAND outputs of per capita consumption, real interest rate, and carbon price path for each of the 64 runs, which are used as inputs to GTM, generating 64 concomitant GTM runs; and (3) comparing the forest GHG emissions paths for each of the 64 runs across the two models using root mean squared difference (RMSD).[†] The run with the lowest

[†] $RMSD = (\frac{1}{T}\sum_{t=1}^{T}(E_{D,t} - E_{G,t})^2)^{0.5}$ where $t = 1,\ldots,T$ represents each 10 year time step, $E_{D,t}$ is DICELAND forest sector emissions in time step t, and $E_{G,t}$ is GTM forest sector emissions in time step t.

RMSD is used to set a tighter parameter grid search around the 3 candidate parameter values. This process iterates until there is adequate convergence.

We performed this convergence process for each of four climate policy-carbon accounting scenarios: (1) *Optimal* climate policy, *Traditional* carbon accounting; (2) *Optimal* climate policy, *Integrative* carbon accounting; (3) *2 Degree* climate policy, *Traditional* carbon accounting; and (4) *2 Degree* climate policy, *Integrative* carbon accounting.

The DICELAND-GTM convergence process resulted in RMSDs across scenarios of 1.73-2.38 Gt CO_2 between the two model's forest emissions pathways from 2020-2100 (for reference, the maximum annual forest mitigation achieved across scenarios is 16.5 Gt CO_2), the timeframe used for model convergence. Years after 2100 are less useful due to terminal condition assumptions in GTM. The DICELAND forest CO_2 emissions pathway can be best interpreted as representing long term GTM emissions trends for a given carbon price path.

DICELAND forest mitigation cost parameters for the lowest RMSD pathways are distinct across forest carbon accounting scenarios, as well as across global climate policy scenario. This indicates that, while it is meaningful to assess effects of forest carbon accounting approaches on efficient carbon prices, parameterization needs to be redone for any significant changes in climate policy (Table 2).

		Optimal		*2 Degree*	
	Units	***Traditional***	***Integrative***	***Traditional***	***Integrative***
Land backstop price (PB_L)	\$/ton CO_2	200	200	200	1467
Annual decrease in PB_L (ΔPB_L)	Ratio	0.005	0.005	0.005	0.0867
Land cost function exponent (θ_4)	Unitless	5	3.7	5	5

Table 2. DICELAND forest mitigation cost parameters for four forest carbon accounting-climate policy scenarios.

3.2 Traditional net albedo *ex ante* calculations

The *Traditional* accounting scenario ignores albedo effects when determining efficient forest sector mitigation activity. To estimate total temperature change and climate damages under the *Traditional* scenario, we must calculate incremental temperature change and climate damages due to albedo to generate the *Traditional Net Albedo* (*TNA*) results. First, we run DICELAND using the *Traditional* parameters (Table 2) for either *Optimal* or *2 Degree* policy and record all results offline. We then take the appropriate GTM time series of albedo change CO_2-equivalent emissions (consistent with the DICELAND parameters used in the previous step) and add albedo CO_2-equivalent emissions to the DICELAND forest sector emissions derived from the previous step. Since DICELAND operates over 5-year time steps and GTM over 10, the *TNA* forest sector emissions must be fit to a spline, the interpolated results of which are used as the input into DICELAND dynamic equations. The result is a *TNA* forest sector emissions pathway. We then use an offline version of the DICELAND dynamic equations (equations (4), (7)-(9), (11)-(12)) that

takes all offline DICELAND results and the *TNA* forest sector emissions pathway as inputs to generate updated temperature and climate damage results.

4. Results

4.1 The role of forests in climate change mitigation

In Figure 2, we show that the carbon price under *Optimal* and *2 Degree* policies drives large increases in global forest carbon stock, even when accounting for albedo effects (Figure 2.a, 2.b), compared to a global climate policy that does not include the forest sector as a mitigation option (*No Land*). Note that in Figure 2 forest carbon stock levels under *Integrative* and *TNA* scenarios reflect albedo effects in terms of carbon stock equivalent on a radiative forcing basis, consistent with methods in Favero et al. (2018). Thus, DICELAND indicates the forest sector provides climate mitigation benefits even when albedo effects are accounted for.

Accounting for albedo *ex ante* under the *Integrative* scenario affects total efficient mitigation provided by forests. By 2100, under the *Integrative* scenario forest carbon stock is 5% (*Optimal* policy) and 6% (*2 Degree* policy) higher compared to *TNA*. While the higher *Integrative* forest carbon stock is primarily due to more efficient allocation of forest expansion over space, consistent with Favero et al. (2018) results, under a *2 Degree* policy 25% of the difference between *Integrative* and *TNA* forest carbon stock is due to higher albedo-sensitive carbon prices (Figure 2.b, compare *Integrative* and *Integrative, same carbon price as Traditional* results).

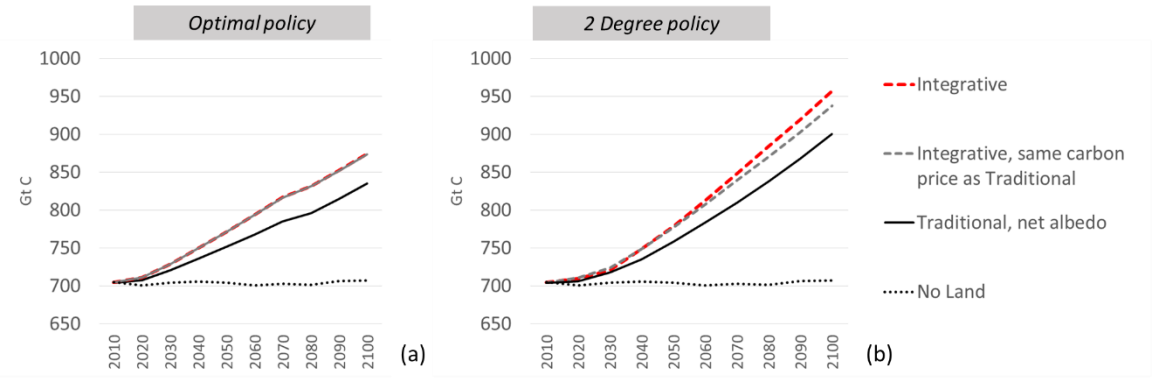

Figure 2. Forest sector Global Timber Model outputs: a. Forest carbon stock, net albedo (GtC), Optimal policy; b. Forest carbon stock, net albedo (GtC), 2 Degree policy.

4.2 Effects on carbon price and forest mitigation cost-effectiveness

The *No Land* policy results in higher carbon prices than when the forest sector is included in climate policy under either *Traditional* or *Integrative* accounting approaches. The 2100 *Traditional* carbon prices are 7% (*Optimal* policy) and 85% (*2 Degree* policy) lower than the *No Land* scenarios.[‡]

The *Integrative* scenario is characterized by more costly forest sector mitigation than under *Traditional* forest carbon accounting, resulting in 2100 carbon prices that are 3% (*Optimal* policy) and 36% (*2 Degree* policy) higher (Figure 3.a, Figure 3.b).

We compare the forest carbon stock accumulated under climate policy with the carbon prices required to reach increasing forest mitigation levels (Figure 3.c, 3.d). While *Traditional* carbon accounting appears to allow for the least costly forest carbon accrual, this is an artifact of

[‡] Note for DICELAND to generate a solution for the *No Land – 2 Degree* policy scenario, the start of the 2 degree constraint is delayed until 2200 (compared to a start year of 2110 for *Traditional* and *Integrative* scenarios). This reflects the difficulty of meeting the 2 degree temperature target without employing the land sector.

the albedo omission accounting error – the *TNA* scenario has the highest marginal cost of increasing forest carbon stock for all mitigation quantities. The average cost of generating the highest forest mitigation quantity under *TNA* carbon accounting is 34% higher (*Optimal* policy) and 9% higher (*2 Degree* policy) than *Integrative* carbon accounting.

Note that there is less of an efficiency gain from using *Integrative* accounting under the *2 Degree* policy compared to *Optimal* policy. This is because under the higher carbon prices of *2 Degree* policy, forests are approaching maximum potential area and carbon storage. This dynamic results in little difference in the costs of *Integrative* versus *TNA* carbon accounting, since both account for albedo effects and exhibit similar forest area and management characteristics. Yet as shown by Figure 3.b, accounting for albedo *ex ante* remains important under *2 Degree* policy for purposes of estimating an efficient carbon price pathway, which in turn affects mitigation levels in other sectors, global temperature change, and climate damages.

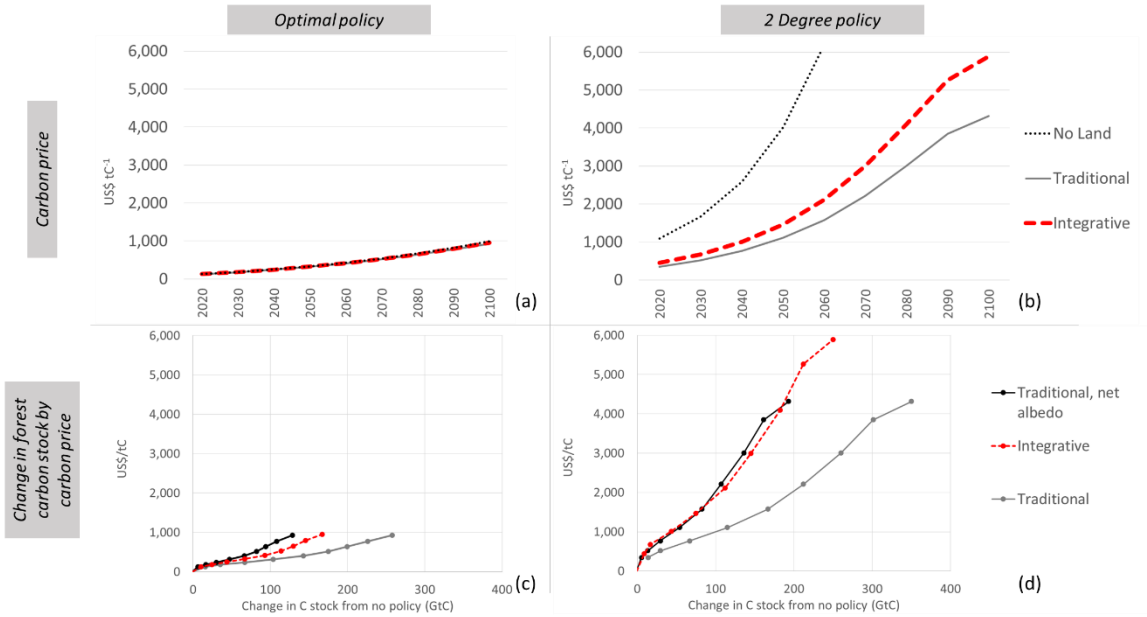

Figure 3. Carbon price and forest mitigation cost-effectiveness: a. DICELAND carbon price (US$ tC^{-1}), Optimal policy; b. DICELAND carbon price (US$ tC^{-1}), 2 Degree policy; c. GTM change in forest carbon stock compared to no climate policy (Gt C), by DICELAND carbon price (US$ tC^{-1}), Optimal policy; d. GTM change in forest carbon stock compared to no climate policy (Gt C), by DICELAND carbon price (US$ tC^{-1}), 2 Degree policy.

Table 3 shows the consistency of carbon price results across two DICELAND *No Land* (*Optimal*; *2.5 degree maximum*) scenarios and equivalent conventional DICE (*Optimal controls*; *2.5 degree maximum*, respectively) scenarios. Here we have added the *2.5 degree maximum* scenario in order to compare to Nordhaus (2016) results, which constrains temperature change below 2.5 degrees Celsius for the entire optimization time frame. The differences in DICE and DICELAND carbon prices for these scenarios result from the DICELAND baseline land sector having larger emissions, derived from the GTM base case, than the DICE exogenous land sector. There are also differences due to the fact that the DICELAND *No Land* carbon prices are a function of the marginal benefit of easing the forest sector mitigation constraint, unlike

conventional DICE which does not account for the potential for land sector mitigation. The difference between DICELAND *No Land* and DICE carbon prices under the *Optimal* scenario is 1% by 2055, while the difference between DICELAND No Land and DICE under the *2.5 degree maximum* scenario reaches 11% by 2055, reflecting the increasing marginal cost of constraining mitigation from the forest sector. Including the land sector as a mitigation option results in lower carbon prices for DICELAND under both *Optimal* and *2 Degree* policies compared to DICE *Optimal controls* and *2.5 degree maximum* scenarios, respectively.

Model	Assumptions	2015	2020	2025	2030	2055
DICE	Optimal	30.7	37.3	44.0	51.6	102.5
DICE	2.5 degree maximum	184.4	229.1	284.1	351.0	1,006.2
DICELAND	No Land, Optimal	30.7	36.7	43.6	51.2	103.7
DICELAND	No Land, 2.5 degree maximum	204.0	253.1	313.4	387.0	1,119.3
DICELAND	Optimal, Traditional	29.6	35.4	42.0	49.3	99.2
DICELAND	Optimal, Integrative	30.0	35.9	42.6	50.0	101.0
DICELAND	2 Degree, Traditional	75.8	94.0	115.8	141.9	361.8
DICELAND	2 Degree, Integrative	98.0	121.7	150.4	184.8	480.2

Table 3. Comparison of carbon price (2010 US$ tCO_2^{-1}) series across DICE (2016 parameters) and DICELAND scenarios. DICE values are derived from Table 1 in Nordhaus (2016).

4.3 The industrial sector adjusts to higher albedo-sensitive carbon prices

The *No Land* scenario exhibits the lowest industrial sector GHG emissions under both *Optimal* and *2 Degree* climate policy, since the industrial sector provides the only mitigation option and there is no flexibility to provide large-scale forest carbon sequestration.

Again, forest mitigation is more expensive under *Integrative* accounting compared to *Traditional* accounting, resulting in higher mitigation effort from the industrial sector. For instance, under *Optimal* climate policy, the industrial sector has an average 0.5% lower annual CO_2 emissions between 2020-2060 under *Integrative* forest carbon accounting compared to

Traditional (Figure 4.a), while *2 Degree* climate policy results in 43% lower annual industrial sector emissions on average under *Integrative* accounting for 2020-2060 (Figure 4.b).

Across both *Optimal* and *2 Degree* climate policy scenarios, total global emissions are therefore lower under the *Integrative* approach, due to both lower land sector emissions as well as lower industrial sector emissions, driven by the higher carbon price. This is the price paid for a more accurate accounting of forest mitigation potential.

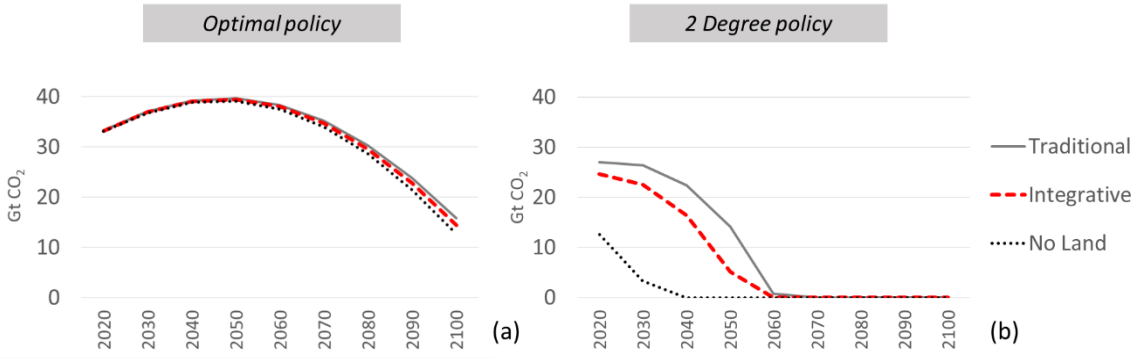

Figure 4. *Industrial sector CO_2 emissions (Gt CO_2), 2020-2100. (a) Optimal policy; (b) 2 Degree policy.*

4.4 Temperature change and climate damages from albedo

Results illustrate that not accounting for albedo has the potential to significantly influence the global average temperature trajectory and thereby climate damages. In fact, Ignoring albedo effects of forest mitigation could lead to 0.14 degrees Celsius (*Optimal* policy) or 0.27 degrees Celsius (*2 Degree* policy) of unexpected temperature change in 2100 (Figure 5.a and 5.b), reaching 5% and 11% of total 2100 temperature change from pre-industrial levels, respectively. These

values reflect the difference in 2100 between temperature increase under the *Traditional* and *TNA* scenarios.

Under *Optimal* policy, 2100 annual unexpected climate damages due ignoring albedo effects could reach 0.2% of global gross economic output while the *2 Degree* policy would see unexpected damages accounting for 0.3% of global gross economic output in 2100. By the end of the century, the unexpected annual climate damages attributable to albedo change reach 22% of total 2100 climate changes.

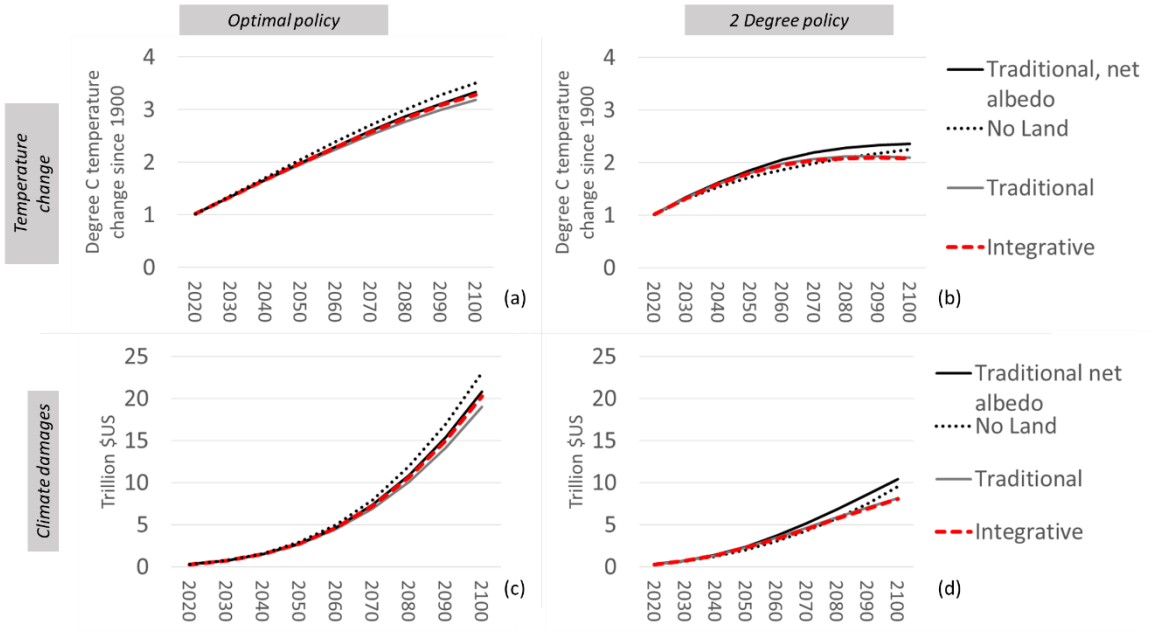

Figure 5. Temperature change and climate damage results: a. Global temperature change since 1900 (degree Celsius), Optimal policy; b. Global temperature change since 1900 (degree Celsius), 2 Degree policy; c. Global climate damages (trillion US$), Optimal policy; d. Global climate damages (trillion US$), 2 Degree policy.

5. Discussion

We find that accounting for albedo effects from forest mitigation activity has potential to meaningfully impact global carbon prices and mitigation levels across economic sectors, particularly under a *2 Degree* global climate policy. Under *Optimal* climate policy, the unexpected damages from ignoring albedo effects (9% of total climate damages by 2100, Figure 5.c) as well as the potential cost reductions from adopting albedo-sensitive forest carbon incentives (34% reduction in average forest mitigation cost; Figure 3.c) are substantial. Unexpected albedo-driven climate damages are even larger under the *2 Degree* policy (22% of total climate damages by 2100, Figure 5.d). It is also more important under *2 Degree* policy to capture the effects of albedo when estimating efficient carbon prices: albedo-sensitive carbon prices could be 36% higher in 2100 than carbon prices that do not consider the albedo effects of forest mitigation (Figure 3.b). Albedo-sensitive accounting also requires substantially higher industrial sector mitigation under *2 Degree* policy, decreasing average annual industrial emissions by 43% between 2020 and 2060 (Figure 4.b).

		Optimal			*2 Degree*		
	Units	*Traditional, Net Albedo*	*Integrative*	*No Land*	*Traditional, Net Albedo*	*Integrative*	*No Land*[b]
Aggregate discounted net economic output, 2020-2100[a]	US$ trillion	1,733	1,733	1,730	1,705	1,700	1,693
Carbon price, 2100	US$ tCO_2^{-1}	252	260	271	1,177	1,606	8,110
Forest sector contribution to total CO_2 mitigation, average, 2020-2100	Percent	22.3	23.0	0	18.2	18.6	0
Global average temperature, 2100	°C change from 1900	3.3	3.3	3.5	2.4	2.1	2.3
Cumulative discounted climate damages, 2020-2100	US$ trillion	26.1	25.6	28.5	17.1	14.6	14.8

Table 4. DICELAND results for six accounting-policy scenarios. a. Discounted aggregate net economic output is the sum of discounted global gross economic output net climate mitigation costs and climate damages for each 10-year time step 2020-2100. The pure rate of social time preference used in DICELAND is 1.5% and the elasticity of the marginal utility of consumption is 1.45. This results in a real interest rate ranging between 3.0% and 5.1% across scenarios and time steps. For consistency we use the PRTP across scenarios and time steps to discount 2020-2100 net economic output. b. For the No Land-2 Degree scenario the start year for the 2 degree constraint is 2200, the earliest start year possible for DICELAND to generate a solution. All other 2 Degree scenarios require temperature change below 2 degrees C following 2110.

To assess the social welfare outcomes across scenarios, we calculate aggregate discounted net economic output for 2020-2100 (Table 4, row 1). The *No Land* scenarios exhibit the lowest

total welfare for both *Optimal* and *2 Degree* policies. This indicates that even if albedo cannot be incorporated into climate policy *ex ante*, whether due to data constraints or analytical uncertainty, the *TNA* scenario is preferable to excluding the land sector from climate mitigation efforts entirely. Forestry mitigation provides flexibility to reduce CO_2 emissions in the event of global temperature goal overshoot, a role it can play even if albedo is incorrectly ignored.

Note that under *2 Degree* policy, the *TNA* scenario exhibits higher discounted net economic output than *Integrative* (Table 4, row 1). This is due to the fact that *Integrative* carbon prices start higher than *TNA* carbon prices early in the time series, resulting in higher mitigation costs, but the benefits of avoided albedo are largest later in the time series. To observe the social welfare benefits of the *Integrative* scenario, we would need to show DICELAND outputs over a longer time period, but this is limited by the GTM optimization timeframe.

Even when considering albedo effects, using either *Traditional* or *Integrative* carbon accounting approaches would allow forests to contribute nearly a quarter of global CO_2 mitigation on average between 2020-2100 (Table 4, row 3), largely consistent with countries' Paris Agreement commitments. The *2 Degree* policy requires significantly more effort from the industrial sector, resulting in lower percentage contribution from the land sector.

Given the potential impact of albedo effects on efficient global carbon prices, forestry and industrial sector mitigation activity, and global climate damages, we suggest policy-makers carefully consider this issue in climate mitigation planning. While greenhouse gases continue to be the dominant driver of anthropogenic climate change, moving toward a more comprehensive recognition of the major factors influencing radiative forcing can help avoid unintended and costly

outcomes. Forest-driven albedo effects are not currently addressed in documents like the 2006 IPCC Guidelines for National Greenhouse Gas Inventories or its 2019 Refinement (IPCC 2006, IPCC 2019a). The recent IPCC Special Report on Climate Change and Land points to the effects of land cover on surface albedo, yet does not provide guidance for how governments should incorporate this issue into policy planning (IPCC 2019b). As governments put in place forest carbon programs to meet Paris Agreement commitments and beyond, our analysis suggests some mechanism is needed to avoid significant albedo change.

As with any integrated assessment model, DICELAND uses a particular model structure and set of parameter assumptions that affect the results of this analysis. Given the potential scale of impact we identify here, we welcome further analysis using alternative models that can assess the economic implications of albedo changes on global climate policy. Future work would usefully incorporate additional interactions between forest ecosystems and the global climate system, such as the role of forest-cloud interactions and accounting for the impacts of changes in evapotranspiration by region.

References

Arora, Vivek, and Alvaro Montenegro. 2011. "Small Temperature Benefits Provided by Realistic Afforestation Efforts." *Nature Geosci* 4: 514–18. https://doi.org/10.1038/ngeo1182.

Bala, G., K. Caldeira, M. Wickett, T. J. Phillips, D. B. Lobell, C. Delire, and A. Mirin. 2007. "Combined Climate and Carbon-Cycle Effects of Large-Scale Deforestation." *Proceedings of the National Academy of Sciences* 104 (16): 6550. https://doi.org/10.1073/pnas.0608998104.

Betts, Richard A. 2000. "Offset of the Potential Carbon Sink from Boreal Forestation by Decreases in Surface Albedo." *Nature* 408 (6809): 187–90. https://doi.org/10.1038/35041545.

Bonan, Gordon B. 2008. "Forests and Climate Change: Forcings, Feedbacks, and the Climate Benefits of Forests." *Science* 320 (5882): 1444. https://doi.org/10.1126/science.1155121.

Cropper, Maureen L, and Wallace E Oates. 1992. "Environmental Economics: A Survey." *Journal of Economic Literature* 30: 675–740.

Dasgupta, Partha. 2014. "Pricing Climate Change." *Politics, Philosophy & Economics* 13 (4): 394–416. https://doi.org/10.1177/1470594X14541521.

Duveiller, Gregory, Josh Hooker, and Alessandro Cescatti. 2018. "The Mark of Vegetation Change on Earth's Surface Energy Balance." *Nature Communications* 9 (1): 679. https://doi.org/10.1038/s41467-017-02810-8.

EPA. 2009. "An Urgent Call to Action: Report of the State-EPA Nutrient Innovations Task Group." Washington, DC.

Eriksson, Mathilda. 2015. "The Role of the Forest in an Integrated Assessment Model of the Climate and the Economy." *Climate Change Economics* 6 (3): 35.

FAO. 2010. "Global Forest Resources Assessment 2010: Main Report." FAO Forestry Paper 163. Rome: Food and Agriculture Organization of the United Nations. http://www.fao.org/3/a-i1757e.pdf.

Faulwasser, Timm, Christopher Kellett, and Steven Weller. 2016. "DICE2013R-Mc." https://github.com/cmkellett/DICE2013R-mc.

Favero, Alice, Robert Mendelsohn, and Brent Sohngen. 2017. "Using Forests for Climate Mitigation: Sequester Carbon or Produce Woody Biomass?" *Climatic Change* 144 (July). https://doi.org/10.1007/s10584-017-2034-9.

Favero, Alice, Brent Sohngen, Yuhan Huang, and Yufang Jin. 2018. "Global Cost Estimates of Forest Climate Mitigation with Albedo: A New Integrative Policy Approach." *Environmental Research Letters* 13 (12): 125002. https://doi.org/10.1088/1748-9326/aaeaa2.

Freeman, A.M. III. 1982. "Air and Water Pollution Control: A Benefit-Cost Assessment."

Gibbard, S., K. Caldeira, G. Bala, T. J. Phillips, and M. Wickett. 2005. "Climate Effects of Global Land Cover Change." *Geophysical Research Letters* 32 (23). https://doi.org/10.1029/2005GL024550.

Grassi, Giacomo, Jo House, Frank Dentener, Sandro Federici, Michel den Elzen, and Jim Penman. 2017. "The Key Role of Forests in Meeting Climate Targets Requires Science for Credible Mitigation." *Nature Climate Change* 7 (February): 220.

Griscom, Bronson W., Justin Adams, Peter W. Ellis, Richard A. Houghton, Guy Lomax, Daniela A. Miteva, William H. Schlesinger, et al. 2017. "Natural Climate Solutions." *Proceedings of the National Academy of Sciences* 114 (44): 11645–11650. https://doi.org/10.1073/pnas.1710465114.

Hsueh, Lily. 2017. "Quasi-Experimental Evidence on the 'Rights to Fish': The Effects of Catch Shares on Fishermen's Days at Sea." *Journal of the Association of Environmental and Resource Economists* 4 (2): 407–45. https://doi.org/10.1086/691555.

IIASA. 2019. "SSP Scenario Database." 2019. http://www.iiasa.ac.at/web/home/research/researchPrograms/Energy/SSP_Scenario_Database.html.

Integrated Assessment Modeling Consortium. 2018. "The Common Integrated Assessment Model (IAM) Documentation." IAMC Wiki. June 28, 2018. https://www.iamcdocumentation.eu/index.php/IAMC_wiki.

IPCC. 2006a. "2006 IPCC Guidelines for National Greenhouse Gas Inventories. Volume 4: Agriculture, Forestry and Other Land Use." https://www.ipcc-nggip.iges.or.jp/public/2006gl/vol4.html.

———. 2006b. "Volume 4: Agriculture, Forestry and Other Land Use." In *2006 IPCC Guidelines for National Greenhouse Gas Inventories*. https://www.ipcc-nggip.iges.or.jp/public/2006gl/vol4.html.

———. 2014. "IPCC, 2014: Summary for Policy Makers." In *Climate Change 2014: Mitigation of Climate Change. Contribution of Working Group III to the Fifth Assessment Report of the Intergovernmental Panel on Climate Change*. Cambridge: Cambridge University Press.

———. 2019a. "2019 Refinement to the 2006 IPCC Guidelines for National Greenhouse Gas Inventories." https://www.ipcc-nggip.iges.or.jp/public/2019rf/index.html.

———. 2019b. "Climate Change and Land: An IPCC Special Report on Climate Change, Desertification, Land Degradation, Sustainable Land Management, Food Security, and Greenhouse Gas Fluxes in Terrestrial Ecosystems." https://www.ipcc.ch/report/srccl/.

Joint Global Change Research Institute. 2019. "GCAM v5.1 Documentation." 2019. http://jgcri.github.io/gcam-doc/toc.html.

Jones, Andrew D., Katherine V. Calvin, William D. Collins, and James Edmonds. 2015. "Accounting for Radiative Forcing from Albedo Change in Future Global Land-Use Scenarios." *Climatic Change* 131 (4): 691–703. https://doi.org/10.1007/s10584-015-1411-5.

Kauppi, Pekka E., Jesse H. Ausubel, Jingyun Fang, Alexander S. Mather, Roger A. Sedjo, and Paul E. Waggoner. 2006. "Returning Forests Analyzed with the Forest Identity." *Proceedings of the National Academy of Sciences* 103 (46): 17574. https://doi.org/10.1073/pnas.0608343103.

Kirschbaum, M. U. F., D. Whitehead, S. M. Dean, P. N. Beets, J. D. Shepherd, and A.-G. E. Ausseil. 2011. "Implications of Albedo Changes Following Afforestation on the Benefits of Forests as Carbon Sinks." *Biogeosciences* 8 (12): 3687–96. https://doi.org/10.5194/bg-8-3687-2011.

Kroetz, Kailin, James N. Sanchirico, and Daniel K. Lew. 2015. "Efficiency Costs of Social Objectives in Tradable Permit Programs." *Journal of the Association of Environmental and Resource Economists* 2 (3): 339–66. https://doi.org/10.1086/681646.

Linn, Joshua, Erin Mastrangelo, and Dallas Burtraw. 2014. "Regulating Greenhouse Gases from Coal Power Plants under the Clean Air Act." *Journal of the Association of Environmental and Resource Economists* 1 (1/2): 97–134. https://doi.org/10.1086/676038.

Lyon, Randolph M., and Scott Farrow. 1995. "An Economic Analysis of Clean Water Act Issues." *Water Resources Research* 31 (1): 213–23. https://doi.org/10.1029/94WR02047.

Muller, Nicholas Z., and Robert Mendelsohn. 2009. "Efficient Pollution Regulation: Getting the Prices Right." *American Economic Review* 99 (5): 1714–39. https://doi.org/10.1257/aer.99.5.1714.

Myhre, Gunnar, Drew Shindell, François-Marie Bréon, William Collins, Jan Fuglestvedt, Jianping Huang, Dorothy Koch, et al. 2013. "8 Anthropogenic and Natural Radiative Forcing." In

Climate Change 2013: The Physical Science Basis. Contribution of Working Group I to the Fifth Assessment Report of the Intergovernmental Panel on Climate Change, 82. Cambridge: Cambridge University Press.

Mykleby, P. M., P. K. Snyder, and T. E. Twine. 2017. "Quantifying the Trade-off between Carbon Sequestration and Albedo in Midlatitude and High-latitude North American Forests." *Geophysical Research Letters* 44 (5): 2493–2501. https://doi.org/10.1002/2016GL071459.

Nordhaus, William. 2014. "Estimates of the Social Cost of Carbon: Concepts and Results from the DICE-2013R Model and Alternative Approaches." *Journal of the Association of Environmental and Resource Economists* 1 (1/2): 273–312. https://doi.org/10.1086/676035.

———. 2018. "Evolution of Modeling of the Economics of Global Warming: Changes in the DICE Model, 1992–2017." *Climatic Change* 148 (4): 623–40. https://doi.org/10.1007/s10584-018-2218-y.

Nordhaus, William D. 1992. "An Optimal Transition Path for Controlling Greenhouse Gases." *Science* 258 (5086): 1315. https://doi.org/10.1126/science.258.5086.1315.

———. 2017. "Revisiting the Social Cost of Carbon." *Proceedings of the National Academy of Sciences* 114 (7): 1518–23. https://doi.org/10.1073/pnas.1609244114.

Nordhaus, William, and Paul Sztorc. 2013. "DICE 2013R: Introduction and User's Manual." www.dicemodel.net.

Pigou, A. C. (Arthur Cecil), 1877-1959. 1924. The Economics of Welfare. Second edition. London : Macmillan, 1924.

Riahi, Keywan, Detlef P. van Vuuren, Elmar Kriegler, Jae Edmonds, Brian C. O'Neill, Shinichiro Fujimori, Nico Bauer, et al. 2017. "The Shared Socioeconomic Pathways and Their Energy, Land Use, and Greenhouse Gas Emissions Implications: An Overview." *Global Environmental Change* 42 (January): 153–68. https://doi.org/10.1016/j.gloenvcha.2016.05.009.

Rogelj, Joeri, Drew Shindell, Kejun Jiang, Solomone Fifita, Piers Forster, Veronika Ginzburg, Collins Handa, et al. 2018. "Mitigation Pathways Compatible with 1.5°C in the Context of Sustainable Development. In: Global Warming of 1.5°C. An IPCC Special Report on the Impacts of Global Warming of 1.5°C above Pre-Industrial Levels and Related Global Greenhouse Gas Emission Pathways, in the Context of Strengthening the Global Response to the Threat of Climate Change, Sustainable Development, and Efforts to Eradicate Poverty."

Rose, Steven, Helal Ahammad, Bas Eickhout, Brian Fisher, Atsushi Kurosawa, Shilpa Rao, Keywan Riahi, and Detlef van Vuuren. 2008. "Land in Climate Stabilization Modeling: Initial Observations." EMF Report 21. Land Modeling Subgroup.

Rose, Steven K., Elmar Kriegler, Ruben Bibas, Katherine Calvin, Alexander Popp, Detlef P. van Vuuren, and John Weyant. 2014. "Bioenergy in Energy Transformation and Climate Management." *Climatic Change* 123 (3–4): 477–93. https://doi.org/10.1007/s10584-013-0965-3.

Smith, P., M. Bustamante, H. Ahammad, H. Clark, H. Dong, E. Elsiddig, H. Haberl, et al. 2014. "11 Agriculture, Forestry and Other Land Use (AFOLU)." In *Climate Change 2014: Mitigation of Climate Change. Working Group III Contribution to the Fifth Assessment Report of the Intergovernmental Panel on Climate Change*. Cambridge: Cambridge University Press. https://doi.org/10.1017/CBO9781107415416.

Smith, Pete, Helmut Haberl, Alexander Popp, Karl-heinz Erb, Christian Lauk, Richard Harper, Francesco N. Tubiello, et al. 2013. "How Much Land-Based Greenhouse Gas Mitigation Can Be Achieved without Compromising Food Security and Environmental Goals?" *Global Change Biology* 19 (8): 2285–2302. https://doi.org/10.1111/gcb.12160.

Sohngen, Brent, and Robert Mendelsohn. 2003. "An Optimal Control Model of Forest Carbon Sequestration." *American Journal of Agricultural Economics* 85 (2): 448–57. https://doi.org/10.1111/1467-8276.00133.

Sohngen, Brent, Robert Mendelsohn, and Roger Sedjo. 1999. "Forest Management, Conservation, and Global Timber Markets." *American Journal of Agricultural Economics* 81 (1): 1–13. https://doi.org/10.2307/1244446.

Spracklen, Dominick V, Boris Bonn, and Kenneth S Carslaw. 2008. "Boreal Forests, Aerosols and the Impacts on Clouds and Climate." *Philosophical Transactions of the Royal Society A: Mathematical, Physical and Engineering Sciences* 366 (1885): 4613–26. https://doi.org/10.1098/rsta.2008.0201.

Stehfest, E, L de Waal, and R Oostenrijk. 2010. "IMAGE User Manual." 500110006. Netherlands Environmental Assessment Agency. https://www.pbl.nl/sites/default/files/downloads/500110006_0.pdf.

Stern, Nicholas. 2008. "The Economics of Climate Change." *American Economic Review* 98 (2): 1–37. https://doi.org/10.1257/aer.98.2.1.

Thompson, Matthew P., Darius Adams, and John Sessions. 2009. "Radiative Forcing and the Optimal Rotation Age." *Ecological Economics* 68 (10): 2713–20. https://doi.org/10.1016/j.ecolecon.2009.05.009.

Tian, Xiaohui, Brent Sohngen, Justin Baker, Sara Ohrel, and Allen A. Fawcett. 2018. "Will U.S. Forests Continue to Be a Carbon Sink?" *Land Economics* 94 (1): 97–113. https://doi.org/10.3368/le.94.1.97.

US EPA, OAR. 2019. "Inventory of U.S. Greenhouse Gas Emissions and Sinks: 1990-2017." Reports and Assessments. US EPA. February 11, 2019. https://www.epa.gov/ghgemissions/inventory-us-greenhouse-gas-emissions-and-sinks-1990-2017.

Van Houtven, George, Ross Loomis, Justin Baker, Robert Beach, and Sara Casey. 2012. "Nutrient Credit Trading for the Chesapeake Bay: An Economic Study," May, 60.

Wang, Chenghao, Zhi-Hua Wang, and Jiachuan Yang. 2018. "Cooling Effect of Urban Trees on the Built Environment of Contiguous United States." *Earth's Future* 6 (8): 1066–81. https://doi.org/10.1029/2018EF000891.

Weitzman, Martin L. 2009. "Some Basic Economics of Climate Change." In *Changing Climate, Changing Economy*, edited by J.-P. Touffut. Edward Elgar. http://dx.doi.org/10.4337/9781781953280.00016.

White House. 2016. "United States Mid-Century Strategy for Deep Decarbonization." November 2016. https://unfccc.int/files/focus/long-term_strategies/application/pdf/us_mid_century_strategy.pdf.

Wilen, James E. 2006. "Why Fisheries Management Fails: Treating Symptoms Rather than the Cause." *Bulletin of Marine Science* 78 (3): 529–46.

World Bank. n.d. “Land Area (Sq. Km) - China, Australia | Data.” Accessed October 8, 2019. https://data.worldbank.org/indicator/AG.LND.TOTL.K2?locations=CN-AU.